A Thesis

entitled

Verification and Validation Method for

an Acoustic Mode Prediction Code for Turbomachinery Noise

by

Jeffrey Severino

Submitted to the Graduate Faculty as partial fulfillment of the requirements for the

Masters of Science Degree in Mechanical Engineering

_____
Dr. Ray Hixon, Committee Chair

_____
Dr. Chinhua Sheng, Committee Member

_____
Dr. Soric Cioc, Committee Member

_____
Dr. Patricia R. Komuniecki, Dean
College of Graduate Studies

The University of Toledo

- 2022

An Abstract of

Verification and Validation Method for
an Acoustic Mode Prediction Code for Turbomachinery Noise

by

Jeffrey Severino

Submitted to the Graduate Faculty as partial fulfillment of the requirements for the
Masters of Science Degree in Mechanical Engineering

The University of Toledo
- 2022

Over the last 20 years, there has been an increase in computational fluid dynamic codes that have made numerical analysis more and more readily available, allowing turbomachine designers to create more novel designs. However, as airport noise limitations become more restrictive over time, reducing aircraft takeoff and landing noise remains a prominent issue in the aviation community. One popular method to reduce aircraft noise is using acoustic liners placed on the walls of the engine inlet and exhaust ducts. These liners are designed to reduce the amplitude of acoustic modes emanating from the bypass fan as they propagate through the engine. The SWIRL code is a frequency-domain linearized Euler equation solver that is designed to predict the effect of acoustic liners on acoustic modes propagating in realistic sheared and swirling mean flows, guiding the design of more efficient liner configurations. The purpose of this study is to validate SWIRL using the Method Of Manufactured Solutions (MMS). This study also investigated the effect of the integration and spatial differencing methods on the convergence for a given Manufactured Solution. In addition, the effect of boundary condition implementation was tested. The improved MMS convergence rates shown for these tests suggest that the revised SWIRL code provides more accurate solutions with less computational effort than the original formulation.

Acknowledgments

Contents

List of Tables

List of Figures

List of Symbols

A .... mean flow speed of sound

A_T .... speed of sound at the duct radius

$\tilde{A}$ .... dimensionless speed of sound, $\frac{A}{A_T}$

D/Dt ...... material derivative, $\partial/\partial t + V \cdot \nabla$

D_N .... derivative matrix using N points

$\mathbf{e}_x, \mathbf{e}_\theta$ .... unit vectors for the axial and tangential directions

k_x .... perturbation axial wavenumber

k .... reduced frequency, $\omega r_{max}/A_T$

m .... number of nodal diameters, i.e. azimuthal mode number

M_x .... axial Mach number

M_θ .... tangential Mach number

P .... mean pressure

p' .... perturbation pressure

r .... radial coordinate

r_{min} .... hub radius, i.e. minimum radius

r_{max} .... hub radius, i.e. maximum radius

$\bar{r}$ .... dimensionless radial coordinate, r/r_{max}

$\bar{r}_{Shankar}$ .... dimensionless radial coordinate in **??** , $r/b = r/(r_{max} - r_{min})$

S .... mean entropy

s' .... perturbation entropy

t .... time

$\vec{V}$ .... mean flow velocity vector

v .... mean flow velocity

v' .... perturbation flow velocity

v_x .... axial component of mean flow velocity

v_θ .... tangential component of mean flow velocity

v'_r .... axial component of perturbation velocity

v'_x .... axial component of perturbation velocity

v'_θ .... tangential component of perturbation flow velocity

v_ϕ .... phase velocity,$k/\bar{\gamma}$

v_g .... group velocity,$dk/d\bar{\gamma}$

x .... axial coordinate

Greek Symbols

$\bar{\gamma}$ .... dimensionless axial wavenumber, $k_x r_{max}$

Γ .... free vortex strength

$\bar{\Gamma}$ .... $\Gamma/(r_T A_T)$

δ .... Kronecker delta

η_H .... hub acoustic liner admittance (at r_{min})

η_T .... tip acoustic liner admittance (at r_{max})

Θ .... circumferential/azimuthal coordinate

κ .... ratio of specific heats

$\kappa_{m\mu}$ .... modal separation constant

λ .... eigenvalue, $-i\bar{\gamma}$

μ .... radial mode index

$\bar{\rho}$ .... mean density

ρ' .... perturbation density

σ .... hub-to-tip radius ratio, r_{min}/r_{max}

Ω .... angular frequency for solid body swirl

$\bar{\Omega}$ .... $\Omega r_T/A_T$

ω .... perturbation angular frequency

List of Abbreviations

CAA .... Computational Aeroacoustics
CFD .... Computational Fluid Dynamics
MMS .... Method of Manufactured Solutions
TSM .... Tanh Summation Method
NS .... Navier-Stokes
RK .... Runge-Kutta

Preface

Chapter 1

Introduction

1.1 Overview

Since the dawn of commerical airlines in the early 20th centurty, the increased demand for aircraft transport introduced jet engines to support large cargo and passengers. Consequently, this rise in innovation resulted in high volume engine noise due to the frequency of flights. After 1975, efforts to reduce aircraft noise eliminated the noise pollution for 90% of the population [2]. However, given the rapid increase in aircraft movements and consequently increase in noise exposure to larger populations, the advancement in noise reduction technologies has only been moderately increasing, leaving a requirement for in aeroacoustic modeling techniques and treatment strategies to compete with the demand for quiet subsonic flight [3]. Between the 1950s and 1960's jet engine designs shifted to higher by pass ratios with two or three shafts. The high by pass ratio (HBP) fan utilized multiple stages of fans and air streams [1]. The efficiency of these engines rose with the availablility of materials that are able to cool flows passing over the turbofan, thus slowing the overall jet velocity but maintaining the efficiency of the engine. Due to the increase in high-bypass-ratio of turbomachines, the newest models of engines have a significantly larger diameter and a shorter nacelle, leaving less room to place acoustic treatments in regions where it
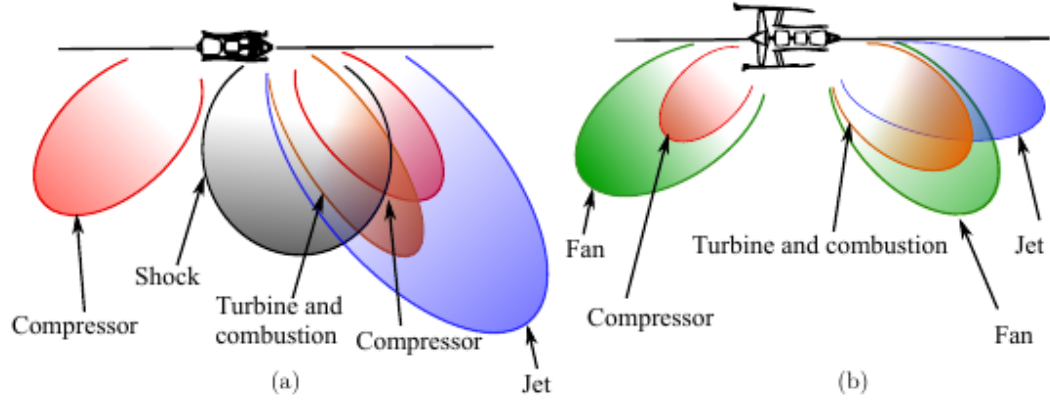
Figure 1-1:   The evolution of the directivity and the relative levels of sources as a function of engine architecture (a)low bypass-ratio (b) high bypass ratio [1]

will be effective [4]. Figure 1-1 shows the evolution of directivity for turbomachines as the use of HBR fans became more popular. As these engines continue to develop, an increased understanding of sound propagation within the interstage of the engine is gong to be needed due to flow behavior (high compressibility and rotational effects). While a turbomachine's general flow condition includes a series of axial, tangential, and radial velocity components that vary depending on the location of concern, the swirling flow between fan stages has been an area of interest due to the potential for acoustic treatment in a location previously avoided for its flow complexity. This work will explore how sound propagation is modeled and how the current state of code verification and validation (V&V) currently stands. This introduction will describe how fluid mechanics is utlized to establish an aeroacoustic model for various ducted flows. It will also discuss how code verification is used in the computational and numerical fields but will show the need for the use of these code verification techniques for a frequency domain CAA code.

In general, jet engine designers can model flow within a turbomachine with the Navier Stokes (N-S) Equations, a set of partial differential equations that describe

the mass, momentum and energy of a given viscous fluid, however these equations can be computationally expensive as they are used in the most general cases.

For aeroacousticians, the N-S equations can be to identify sound generation and propagation because acoustic waves are low amplitude (only a fraction of atmospheric pressure) and are not strongly influenced by viscosity.

As a result, it is common in practice to utilize the Linearized Euler equations (LEE), a closely related set of PDEs that model inviscid fluid, as they provide an approximation for higher Reynold number flows where viscosity does not play a critical role. ach to modeling sound propagation within a flow is to "linearize" the Euler equations, which decomposes the flow solution into a mean and fluctuating component . The decomposition is done in a linear fashion because the sound propagation amplitude is small with respect to the mean flow, and their presence does not appreciable change the mean flow field. The flow solutioń decomposition gives rise to linear and nonlinear terms in the Euler equations where the non-linear fluctuating components are neglected.

The LEE provides a system of linear equations where the solution is a family of wavenumbers and radial mode shapes that arise from unsteady disturbances for flows within a cylindrical duct. Another method decomposes the flow into vortical and potential parts [5]. In either case, this presents an initial value problem which in limited cases can obtain analytical solutions for simplified mean flow. Once a mean flow is contains a tangential component, the LEE equations must be solved numerically. For uniform flows in a hard wall duct , the waves are categorized as vortical ,entropical, and acoustic waves. The vortical and entropic waves soley convect with the mean flow, where as the acoustic wave can propagate without damping or decay exponentially. However, for swiriling flows, the waves are partially coupled and are not easily categorized due to an additonal category of "nearly convecting" modes [6],[7] . Therefore, the families of waves must be found numerically [8] making the

ducted acoustic propagtion in swirling flow a problem without an analytical solution but has a framework for a numerical solution. Swirling flow has been a difficult problem to investigate in comparison to flows parallel to the wall domain of a duct [9] because of the lack of an analytical solution and thus cannot be described from a single convective wave equation. However, the solution for sheared mean flows was first presented by Goldstein [10],[11]. Various special cases of swirling flow (free vortex and solid body swirl) was examined in [12] [6], [7]. In recent years V & V has been done given the rise in technologies capabale of experimentally measuring the acoustic modes within a turbomachine [13]. This work aims offer additional insight to the V & V process by expanding on techniques used in this field.

Computational codes are widely used in the field of aeroacoustics and concerted effort has recently been made to improve V & V techniques by Ingraham and Hixon [14, 15]. The question of getting the correct answer was a large focus of this work.

This thesis aims to continue this effort by conducting code verification and validation on a frequncy domain Linearized Euler equation approximation on previous work done by Pratt & Whitney and NASA Glenn Research Center though techical contract [16, 17].

The algorithms presented in this thesis have been written using FORTRAN 77 and has been updated to FORTRAN 90, and implemented into a code named SWIRL. The foundational work has been started by Pratt and Whitney by Kenneth Kousen [16] and continuted by Dr. Ray Hixon. SWIRL analyzes axial flows with mean shear and swirl in hard wall and acoustically lines ducts. The Method of Manufactured Solutions (MMS) is a process for generating an analytical solution for a code that provides the numerical solution for a given domain. The goal of MMS is to establish a manufactured solution that can be used to establish the accuracy of the code within question. For this study, SWIRL, a code used to calculate the radial modes within an infinitely long duct is being validated through code verification. SWIRL accepts a

given mean flow and uses numerical integration to obtain the speed of sound. The integration technique is found to be the composite trapezoidal rule through asymptotic error analysis.

Prior work has largly depended on conducting code validation through exact solutions to the partial differential equation (PDE) , the convective wave equation . Such a procedure formally known as the method of exact solutions (MES) [18]. MES has the advantage in that the output of SWIRL can be directly compared to the solution of the PDE, however available solutions are limited for sound propagation in ducted flows.

The literature review in the next chapter will discuss the governing equations that are used to predict the acoustic behavior in a fluid flowing internally, followed by the research problem that arises in swirling flow, the objectives and questions, the significance and finally the limitations. The proposed research aims to determine the impact of the numerical schemes used in the swirling flow problem and how it effects the family of waves that are produced from the problem formulation so a better understanding of the acoustic phenomena as the flow under goes a compressible rotational flow. The use of the method of manufactured solutions is used as a means of ensuring the code is correctly approximating the goverining equations and will check the effect of the numerical schemes on the axial wavenumbers produced.

The use of numerical approximations are powerful for cases where there is no analytical solution, thus leaving multiple ways of arriving at a numerical solution. The use of MMS allows the user to obtain various metrics such as the approximated asymptotic rate of convergence, or the grid convergence index, to identify if the code is performing as intended , i.e. using the right equations.

The goal of this research is to conduct component level code verification tests for the problem of characterizing the duct acoustics for flow using a LEE model by looking at the two numerical components for SWIRL.

The goal o The proposed component verification from Kleb and Wood will be presented to addreess the characterization of modes and the presence of numerical ones.

Hypothesis. further improve the result.

Chapter 2

Chapter 2: Literature Review

2.1 Introduction

2.1.1 The problem to be addressed and its significance

The impact of swirling flow has been , there has been a concerted effort to model sound propagation under such conditions. This has lead to a number of publications that attempt to discern the acoustic signature of swirling flow through a cylindrical domain [6] , [7], [16], [17], [5] ,[19],[20], [21], [22], [23], [9], [24], [25], [26].

2.1.2 Establish reasoning - i.e. point - of - view for reviewing the literature

A large amount of aircraft noise was reduced from 1975-2000, effectively eliminating the noise pollution for 90% of the population [2]. Since the early 2000's, the advancement in noise reduction technologies has been gradual, leaving a requirement for drastic improvement in aeroacoustic treatment strategies to compete with the demand of quiet subsonic flight. A previous theoretical review by Envia has been suggested that a non linear time domain computation could capture the source gen-

eration (incident turbulence) in addition to the broadband noise. Such a process would have the capabilities of of solving all components of noise generation in an individual calculation [8]. This would at minimum, require an "LES-type" fidelity code, which can tend to be computationally expensive. A promising option is NASA GRC's Broadband Aeroacoustic Stator Simulation (BASS). BASS is a high-order, high accuracy computational aeroacoustics (CAA) code which has been used to study non linear provides mean an extensive study of non linear phenomena in turbomachinery flow, and in particular, mechanisms of noise generation that are produced from unsteady disturbances. This code allows for a wide variety of finite differencing and time marching schemes as well as artificial dissipation methods. This effective computational tool allows for an in-depth modeling of realistic velocity profiles that would be representative of flow produced from a rotor blade row. In recent work, a new method of implementing realistic, three-dimensional rotor wakes free from acoustics was validated [27]. This provides a means of studying acoustic responses non linear swirling flows within pragmatic geometric configurations, while simultaneously allow for the modeling of sources generation produced from the incident turbulence.

Over the last 40 years, several studies have investigated the impact of swirling flow on the sound propagation with the use of the 3D linearized Euler equations, directly solving the unsteady equations as opposed to approximating the solutions to both steady and unsteady flow problems. Another NASA code, LINFLUX predict acoustic disturbances from blade movements in subsonic flows. While LINFLUX demostrates capabillities to model three dimensional steady and unsteady flows, the computational time is larger compared to lower fidelity codes that only compute the unsteady portion of the problem. The benefit of such a code is beneficial to engine and liner designers who are interested in a wide range of configurations, requiring a parametric study. SWIRL [17], is a code that coducts an eigenmode analysis by assuming a constant radius annular or cylindrical duct with acoustically lined walls

using the linearized unsteady Euler equations. Such a code is needed to identify the modal content and can be used as a boundary condition with LINFLUX by using a mode matching technique. The goal of this theoretical review is to see the current state of low-fidelity frequency domain LEE codes and where the foundational model differs depending on the problem formulation.

2.1.3 Explain the order/sequence of the review

This review will compare studies that have considered the applicability of unsteady linearized Euler equations on cylindrical and annular ducts. First the work of Kousen will breifly summarized [17, 16]. Secondly, the alternate approached shown by Golubev and Atassi used in [19, 20] were also compared. These works have utilized a standard normal mode approach to determine the modal response of inviscid, compressible, swirling flow within a cylindrical and annular ducts. Results and findings have revealed three categories of associated wave - modes, acoustic, nearly convected, and nearly sonic. Detailed examination of the literature indicate that the hierarchical system was not initially apparent. A qualitative description of the numerical methods used to evaluate the eigensystem of solutions will be described. The use of the Method of Manufactured Solutions will also be described. While it's use is widespead in the verification and validation community, very little aeroacoustic codes utlize the MMS to apply code verification. This review will discuss the procedures and guidelines associated with the MMS, and some specific measures that were taken to ensure that the guidelines were met and that the suggestions used in literature were expanded upon.

2.1.4 The theoretical foundation of conceptual framework

One key question that remains, is how well do unsteady linearized equations capture the mechanisms of noise generation within realistic turbomachinery flow? There exists a copious amount of published work describing the use of wave equations to describe the governing behavior of ducted sound propagation. However, turbomachines inherently rely on high velocities, high temperatures to maximize efficiencies. Such mechanisms need a more thorough formulation so that a complete acoustic description of the flow can be provided.

To begin exploring various geometries, we must first ask: what are the central theories that have been used to explain the acoustic behavior of unsteady swirling flows? Do the linearized Euler equations provide an adequate means of capturing the mechanisms of noise generation within realistic turbomachinery flow? The study was expanded by [7, 28] who included cases of solid body swirl. Wundrow studied the swirling potential flows using Goldstein's disturbance velocity decomposition [10] using a numerical approach and found that the solutions were more accurate and found more efficiently [7]. Kousen expanded these efforts by including [16, 17] the effect unsteady disturbances in the presence of forced solid body-swirl and free-vortex flow without the use of potential flow theory. Using normal mode analysis along with a radial spatial differencing scheme, the wave modes produced within cylindrical and annular ducts was reported. Results show (figure 4.7) two distinct families of modes, purely convected and acoustic modes. The presence of axial shear in combination solid body flows can endue coupling between these modes, which in theory would not appear unless viscous terms were present in the eigenvalue analysis. Lack of available swirl flow results "hampered" validation attempts. However, this eigenvalue approach was utilized with a new quasi-3D formulation to find the axial wavenumbers from solid body flow was proposed in his next work .

In [17], A quasi 3D formulation was validated and used to predict the appearance of modes due to the interaction of a rotor with spatially uniform steady and unsteady flow. These modes were first classified by [29] as "spinning modes". In addition, further investigation was done on the results shown in [17]. The axial wavenumbers that were previously found to be purely convective were shown to be in part ,"nearly convective" (shear) pressure modes. These were found to propagate in the axial direction with no loss in amplitude, thus never satisfying the cut-off condition.

2.2 Review of the assessment of the numerical techniques

Kousen assesed the accuracy of the numerical discretication technique for a series of test cases using three sources [30] [31] and [32] ([10] [15] and [45] in Kousen's work [16] respectively). The results were assesed by using various literature comparisons. The methodology was presented of uniform mean axial flows, but results for hard wall cases were presented by computing the order of accuracy for the first four radial modes (See Figures 4.1-4.4), . (Explain why this is MES and offer MMS as a source of verification and explain that MES is validation [33] [34]). For a uniform axial flow, the axial wavenumbers can be computed from an analytical solution, where one of the key input parameters are the zero crossings of the derivative of the Bessel Function of the first kind . The values are presented [35] and are often refered to as separation constants for a circumfirential and radial mode pair ; which are needed to compute the solution of the convective wave equation.

The axial wavenumber is found by using second-order differential convective wave equation for pressure using a fourth order accurate Runge-Kutta(RK) method [17] which was done to check against the results in [36] (Table 4.1 and 4.2 in [17]). The output parameter was γ/k. Each axial wave number can then be used to compute

the analytical radial mode using the exponential assumption. Axial wavenumbers from annular and cylindrical ducts with lined walls were compared to findings from Astley and Eversman [32] for uniform and sheared axial flow with liner (Table 4.3). The results taken were from a "high-order" RK scheme used. Axial wavenumbers from cylindrical ducts with hard walls were compared to findings from Shankar [30] in Table 4.4 of [17].

In recent years Maldonado et. al, [13] has made significant contributions in solution verification given the recent improvements in experimental measurement techniques. The work has presented test cases for lined ducts that have been compared to Kousen [17], Nijboer [22] and Peake [25] and show excellent comparison. The goal of this work is to contribute these efforts by conducting the method of manufactured solutions to offer clarity in using techniques often used in other verification and validation (V&V) studies.

2.2.1   The research questions, hypotheses, foreshadowed problems, or conjectures

While these results confirm the findings of SWIRL and other LEE codes, this does not check if the equations that were programmed were entered correctly. While an emphasis on solution verification is vital, it should be coupled with code verification to determine the robustness and consistency of the algorithm. The method of manufactured solutions combined with order of accuracy verification is often used as a gold standard of code verification [33] and has been shown to provide an estimate of discretization error that can be computed before the final answer is obtained. Since the mid 2000's, code verification literature has grown popular in the field of computational mathematics and physics due to its ability to conduct tests for numerical approximations of partial and ordinary differential equations. The MMS offers

a means of "manufacturing" an arbitrary solution by define functions for each term in the governing equation. Common practices and guidelines are offered in [34] to choose the fuunctions, but are phrased such that MMS can be widely applied. Since various numerical problems are unique in their treatment of spatial discretization, and boundary condtions , this work will describe the use of these guidelines and the nuances that have been taken to check the boundary conditon and radial derivatives used in SWIRL.

Knupp in Code Verification by the MMS [34] provides guidelines for creating manufactured soultions which states,

1. The manufactured solutions should be composed of smooth analytic functions

2. The manufactured solutions should exercize every term in the governing equation that is being tested,

3. The solution should have non trivial derivatives.

4. The solution derivatives should be bounded by a small constant. In this case this constant should prevent the function from becoming greater than one.

5. The solution should not prevent the code from running

6. The solution should be defined on a connected subset of two- or three- dimensional space to allow flexibility in chosing the domain of the PDE.

7. The solution should coincide with the differential operators of the PDE. For example, the flux term in Fourier's law of conduction requires T to be differentiable.

The goal is the to calculate an observed order of accuracy.

2.2.2 Calculation of Observed Order-of-Accuracy

To begin the method of manufactured solutions, the discretization error, ϵ is defined as a function of radial grid spacing, Δr

$$\epsilon = \epsilon(\Delta r)$$

The discretization error in the solution should be proportional to $(\Delta r)^\alpha$ where $\alpha > 0$ is the theoretical order for the computational method. The error for each grid is expressed as

$$\epsilon_{M_\theta}(\Delta r) = |M_{\theta,Analytic} - M_{\theta,calc}|$$

where $M_{\theta,Analytic}$ is the tangential mach number that is defined from the speed of sound we also defined and the $M_{\theta,calc}$ is the result from SWIRL. The Δr is to indicate that this is a discretization error for a specific grid spacing. Applying the same concept to to the speed of sound,

If we define this error on various grid sizes and compute ϵ for each grid, the observed order of accuracy can be estimated and compared to the theoretical order of accuracy. For instance, if the numerical soution is second-order accurate and the error is converging to a value, the L2 norm of the error will decrease by a factor of 4 for every halving of the grid cell size. Since the input variables should remain unchanged, the error for the axial and tangential mach number should be zero. As for the speed of sound, since we are using an analytic expression for the tangential mach number, we know what the theoretical result would be from the numerical integration technique as shown above. Similarly we define the discretization error for the speed of sound.

$$\epsilon_A(\Delta r) = |A_{Analytic} - A_{calc}|$$

For a perfect answer, we expect ϵ to be zero. Since a Taylor series can be used to derive the numerical schemes, we know that the truncation of higher order terms is what indicates the error we expect from using a scheme that is constructed with such truncated Taylor series.

The expectation is that the error at each grid point j to satisfy the following,

$$0 = |A_{Analytic}(r_j) - A_{calc}(r_j)|$$

$$\widetilde{A}_{Analytic}(r_j) = \widetilde{A}_{calc}(r_j) + (\Delta r)^\alpha \beta(r_j) + H.O.T$$

where the value of $\beta(r_j)$ does not change with grid spacing, and α is the asymptotic order of accuracy of the method. It is important to note that the numerical method recovers the original equations as the grid spacing approached zero.

Subtracting $A_{Analytic}$ from both sides gives

$$A_{calc}(r_j) - A_{Analytic}(r_j) = A_{Analytic}(r_j) - A_{Analytic}(r_j) + \beta(r_j)(\Delta r)^\alpha$$

$$\epsilon_A(r_j)(\Delta r) = \beta(r_j)(\Delta r)^\alpha$$

To estimate the order of accuracy of the accuracy, the global errors are calculated by taking the L2 Norm of the error which is denoted as $\hat{\epsilon}_A$

$$\hat{\epsilon}_A = \sqrt{\frac{1}{N}\sum_{j=1}^{N} \epsilon(r_j)^2}$$

$$\hat{\beta}_A(r_j) = \sqrt{\frac{1}{N}\sum_{j=1}^{N} \beta(r_j)^2}$$

As the grid density increases, $\hat{\beta}$ should asymptote to a constant value. Given two grid densities, Δr and $\sigma \Delta r$, and assuming that the leading error term is much larger than any other error term,

$$\hat{\epsilon}_{grid1} = \hat{\epsilon}(\Delta r) = \hat{\beta}(\Delta r)^\alpha$$

$$\hat{\epsilon}_{grid2} = \hat{\epsilon}(\sigma \Delta r) = \hat{\beta}(\sigma \Delta r)^\alpha$$

$$= \hat{\beta}(\Delta r)^\alpha \sigma^\alpha$$

The ratio of two errors is given by,

$$\frac{\hat{\epsilon}_{grid2}}{\hat{\epsilon}_{grid1}} = \frac{\hat{\beta}(\Delta r)^\alpha}{\hat{\beta}(\Delta r)^\alpha} \sigma^\alpha$$

$$= \sigma^\alpha$$

Thus, α,the asymptotic rate of convergence is computed as follows

$$\alpha = \frac{\ln \frac{\hat{\epsilon}_{grid2}}{\hat{\epsilon}_{grid1}}}{\ln(\sigma)}$$

For example ,a doubling of grid points has $\sigma = 1/2$,

$$\alpha = \frac{\ln\left(\hat{\epsilon}\left(\frac{1}{2}\Delta r\right)\right) - \ln\left(\hat{\epsilon}\left(\Delta r\right)\right)}{\ln\left(\frac{1}{2}\right)}$$

2.3 Conclusion

This review discusses the development of the unsteady linearized equations, and how improvements in the modal analysis capture more families of mechanisms of noise generation within non-uniform swirling flow turbomachinery flow. While the literature presented offers a measure of verification and validation through the use of the Method of Exact Solutions, the Method of Manufactured Solutions offers a level of code verification which allows for error checking by computing the approximate order of accuracy for a given numerical scheme, which is independent of the final answer, which in this case is the axial wavenumber. The next chapter will outline the methodology and techniques used when applying MMS to SWIRL. The methods consist of unique treatment of boundary conditions using fairing functions as well as an example of using a summation to generate arbitrary functions as manufactured solutions which has the dual benefit of giving a large number of derivatives but allows for high gradients in specific locations along the domain of the MS. The use of open-source widely available functions in Python were used to symbolically create the MS and then used to generate FORTRAN code that will compute the MS for code comparison.

Chapter 3

Chapter 3: Theoretical Framework and Methods

3.1 Introduction

This chapter will outline the steady and unsteady aerodynamic models used for this study. The MMS procedure as it is used in this study will be described. The summation method used to generate symbolic expression will be breifly described. This chapter will also present the use of fairing functions to impose the equivallent boundary conditions used in the numerical approximation. The procedure for calculating the approximated rate of convergence for a system of equations is also presented.

3.2 Steady Flow Aerodynamic Model

3.2.1 Compressible Euler Equations

For an ideal polytropic gas with density, ρ, velocity, $\vec{V}$, and pressure, p , the Euler equations are,

$$\frac{D\rho}{Dt} = -\rho\nabla \cdot \vec{V} \tag{3.1}$$

$$\frac{D\vec{V}}{Dt} = -\frac{\nabla p}{\rho} + \vec{g} \tag{3.2}$$

$$\frac{Dp}{Dt} = -\gamma p\nabla \cdot \vec{V} \tag{3.3}$$

$$\tag{3.4}$$

where Equations (3.1, 3.2, 3.3) are the conservation of mass, momentum, and energy equations respectively.

If the flow is assumed to be asymmetric, then the radial velocity component is zero. With this considered, the velocity vector ,$\vec{V}$ in cylindrical coordinates become,

$$\vec{V}(r,\theta,x) = v_x(r)\hat{e}_x + v_\theta(r)\hat{e}_\theta \tag{3.5}$$

where $\hat{e}_x$ and $\hat{e}_\theta$ are unit vectors for the axial and tangential directions.The gradient operator ,∇ in cylindrical coordinates, is

$$\vec{\nabla} = \hat{e}_r\frac{\partial}{\partial r} + \frac{1}{r}\hat{e}_\theta\frac{\partial}{\partial\theta} + \frac{\partial}{\partial z}\hat{e}_z = 0 \tag{3.6}$$

Expanding Equations (3.1, 3.2, 3.3) with the corresponding cylindrical expressions become,

$$\frac{\partial \rho}{\partial t} + v_r \frac{\partial \rho}{\partial r} + \frac{v_\theta}{r} \frac{\partial \rho}{\partial \theta} + v_x \frac{\partial \rho}{\partial \theta} + \rho \left(\frac{1}{r} \frac{\partial (r v_r)}{\partial r} + \frac{1}{r} \frac{\partial v_\theta}{\partial \theta} + \frac{\partial v_x}{\partial x} \right) = 0 \qquad (3.7)$$

$$\frac{\partial v_r}{\partial t} + v_r \frac{\partial v_r}{\partial r} + \frac{v_\theta}{r} \frac{\partial v_r}{\partial \theta} - \frac{v_\theta^2}{r} + v_x \frac{\partial v_r}{\partial x} = -\frac{1}{\rho} \frac{\partial p}{\partial r} \qquad (3.8)$$

$$\frac{\partial v_\theta}{\partial t} + v_r \frac{\partial v_\theta}{\partial r} + \frac{v_\theta}{r} \frac{\partial v_\theta}{\partial \theta} + \frac{v_r v_\theta}{r} + v_x \frac{\partial v_\theta}{\partial x} = -\frac{1}{\rho r} \frac{\partial p}{\partial \theta} \qquad (3.9)$$

$$\frac{\partial v_x}{\partial t} + v_r \frac{\partial v_x}{\partial r} + \frac{v_\theta}{r} \frac{\partial v_x}{\partial \theta} + v_x \frac{\partial v_x}{\partial x} = -\frac{1}{\rho} \frac{\partial p}{\partial x} \qquad (3.10)$$

$$\frac{\partial p}{\partial t} + v_r \frac{\partial p}{\partial r} + \frac{v_\theta}{r} \frac{\partial p}{\partial \theta} + v_x \frac{\partial p}{\partial \theta} + \gamma p \left(\frac{1}{r} \frac{\partial (r v_r)}{\partial r} + \frac{1}{r} \frac{v_\theta}{\partial \theta} + \frac{\partial v_x}{\partial x} \right) = 0 \qquad (3.11)$$

For a steady flow, $(\partial/\partial t = 0)$, the compressible flow equations can be further reduced to,

$$\nabla(\vec{V} \rho) = 0 \qquad (3.12)$$

$$(\vec{V} \cdot \nabla)\vec{V} = 0 \qquad (3.13)$$

$$\nabla S = 0 \qquad (3.14)$$

where S represents the entropy in the mean flow.

3.2.2 Nonuniformities from swirling mean flow

If the mean flow contains a swirling component, i.e. a velocity vector in the tangential direction, the mean quantities, pressure , density are non-uniform, thus also changing the speed of sound. By integrating the radial momentum equation, an expression for the speed of sound was established to account for the resulting nonuniformities due to rotations in the flow.

$$p = \int_{r_{min}}^{r_{max}} \frac{\rho v_\theta^2}{r} dr \tag{3.15}$$

where r_{min} and r_{max} are the bounds of the radius. Since the flow is isentropic, the pressure is related to the speed of sound through $\nabla p = A^2 \nabla \rho$; which is used to compute ρ. With the relationship $A^2 = \kappa p / \rho$, the speed of sound is found to be,

$$\tilde{A}(\tilde{r}) = exp\left[\left(\frac{1-\gamma}{2}\right)\int_{\tilde{r}}^{1} \frac{M_\theta}{\tilde{r}} \partial \tilde{r}\right]$$

For special cases of swirling flow, the relation to between the speed of sound and the tangential velocity can be found. Expressions can be derived for free vortex , and/or solid body swirl.

3.3   Unsteady Flow: Aerodynamic Model

3.4   Non-dimensionalization

Chapter 4

Chapter 4: Numerical Models

4.1 Numerical Integration

4.2 Introduction

The Method of Manufactured Solutions (MMS) is a process for generating an analytical solution for a code that provides the numerical solution for a given domain. The goal of MMS is to establish a manufactured solution that can be used to establish the accuracy of the code within question. For this study, SWIRL, a code used to calculate the radial modes within an infinitely long duct is being validated through code verification. SWIRL accepts a given mean flow and uses numerical integration to obtain the speed of sound. The integration technique is found to be the composite trapezoidal rule through asymptotic error analysis.

For SWIRL, the absolute bare minimum requirement is to define the corresponding flow components for the domain of interest. SWIRL assumes no flow in the radial direction, leaving only two other components, axial and tangential for a 3D cylindrical domain. Since SWIRL is also non dimensionalized, the mean flow components are defined using the Mach number. SWIRL uses the tangential mach number to obtain the speed of sound using numerical integration. The speed of sound is then used to

find the rest of the primative variables for the given flow.

4.3 Methods

SWIRL is a linearized Euler equations of motion code that calculates the axial wavenumber and radial mode shapes from small unsteady disturbances in a mean flow. The mean flow varies along the axial and tangetial directons as a function of radius. The flow domain can either be a circular or annular duct, with or without acoustic liner. SWIRL was originally written by Kousen [insert ref].

The SWIRL code requires two mean flow parameters as a function of radius, M_x, and M_θ. Afterwards, the speed of sound, $\widetilde{A}$ is calculated by integrating M_θ with respect to r. To verify that SWIRL is handling and returning the accompanying mean flow parameters, the error between the mean flow input and output variables are computed. Since the trapezoidal rule is used to numerically integrate M_θ, the discretization error and order of accuracy is computed. Since finite differencing schemes are to be used on the result of this integration, it is crucial to accompany the integration with methods of equal or less order of accuracy. This will be determined by applying another MMS on the eigenproblem which will also have an order of accuracy.

4.3.1 Theory

To relate the speed of sound to a given flow, the radial momentum equation is used. If the flow contains a swirling component,then the primitive variables are nonuniform through the flow, and mean flow assumptions are not valid.

$$\frac{\partial v_r}{\partial t} + v_r \frac{\partial v_r}{\partial r} + \frac{v_\theta}{r} \frac{\partial v_\theta}{\partial \theta} - \frac{v_\theta^2}{r} v_x \frac{\partial v_r}{\partial x} = \frac{1}{\rho} \frac{\partial P}{\partial r}$$

To account to for this, the radial momentum is simplified by assuming the flow is steady, the flow has no radial component. In addition, the viscous and body forces are neglected. Then the radial pressure derivative term is set equal to the dynamic pressure term. Seperation of variables is applied.

$$\frac{v_\theta^2}{r} = \frac{1}{\rho} \frac{\partial P}{\partial r}$$

$$P = \int_r^{r_{max}} \frac{\rho V_\theta^2}{r}$$

To show the work, we will start with the dimensional form of the equation and differentiate both sides. Applying separation of variables,

$$\int_r^{r_{max}} \frac{\bar{\rho} v_\theta^2}{r} \partial r = - \int_{P(r)}^{P(r_{max})} \partial p.$$

Since $\tilde{r} = r/r_{max}$,

$$r = \tilde{r} r_{max}.$$

Taking total derivatives (i.e. applying chain rule),

$$dr = d(\tilde{r} r_{max}) = d(\tilde{r}) r_{max},$$

Substituting these back in and evaluating the right hand side,

$$\int_{\tilde{r}}^{1} \frac{\bar{\rho} v_{\theta}^2}{\tilde{r}} \partial \tilde{r} = P(1) - P(\tilde{r})$$

For reference the minimum value of $\tilde{r}$ is,

$$\sigma = \frac{r_{max}}{r_{min}}$$

For the radial derivative, the definition of the speed of sound is utilized,

$$\frac{\partial A^2}{\partial r} = \frac{\partial}{\partial r} \left(\frac{\gamma P}{\rho} \right).$$

Using the quotient rule, the definition of the speed of sound is extracted,

$$= \frac{\partial P}{\partial r} \frac{\gamma \bar{\rho}}{\bar{\rho}^2} - \left(\frac{\gamma P}{\bar{\rho}^2} \right) \frac{\partial \bar{\rho}}{\partial r}$$

$$= \frac{\partial P}{\partial r} \frac{\gamma}{\bar{\rho}} - \left(\frac{A^2}{\bar{\rho}} \right) \frac{\partial \bar{\rho}}{\partial r}$$

Using isentropic condition $\partial P / A^2 = \partial \rho$,

$$= \frac{\partial P}{\partial r} \frac{\gamma}{\bar{\rho}} - \left(\frac{1}{\bar{\rho}} \right) \frac{\partial P}{\partial r}$$

$$\frac{\partial A^2}{\partial r} = \frac{\partial P}{\partial r} \frac{\gamma - 1}{\bar{\rho}}$$

$$\frac{\bar{\rho}}{\gamma - 1} \frac{\partial A^2}{\partial r} = \frac{\partial P}{\partial r}$$

Going back to the radial momentum equation, and rearranging the terms will simplify the expression. The following terms are defined to start the nondimensionalization.

$$M_\theta = \frac{V_\theta}{A}$$

$$\widetilde{r} = \frac{r}{r_{max}}$$

$$\widetilde{A} = \frac{A}{A_{r,max}}$$

$$A = \widetilde{A} A_{r,max}$$

$$r = \widetilde{r} r_{max}$$

$$\frac{\partial}{\partial r} = \frac{\partial \widetilde{r}}{\partial r} \frac{\partial}{\partial \widetilde{r}}$$

$$= \frac{1}{r_{max}} \frac{\partial}{\partial \widetilde{r}}$$

Dividing by A,

$$\frac{M_\theta^2}{r}(\gamma - 1) = \frac{\partial A^2}{\partial r} \frac{1}{A^2}$$

Now there is two options, either find the derivative of $\bar{A}$ or the integral of M_θ with respect to r.

1. Defining non dimensional speed of sound $\tilde{A} = \frac{A(r)}{A(r_{max})}$

$$\int_{r}^{r_{max}} \frac{M_\theta}{r} (\gamma - 1) \, \partial r = ln\left(\frac{1}{\tilde{A}^2}\right)$$

$$= -2ln(\tilde{A})$$

$$\tilde{A}(r) = exp\left[-\int_{r}^{r_{max}} \frac{M_\theta}{r} \frac{(\gamma - 1)}{2} \partial r\right]$$

$$\text{replacing r with } \tilde{r} \rightarrow \tilde{A}(r) = exp\left[-\int_{r}^{r_{max}} \frac{M_\theta}{r} \frac{(\gamma - 1)}{2} \partial r\right]$$

$$\tilde{A}(\tilde{r}) = exp\left[\left(\frac{1 - \gamma}{2}\right) \int_{\tilde{r}}^{1} \frac{M_\theta}{\tilde{r}} \partial \tilde{r}\right]$$

2. Or we can differentiate

Solving for M_θ ,

$$M_\theta^2 = \frac{\partial A^2}{\partial r} \frac{r}{A^2 (\gamma - 1)}$$

Nondimensionalizing and substituting,

$$M_\theta^2 \frac{(\gamma - 1)}{\tilde{r} r_{max}} = \frac{1}{(\tilde{A} A_{r,max})^2} \frac{A_{r,max}^2}{r_{max}} \frac{\partial \tilde{A}^2}{\partial \tilde{r}}$$

$$M_\theta^2 \frac{(\gamma - 1)}{\tilde{r}} = \frac{1}{\tilde{A}^2} \frac{\partial \tilde{A}^2}{\partial \tilde{r}}$$

$$M_\theta = \sqrt{\frac{\tilde{r}}{(\gamma - 1)\tilde{A}^2} \frac{\partial \tilde{A}^2}{\partial \tilde{r}}} \qquad (4.1)$$

4.3.2 Procedure

There are a few constraints and conditions that must be followed in order for the analytical function to work with SWIRL,

- The mean flow and speed of sound must be real and positive. This will occur is a speed of sound is chosen such that the tangential mach number is imaginary

- The derivative of the speed of sound must be positive

- Any bounding constants used with the mean flow should not allow the total Mach number to exceed one.

- the speed of sound should be one at the outer radius of the cylinder

Given these constraints, $tanh(r)$ is chosen as a function since it can be modified to meet the conditions above. Literature (The tanh method: A tool for solving certain classes of nonlinear evolution and wave equations) is a paper than demonstrates the strength of using tanh functions. One additonal benefit of tanh(r) is that it is bounded between one and negative one, i.e.

- As r $\rightarrow \infty$ tanh(r) $\rightarrow$ 1

- As -r $\rightarrow -\infty$ tanh(r) $\rightarrow$ -1

To test the numerical integration method, M_θ is defined as a result of differentiating the speed of sound, A. This is done opposed to integrating M_θ analytically. However, an analytical function can be defined for M_θ, which can then be integrated to find what $\widetilde{A}$ should be. Instead, the procedure of choice is to back calculate what the appropriate M_θ is for a given expression for $\widetilde{A}$. Since it is easier to take derivatives , we will solve for M_θ using Equation 4.1 ,

4.3.3   Tanh Summaion Formulation

The goal is generate an MS with a number of "stairs" that is bounded between zero and one. Here's what my focus group ideas are,

$$1 = R + L$$

where, 1 is a constraint, and R and L are the two waves when summed need to cancel if it were the exact same amplitude & opposite sign

so ,

$$R + L = \tanh(x) + -\tanh(x) = 0$$

or in our case,

$$R + L = \tanh(x) + -\tanh(x) = 1$$

We can tweak this by adding knobs by adding "knobs" A and B. If we dont want the total to not exceed one then, $A_j + A_{j+1} \cdots A_{last} = 1$. B_1 changes the steepnes of the kink that we want. In order to generalize this,

$$\bar{A} = \sum_{j=1}^{n} R_{ij} + \sum_{j=1}^{n} L_{ij}$$

31

where,

$$R_{ij} = A_j \tanh(B_j(x_i - x_j))$$

$$L_{ij} = A_j \tanh(B_j(x_j - x_n))$$

Letting $n = 3 \ldots$

$$\bar{A} = S_{vert} + \sum_{j=1}^{3} R_{ij} + \sum_{j=1}^{3} L_{ij}$$

$$\bar{A} = A_1 \tanh(B_1(x_i - x_1)) + A_2 \tanh(B_2(x_i - x_2)) + A_3 \tanh(B_3(x_i - x_3)) +$$

$$A_1 \tanh(B_1(x_1 - x_n)) + A_2 \tanh(B_2(x_2 - x_n)) + A_3 \tanh(B_3(x_3 - x_n))$$

and,

$$A_1 = A_2 = A_3 = k_1$$

$$B_1 = B_2 = B_3 = k_2$$

A tanh summation method was constructed to make a manufactured solution with strong changes in slope. This ensures that the numerical approximation will not give trivial answers. then for some functions we need to impose boundary conditions. We will demonstrate how the careless implementation of a boundary condition can lead to close approximations on the interior. The speed of sound is defined with the subscript *analytic* to indicate that this is the analytical function of choice and has no physical relevance to the actual problem.

$$\widetilde{A}_{analytic} = \Lambda + k_1 \tanh \left(k_2 \left(\widetilde{r} - \widetilde{r}_{max} \right) \right),$$

32

where,

$$\Lambda = 1 - k_1 \tanh(k_2(1 - \widetilde{r}_{max})),$$

When, $\widetilde{r} = \widetilde{r}_{max}$, $\widetilde{A}_{analytic} = 1$. Taking the derivative with respect to $\widetilde{r}$,

$$\frac{\partial \widetilde{A}_{analytic}}{\partial \widetilde{r}} = \left(1 - \tanh^2\left((r - r_{max})\, k_2\right)\right) k_1 k_2,$$

$$= \frac{k_1 k_2}{\cosh^2\left((r - r_{max})\, k_2\right)}.$$

Substitute this into the expression for M_θ in Equation 4.1,

$$M_\theta = \sqrt{2} \sqrt{\frac{r k_1 k_2}{(\kappa - 1)\left(\tanh\left((r - r_{max})\, k_2\right) k_1 + \tanh\left((r_{max} - 1)\, k_2\right) k_1 + 1\right) \cosh^2\left((r - r_{max})\, k_2\right)}}$$

Now that the mean flow is defined, the integration method used to obtain the speed of sound

Initially the source terms were defined without mention of the indices of the matrices they make up. In other words, there was no fore sight on the fact that these source terms are sums of the elements within A,B, and X. To investigate the source terms in greater detail, the FORTRAN code that calls the source terms will output the terms within the source term and then sum them, instead

of just their sum. i $[A]x = \lambda[B]x$

which can be rearranged as,

$[A]x - \lambda[B]x = 0$

Here, x is an eigenvector composed of the perturbation variables, v_r, v_θ, v_x, p and λ is the associated eigenvalue, (Note: $\lambda = -i\bar{\gamma}$)

Writing this out we obtain $\cdots$.

Linear System of Equations:

$$-i\left(\frac{k}{A} - \frac{m}{r}M_\theta\right)v_r - \frac{2}{r}M_\theta v_\theta + \frac{dp}{dr} + \frac{(\kappa-1)}{r}M_\theta^2 p - \lambda M_x v_r = S_1 \qquad (4.2)$$

Using matrix notation,

$$A_{11}x_1 - A_{12}x_2 + A_{14}x_4 - \lambda B_{11}x_1 = S_1 \qquad (4.3)$$

But A_{14} and A_{41} in Kousen's paper only has the derivative operator. Since I am currntly writing the matrix out term by term and not doing the matrix math to obtain the symbolic expressions, I will define A_{14} with dp/dr and A_{41} with dv_r/dr Similarly,

$$A_{21}x_1 - A_{22}x_2 + A_{24}x_4 \qquad\qquad -\lambda B_{22}x_2 = S_2 \qquad (4.4)$$

$$A_{31}x_1 - A_{33}x_3 \qquad\qquad -\lambda(B_{33}x_3 + B_{34}x_4) = S_3 \qquad (4.5)$$

$$A_{41}x_1 + A_{42}x_2 + A_{44}x_4 \qquad\qquad -\lambda(B_{33}x_3 + B_{44}x_4) = S_4 \qquad (4.6)$$

Now we can begin looking at the source terms, term by term. They each should also converge at a known rate

4.3.4 Calculation of Observed Order-of-Accuracy

The numerical scheme used to perform the integration of the tangential velocity will have a theoretical order-of-accuracy. To find the theoretical order-of-accuracy, the discretization error must first be defined. The error, ϵ, is a function of id spacing, Δr

$$\epsilon = \epsilon(\Delta r)$$

The discretization error in the solution should be proportional to $(\Delta r)^\alpha$ where $\alpha > 0$ is the theoretical order for the computational method. The error for each grid is expressed as

$$\epsilon_{M_\theta}(\Delta r) = |M_{\theta,analytic} - M_{\theta,calc}|$$

where $M_{\theta,analytic}$ is the tangential mach number that is defined from the speed of sound we also defined and the $M_{\theta,calc}$ is the result from SWIRL. The Δr is to indicate that this is a discretization error for a specific grid spacing. Applying the same concept to to the speed of sound,

If we define this error on various grid sizes and compute ϵ for each grid, the observed order of accuracy can be estimated and compared to the theoretical order of accuracy. For instance, if the numerical soution is second-order accurate and the error is converging to a value, the L2 norm of the error will decrease by a factor of 4 for every halving of the grid cell size.

Since the input variables should remain unchanged (except from minor changes from the Akima interpolation), the error for the axial and tangential mach number should be zero. As for the speed of sound, since we are using an analytic expression for the tangential mach number, we know what the theoretical result would be from the numerical integration technique as shown above. Similarly we define the discretization error for the speed of sound.

$$\epsilon_A(\Delta r) = |A_{analytic} - A_{calc}|$$

For a perfect answer, we expect ϵ to be zero. Since a Taylor series can be used to derive the numerical schemes, we know that the truncation of higher order terms is what indicates the error we expect from using a scheme that is constructed with such truncated Taylor series.

The error at each grid point j is expected to satisfy the following,

$$0 = |A_{analytic}(r_j) - A_{calc}(r_j)|$$

$$\widetilde{A}_{analytic}(r_j) = \widetilde{A}_{calc}(r_j) + (\Delta r)^\alpha \beta(r_j) + H.O.T$$

where the value of $\beta(r_j)$ does not change with grid spacing, and α is the asymptotic order of accuracy of the method. It is important to note that the numerical method recovers the original equations as the grid spacing approached zero. It is important to note that β represents the first derivative of the Taylor Series. Subtracting $A_{analytic}$ from both sides gives,

$$A_{calc}(r_j) - A_{analytic}(r_j) = A_{analytic}(r_j) - A_{analytic}(r_j) + \beta(r_j)(\Delta r)^\alpha$$

$$\epsilon_A(r_j)(\Delta r) = \beta(r_j)(\Delta r)^\alpha$$

To estimate the order of accuracy of the accuracy, we define the global errors by calculating the L2 Norm of the error which is denoted as $\hat{\epsilon}_A$

$$\hat{\epsilon}_A = \sqrt{\frac{1}{N}\sum_{j=1}^{N}\epsilon(r_j)^2}$$

36

$$\hat{\beta}_A(r_j) = \sqrt{\frac{1}{N}\sum_{j=1}^{N}\beta(r_j)^2}$$

As the grid density increases, $\hat{\beta}$ should asymptote to a constant value. Given two grid densities, Δr and $\sigma\Delta r$, and assuming that the leading error term is much larger than any other error term,

$$\hat{\epsilon}_{grid1} = \hat{\epsilon}(\Delta r) = \hat{\beta}(\Delta r)^\alpha$$

$$\hat{\epsilon}_{grid2} = \hat{\epsilon}(\sigma\Delta r) = \hat{\beta}(\sigma\Delta r)^\alpha$$

$$= \hat{\beta}(\Delta r)^\alpha \sigma^\alpha$$

The ratio of two errors is given by,

$$\frac{\hat{\epsilon}_{grid2}}{\hat{\epsilon}_{grid1}} = \frac{\hat{\beta}(\Delta r)^\alpha}{\hat{\beta}(\Delta r)^\alpha}\sigma^\alpha$$

$$= \sigma^\alpha$$

Thus, α,the asymptotic rate of convergence is computed as follows

$$\alpha = \frac{\ln\frac{\hat{\epsilon}_{grid2}}{\hat{\epsilon}_{grid1}}}{\ln(\sigma)}$$

Defining for a doubling of grid points ,

$$\alpha = \frac{\ln\left(\hat{\epsilon}\left(\frac{1}{2}\Delta r\right)\right) - \ln\left(\hat{\epsilon}\left(\Delta r\right)\right)}{\ln\left(\frac{1}{2}\right)}$$

Similarly for the eigenvalue problem, Initially the source terms were defined without mention of the indicies of the matricies they make up. In other words, there was no fore sight on the fact that these source terms are sums of the elements within A,B, and X. To investigate the source terms in greater detail, the FORTRAN code that calls the source terms will output the terms within the source term and then sum them, instead of just their sum.

$$[A]x - \lambda[B]x = 0$$

4.4 Fairing Functions

Goal: How can we modify a manufactured solution such that the endpoints are suitable for comparison against a codes boundary condition implementation

4.5 Setting Boundary Condition Values Using a Fairing Function

4.5.1 Using β as a scaling parameter

Defining the nondimensional radius in the same way that SWIRL does:

$$\widetilde{r} = \frac{r}{r_T}$$

where r_T is the outer radius of the annulus.

The hub-to-tip ratio is defined as:

$$\sigma = \frac{r_H}{r_T} = \widetilde{r}_H$$

where $\widetilde{r}_H$ is the inner radius of the annular duct. The hub-to-tip ratio can also be zero indicating the duct is hollow.

A useful and similar parameter is introduced, β, where $0 \leq \beta \leq 1$

$$\beta = \frac{r - r_H}{r_T - r_H}$$

Dividing By r_T

$$\beta = \frac{\frac{r}{r_T} - \frac{r_H}{r_T}}{\frac{r_T}{r_T} - \frac{r_H}{r_T}}$$

$$= \frac{\widetilde{r} - \widetilde{r}_H}{1 - \sigma}$$

Suppose a manufactured solution f_{MS} with boundaries $f_{MS}(r = \sigma)$ and $f_{MS}(\widetilde{r} = 1)$ is the specified analytical solution. The goal is to change the boundary conditions of the manufactured solution in such way that allows us to adequately check the boundary conditions imposed on SWIRL. Defining the manufactured solution, $f_{MS}(\widetilde{r})$, where $\sigma \le \widetilde{r} \le 1$ and there are desired values of f at the boundaries desired values are going to be denoted as f_{minBC} and f_{maxBC}. The desired changes in f are defined as:

$$\Delta f_{minBC} = f_{minBC} - f_{MS}(\widetilde{r} = \sigma)$$

$$\Delta f_{maxBC} = f_{maxBC} - f_{MS}(\widetilde{r} = 1)$$

We'd like to impose these changes smoothly on the manufactured solution function. To do this, the fairing functions, $A_{min}(\widetilde{r})$ and $A_{max}(\widetilde{r})$ where:

$$f_{BCsImposed}(\widetilde{r}) = f_{MS}(\widetilde{r}) + A_{min}(\widetilde{r})\Delta f_{minBC} + A_{max}(\widetilde{r})\Delta f_{maxBC}$$

Then, in order to set the condition at the appropriate boundary, the following conditions are set,

$$A_{min}(\widetilde{r} = \sigma) = 1$$

$$A_{min}(\widetilde{r} = 1) = 0$$

$$A_{max}(\widetilde{r} = 1) = 1$$

$$A_{max}(\widetilde{r} = \sigma) = 0$$

If $A_{min}(\widetilde{r})$ is defined as a function of $A_{max}(\widetilde{r})$ then only $A_{max}(\widetilde{r})$ needs to be defined, therefore

$$A_{min}(\widetilde{r}) = 1 - A_{max}(\widetilde{r})$$

It is also desirable to set the derivatives for the fairing function at the boundaries incase there are boundary conditions imposed on the derivatives of the fairing function.

$$\frac{\partial A_{max}}{\partial \widetilde{r}}\Big|_{\widetilde{r}=\sigma} = 0$$

$$\frac{\partial A_{max}}{\partial \widetilde{r}}\Big|_{\widetilde{r}=1} = 0$$

$$\frac{\partial A_{min}}{\partial \widetilde{r}}\Big|_{\widetilde{r}=\sigma} = 0$$

$$\frac{\partial A_{min}}{\partial \widetilde{r}}\Big|_{\widetilde{r}=1} = 0$$

4.5.2 Minimum Boundary Fairing Function

Looking at A_{min} first, the polynomial is:

$$A_{min}(\beta) = a + b\beta + c\beta^2 + d\beta^3$$

$$A_{min}(\widetilde{r}) = a + b\left(\frac{\widetilde{r} - \sigma}{1 - \sigma}\right) + c\left(\frac{\widetilde{r} - \sigma}{1 - \sigma}\right)^2 + d\left(\frac{\widetilde{r} - \sigma}{1 - \sigma}\right)^3$$

Taking the derivative,

$$A'_{min}(\widetilde{r}) = b\left(\frac{1}{1 - \sigma}\right) + 2c\left(\frac{1}{1 - \sigma}\right)\left(\frac{\widetilde{r} - \sigma}{1 - \sigma}\right) + 3d\left(\frac{1}{1 - \sigma}\right)\left(\frac{\widetilde{r} - \sigma}{1 - \sigma}\right)^2$$

$$A'_{min}(\beta) = \left(\frac{1}{1 - \sigma}\right)\left[b + 2c\beta + 3d\beta^2\right]$$

Now we will use the conditons mentioned earlier as constraints to this system of equations Using the possible values of $\widetilde{r}$,

$$A_{min}(\sigma) = a \qquad\qquad = 1$$

$$A_{min}(1) = a + b + c + d \qquad\qquad = 0$$

$$A'_{min}(\sigma) = b \qquad\qquad = 0$$

$$A'_{min}(1) = b + 2c + 3d \qquad\qquad = 0$$

which has the solution,

$$a = 1$$

$$b = 0$$

$$c = -3$$

$$d = 2$$

giving the polynomial as:

$$A_{min}(\widetilde{r}) = 1 - 3\left(\frac{\widetilde{r} - \sigma}{1 - \sigma}\right)^2 + 2\left(\frac{\widetilde{r} - \sigma}{1 - \sigma}\right)^3$$

4.5.3 Max boundary polynomial

Following the same procedure for A_{max} gives

$$A_{min}(\widetilde{r}) = 3\left(\frac{\widetilde{r} - \sigma}{1 - \sigma}\right)^2 - 2\left(\frac{\widetilde{r} - \sigma}{1 - \sigma}\right)^3$$

4.5.4 Corrected function

The corrected function is then,

$$f_{BCsImposed}(\widetilde{r}) = f_{MS}(\widetilde{r}) \qquad\qquad +A_{min}\Delta f_{minBC} + A_{max}\Delta f_{maxBC}$$

$$= f_{MS}(\widetilde{r}) \qquad + \left(1 - 3\left(\frac{\widetilde{r} - \sigma}{1 - \sigma}\right)^2 + 2\left(\frac{\widetilde{r} - \sigma}{1 - \sigma}\right)^3\right)[\Delta f_{minBC}]$$

$$+ \left(3\left(\frac{\widetilde{r} - \sigma}{1 - \sigma}\right)^2 - 2\left(\frac{\widetilde{r} - \sigma}{1 - \sigma}\right)^3\right)[\Delta f_{maxBC}]$$

$$f_{BCsImposed}(\beta) = f_{MS}(\beta) \qquad +\Delta f_{minBC} + \left(3\beta^2 - 2\beta^3\right)[\Delta f_{maxBC} - \Delta f_{minBC}]$$

Note that we're carrying the correction throughout the domain, as opposed to limiting the correction at a certain distance away from the boundary. The application of this correction ensures that there is no discontinuous derivatives inside the domain; as suggested in Roach's MMS guidelines (insert ref)

What is meant by "just because A_{min} and its first derivative go to zero doesn't mean that the second derivatives"

4.5.5 Symbolic Sanity Checks

We want to ensure that $f_{BCsImposed}$ has the desired boundary conditions, $f_{minBC/maxBC}$ instead of the original boundary values that come along for the ride in the manufactured solutions, $f_{MS}(\widetilde{r} = \sigma/1)$. In another iteration of this method, we will be changing the derivative values, so let's check the values of $\frac{\partial f_{BCsImposed}}{\partial \widetilde{r}}$ to make sure those aren't effected unintentionally.

Symbolic Sanity Check 1

The modified manufactured solution, $f_{BCsImposed}$ with the fairing functions A_{min} and A_{max} substituted in is,

$$f_{BCsImposed}(\widetilde{r}) = \left(3 \left(\frac{\widetilde{r} - \sigma}{1 - \sigma} \right)^2 - 2 \left(\frac{\widetilde{r} - \sigma}{1 - \sigma} \right)^3 \right) [\Delta f_{maxBC}].$$

Further simplification yields,

$$f_{BCsImposed}(\widetilde{r} = \sigma) = \left(f_{MS}(\widetilde{r} = \sigma) + \Delta f_{minBC} + \left(3 \left(\frac{\sigma - \sigma}{1 - \sigma} \right)^2 - 2 \left(\frac{\sigma - \sigma}{1 - \sigma} \right)^3 - \right) [\Delta f_{maxBC} - \Delta f_n$$

$$= f_{MS}(\widetilde{r} = \sigma) + \Delta f_{minBC}$$

$$= f_{MS}(\widetilde{r} = \sigma) + (f_{minBC} - f_{MS}(\widetilde{r} = \sigma))$$

$$= f_{minBC}$$

$$f_{BCsImposed}(\widetilde{r}=1) = \left(f_{MS}(\widetilde{r}=1) + \Delta f_{minBC} + \left(3\left(\frac{1-\sigma}{1-\sigma}\right)^2 - 2\left(\frac{1-\sigma}{1-\sigma}\right)^3 - \right)[\Delta f_{maxBC} - \Delta f_{m\cdots}$$

$$= f_{MS}(\widetilde{r}=1) + \Delta f_{maxBC}$$

$$= f_{MS}(\widetilde{r}=1) + (f_{maxBC} - f_{MS}(\widetilde{r}=1))$$

$$= f_{maxBC}$$

$$\frac{\partial}{\partial \widetilde{r}}\left(f_{BCsImposed}(\widetilde{r}) = \left(3\left(\frac{\widetilde{r}-\sigma}{1-\sigma}\right)^2 - 2\left(\frac{\widetilde{r}-\sigma}{1-\sigma}\right)^3\right)[\Delta f_{maxBC}]\right)$$

$$\frac{\partial f_{MS}}{\partial \widetilde{r}} + \left(\frac{6}{1-\sigma}\right)\left(\left(\frac{\widetilde{r}-\sigma}{1-\sigma}\right) - \left(\frac{r-\sigma}{1-\sigma}\right)^2\right)(\Delta f_{maxBC} - \Delta f_{minBC})$$

At $\widetilde{r}=\sigma$, the derivative is:

$$\frac{\partial f_{MS}}{\partial \widetilde{r}}\bigg|_{\sigma}$$
$$\frac{\partial f_{MS}}{\partial \widetilde{r}}\bigg|_{1}$$

4.5.6 Min boundary derivative polynomial

The polynomial is of the form:

$$B_{min}(\beta) = a + b\beta + c\beta^2 + d\beta^3$$

$$B_{min}(\widetilde{r}) = a + b\left(\frac{\widetilde{r}-\sigma}{1-\sigma}\right) + c\left(\frac{\widetilde{r}-\sigma}{1-\sigma}\right)^2 + d\left(\frac{\widetilde{r}-\sigma}{1-\sigma}\right)^3$$

Taking the derivative,

$$B'_{min}(\widetilde{r}) = b\left(\frac{1}{1-\sigma}\right) + 2c\left(\frac{1}{1-\sigma}\right)\left(\frac{\widetilde{r}-\sigma}{1-\sigma}\right) + 3d\left(\frac{1}{1-\sigma}\right)\left(\frac{\widetilde{r}-\sigma}{1-\sigma}\right)^2$$

$$B'_{min}(\beta) = \left(\frac{1}{1-\sigma}\right)\left[b + 2c\beta + 3d\beta^2\right]$$

Applying the four constraints gives:

$$a = 0$$

$$b = (1-\sigma)$$

$$a + b + c + d = 0$$

$$2 + 2c + 3d = 0$$

$$c + d = -b$$

$$2c + 3d = -b$$

$$c = -2b$$

$$d = b$$

and the min boundary derivative polynomial is:

$$B_{min}(\widetilde{r}) = b\left(\frac{\widetilde{r}-\sigma}{1-\sigma}\right) - 2b\left(\frac{\widetilde{r}-\sigma}{1-\sigma}\right)^2 + b\left(\frac{\widetilde{r}-\sigma}{1-\sigma}\right)^3$$

$$= (1-\sigma)\left(\left(\frac{\widetilde{r}-\sigma}{1-\sigma}\right) - 2\left(\frac{\widetilde{r}-\sigma}{1-\sigma}\right)^2 + \left(\frac{\widetilde{r}-\sigma}{1-\sigma}\right)^3\right)$$

4.5.7   Polynomial function, max boundary derivative

The polynomial is of the form:

The polynomial is of the form:

$$B_{max}\left(\beta\right) = a + b\beta + c\beta^2 + d\beta^3$$

$$B_{max}\left(\widetilde{r}\right) = a + b\left(\frac{\widetilde{r}-\sigma}{1-\sigma}\right) + c\left(\frac{\widetilde{r}-\sigma}{1-\sigma}\right)^2 + d\left(\frac{\widetilde{r}-\sigma}{1-\sigma}\right)^3$$

which has the derivative,

$$B'_{max}\left(\widetilde{r}\right) = b\left(\frac{1}{1-\sigma}\right) + 2c\left(\frac{1}{1-\sigma}\right)\left(\frac{\widetilde{r}-\sigma}{1-\sigma}\right) + 3d\left(\frac{1}{1-\sigma}\right)\left(\frac{\widetilde{r}-\sigma}{1-\sigma}\right)^2$$

$$B'_{max}\left(\beta\right) = \left(\frac{1}{1-\sigma}\right)\left[b + 2c\beta + 3d\beta^2\right]$$

Applying the four constraints gives:

$$a = 0$$

$$b = 0$$

$$a + b + c + d = 0$$

$$b + 2c + 3d = (1-\sigma)$$

working this out:

$$c + d = 0$$

$$2c + 3d = (1-\sigma)$$

gives

47

$$c = -\left(1 - \sigma\right) d \qquad\qquad = \left(1 - \sigma\right)$$

and the max boundary derivative polynomial is:

$$B_{max}\left(\widetilde{r}\right) = \left(1 - \sigma\right)\left(-\left(\frac{\widetilde{r} - \sigma}{1 - \sigma}\right)^2 + \left(\frac{\widetilde{r} - \sigma}{1 - \sigma}\right)^3\right)$$

4.5.8 Putting it together

The corrected function is then:

$$f_{BCsImposed}\left(\widetilde{r}\right) = f_{MS} + B_{min}\left(\widetilde{r}\right)\Delta f'_{minBC} + B_{max}\left(\widetilde{r}\right)\Delta f'_{maxBC}$$

$$= f_{MS} +$$

$$\left(1 - \sigma\right)\left(\left(\frac{\widetilde{r} - \sigma}{1 - \sigma}\right) - \left(\frac{\widetilde{r} - \sigma}{1 - \sigma}\right)^2\right)\Delta f'_{minBC} +$$

$$\left(1 - \sigma\right)\left(-\left(\frac{\widetilde{r} - \sigma}{1 - \sigma}\right)^2 + \left(\frac{\widetilde{r} - \sigma}{1 - \sigma}\right)^3\right)\left(\Delta f'_{minBC} + \Delta f'_{maxBC}\right)$$

Chapter 5

Results and Discusssion

5.1 Verification

5.1.1 Introduction

The frequency domain, linearized Euler equation computer code, SWIRL, was verified through the Methods of Manufactured and Exact solutions. However, while the Method of Exact Solutions (MES) can be used to validate the ouput of SWIRL, there is a limitation on the number of exact solutions available based on the flow and domain. Any changes in a flow configuration (uniform axial flow vs. sheared axial flow, without any tangential component) require a recalculation of the analytical solution. Code validation through MES is for the case of uniform flow in a cylindrical duct since the exact solution requires implementing special Bessel functions . In addition, the exact solution needs to be recomputed for changes in radii and the use of acoustic liner (i.e., boundary conditions). For this reason, the more comprehensive MMS was first used for code verification to test each variable in the governing equations and gain measurable acceptance criteria without relying on expert judgment.

MMS was implemented on a component level since SWIRL consists of two main numerical approximations for flows with axial and tangential components. First, the numerical integration technique required for radial change in sound speed was

verified. Then, the four governing equations that make up the matrices required for the eigenvalue problem were tested. Note that the output of the eigenvalue problem was tested with MMS by recomputing the expression $[A]x - \lambda[B]x = 0$ with a given eigenvalue/vector pair. The calculated $L_{2,norm}$ (i.e. error and the order of accuracy for both numerical methods are discussed below. The MMS was then used to compare against validation cases in literature to outline the methodolody for test cases for which there is no solution.

5.1.2   MMS, Solutions

(insert table instead of equations, check comments in tex file for parameters)

$$\bar{A} \mid \text{test}$$

Table 5.1: Manufactured solution table for the first MMS test case

Figure 5-17 shows the manufactured solution for the mean flow profile. The tangent summation method was used to generate the axial Mach number, the speed of sound, and the perturbation variables. The tangential Mach number was numerically approximated by using the composite trapezoidal rule. The manufactured mean flow profile is unique because it has been generated solely to verify SWIRL and does not have physical significance. The "kinks" in the solution will allow a significant magnitude for the derivatives of these solutions. The results from the numerical integration are presented in Figure 5-2. Although the slope of the line appears linear, the TSM was still used to generate the MS for the speed of sound. Denser grids were used to compute the error by iterating as grid spacing approaches zero. The difference between the expected speed of sound to the actual speed of sound is shown in Figure 5-3 as a function of radius. Note that the error reaches machine precision early in the iterations and approaches zero as more grid points are used.

The error will decrease at a known rate depending on the type of numerical inte-
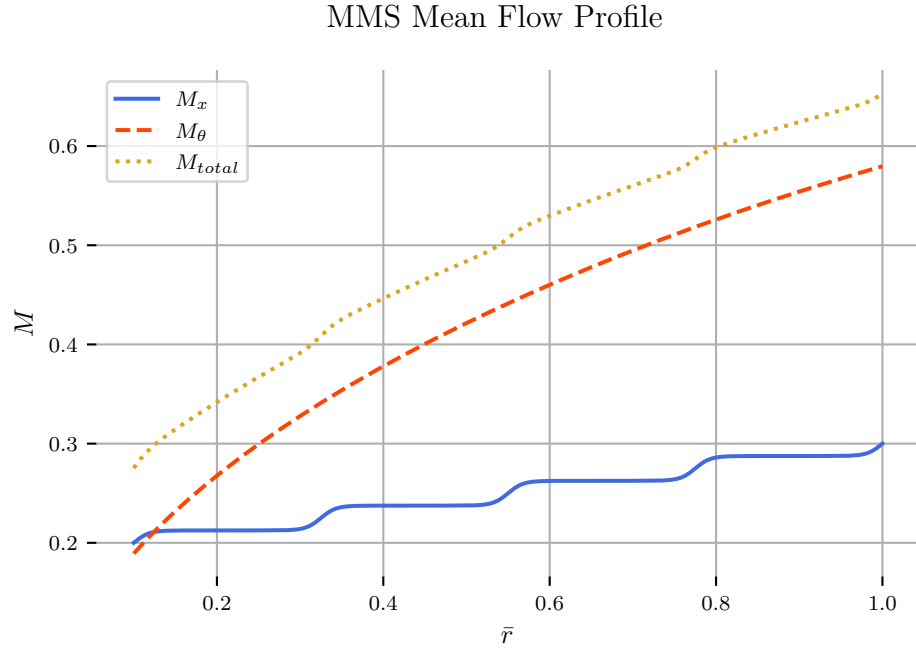
MMS Mean Flow Profile

Figure 5-1: The manufactured mean flow test case using a summation of Tangents for A and M_x
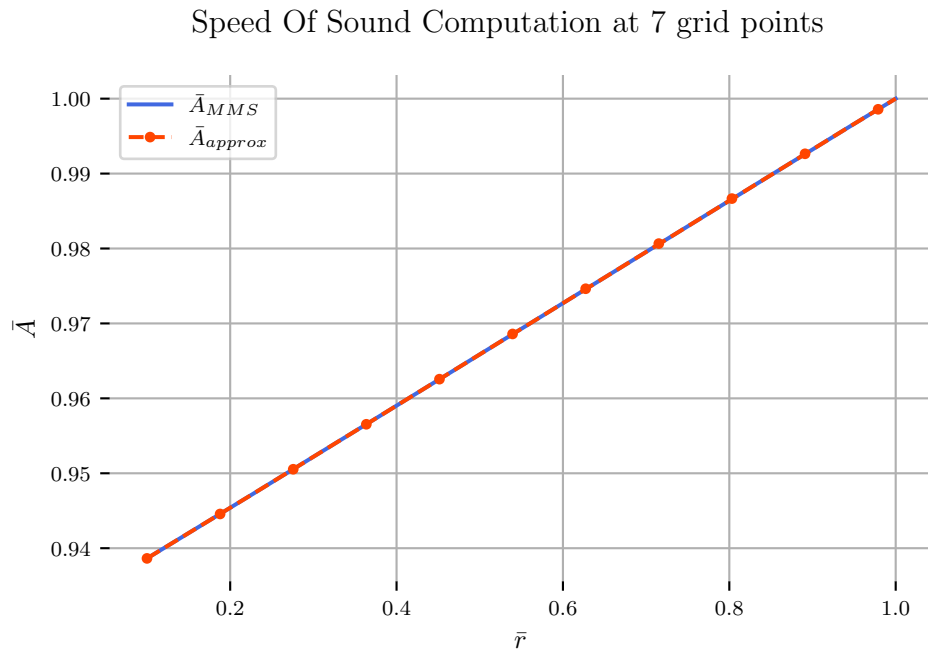

Speed Of Sound Computation at 7 grid points

Figure 5-2: A comparison of the speed of sound, expected vs actual at the lowest grid to show similarities in solution
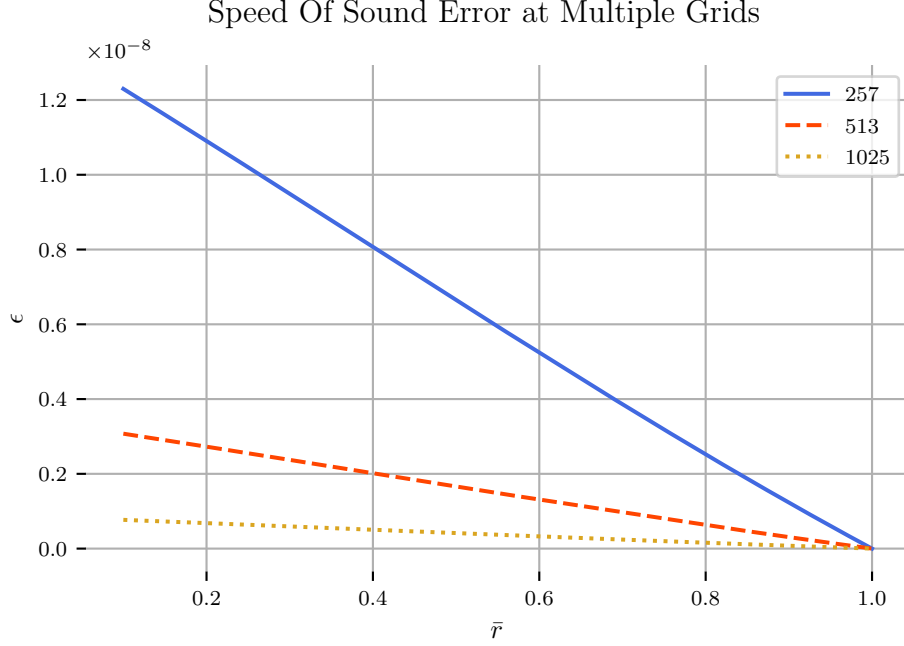
Figure 5-3: A comparison of the speed of sound error at three grid

gration scheme. Since the composite trapezoidal rule has an order of accuracy of 2, it is expected that the approximated order of accuracy will approach two as the error approaches zero. This behavior is shown in Figure 5-4, where the approximated line is the L2 norm of the speed of sound error. The slope (i.e., the asymptotic rate of convergence) approached two for numerical integration as the grid spacing decreases (See Figure 5.1.2) .

The manufactured solution used for the fluctuation variables in the MMS test case is shown in Table 5.1. Recall that the variable B varies the slope around the tangent function at each inflection point; the maximum amplitude of each tangent function was A = 0.1 and was equally spaced between $\tilde{r}_{min}$-$\tilde{r}_{max}$. The boundary conditions for the perturbation variable $\tilde{v}_r$ were set using the fairing functions to impose boundary conditions. Fairing functions also set the derivative of the perturbation variable $\tilde{p}$. Only $\tilde{p}$ is affected by acoustic liners since it alters the rate of change of pressure at the walls, not the pressure or velocity. The subscripts $BCsImposed, diffBCsImposed$
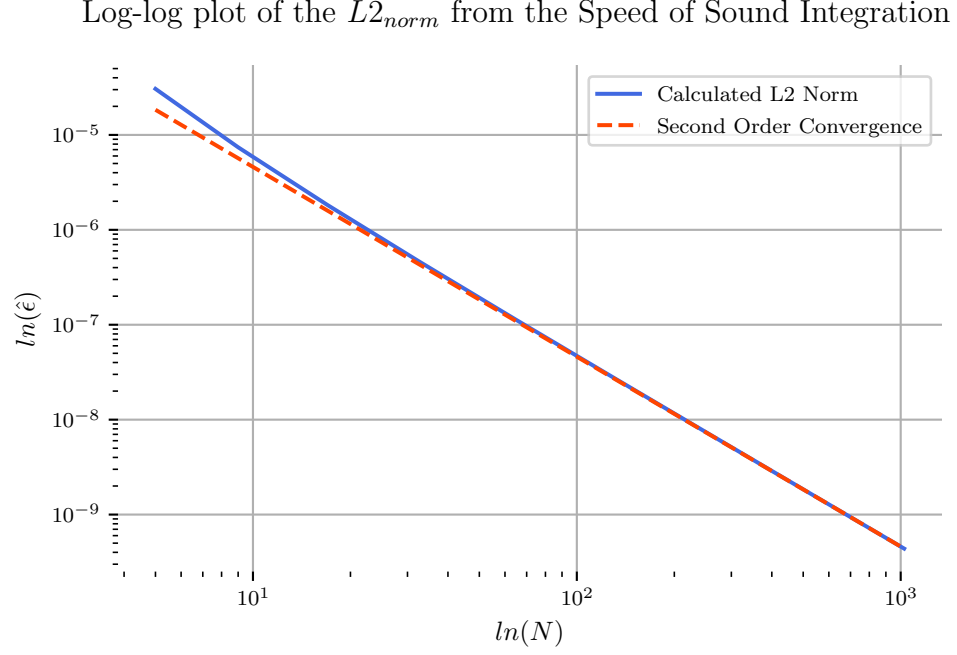
Figure 5-4: L2 Norm comparison for the speed of sound integration for the compound trapezoidal rule

state where the perturbation or its derivative value was altered to be uniform between the code and the manufactured solution.

A second and fourth-order central differencing scheme for the LEE is used for the approximated radial derivatives and compared to the source terms generated for the MMS in Figure 5-10. The L2 norm and the asymptotic rate of convergence is shown for the two diffferencing schemes in 5-15 .

The grid points were doubled, starting at 7 grid points and ending after 9 iterations with 1025 grid points. Both schemes do not have the order of accuracy down to machine precision but get down to 10^-6 For the LEE, a second and fourth order central differencing scheme is used for the approximated radial derivatives and then compared to the source terms generated for the MMS in Figure 5-10.
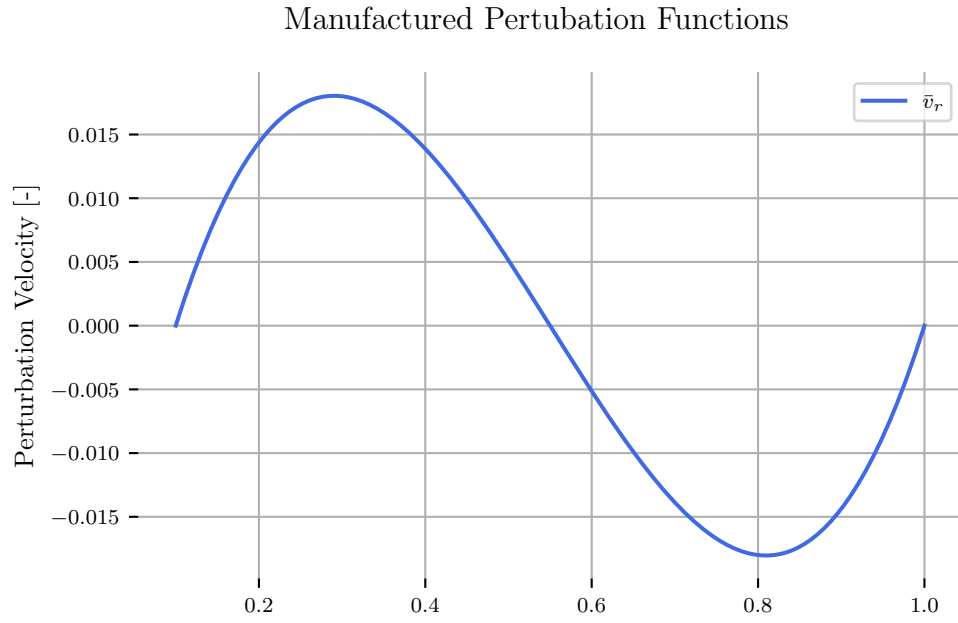
Manufactured Pertubation Functions

Figure 5-5: The manufactured perturbation functions $,v_r$
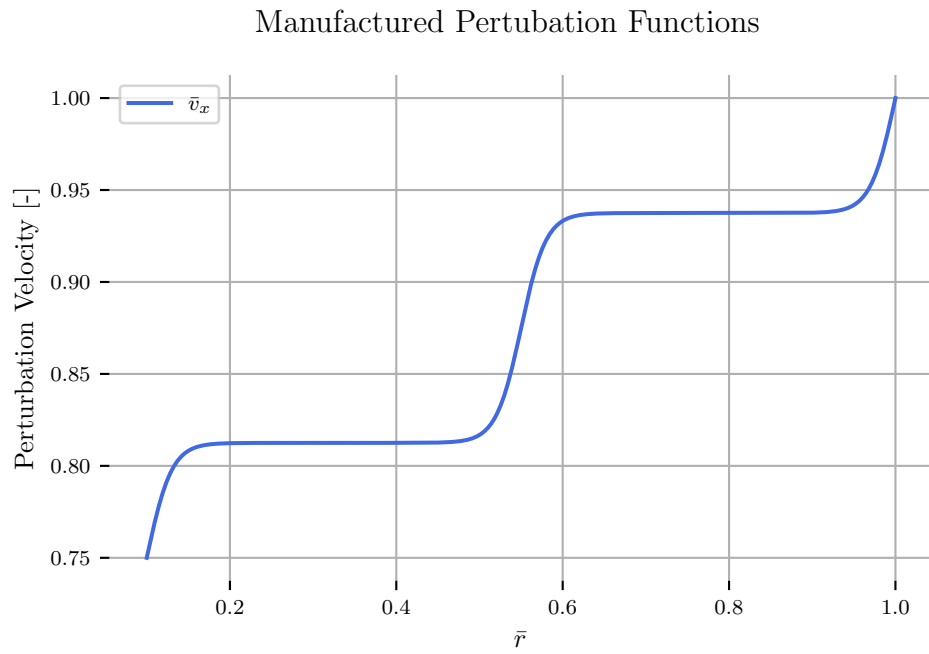
Manufactured Pertubation Functions

Figure 5-6: The manufactured perturbation functions $,v_x$

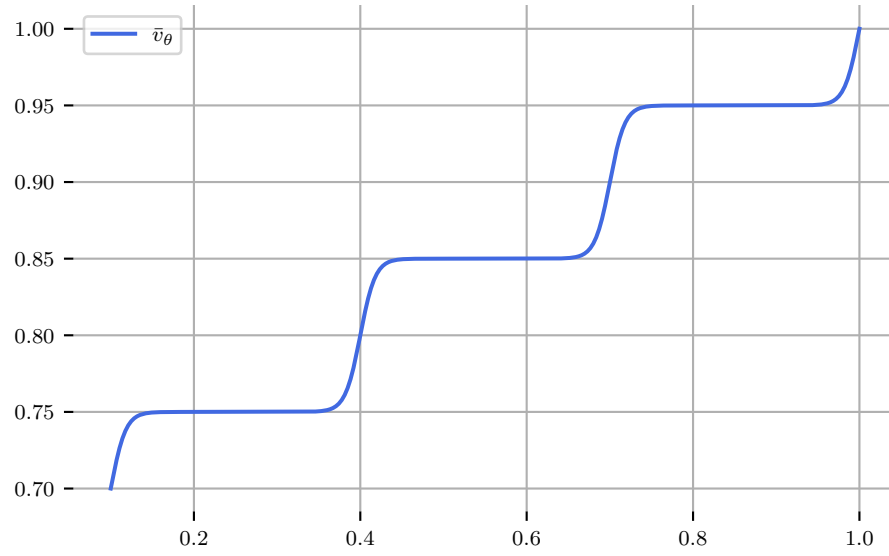Manufactured Pertubation Functions

Figure 5-7: The manufactured perturbation functions ,v_θ

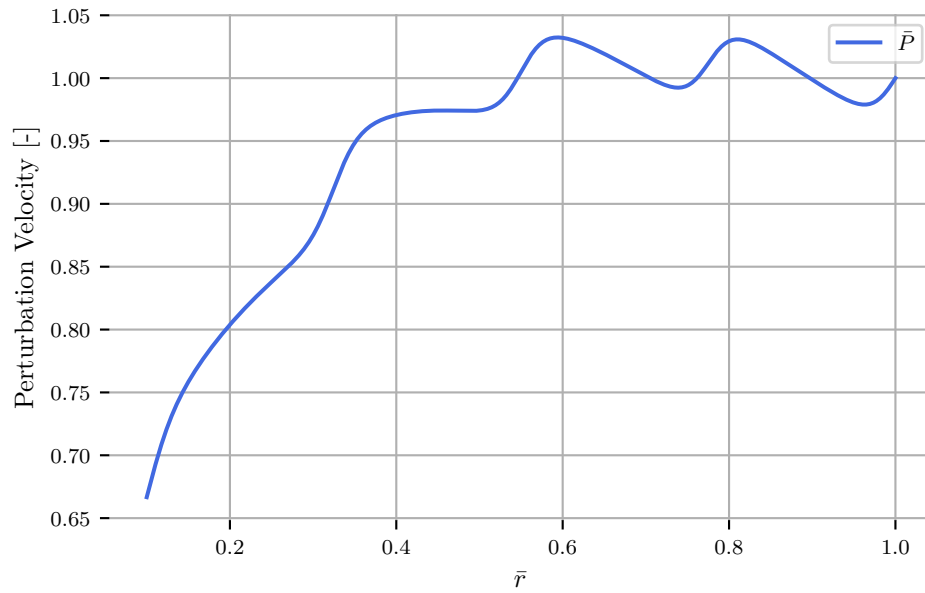Manufactured Pertubation Functions

Figure 5-8: The manufactured perturbation functions ,P

5.1.2.1 Test Case 1

A comparison was conducted for a hollow cylinder undergoing uniform flow with acoustic liners along the outer duct perimeter. The azimuthal mode number, reduced
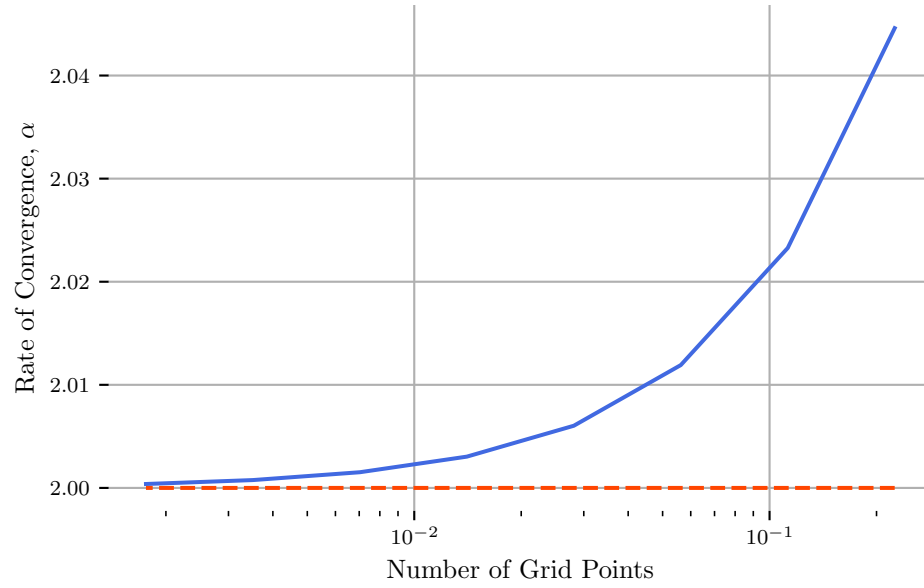
Figure 5-9: Speed of Sound Rate Of Convergence

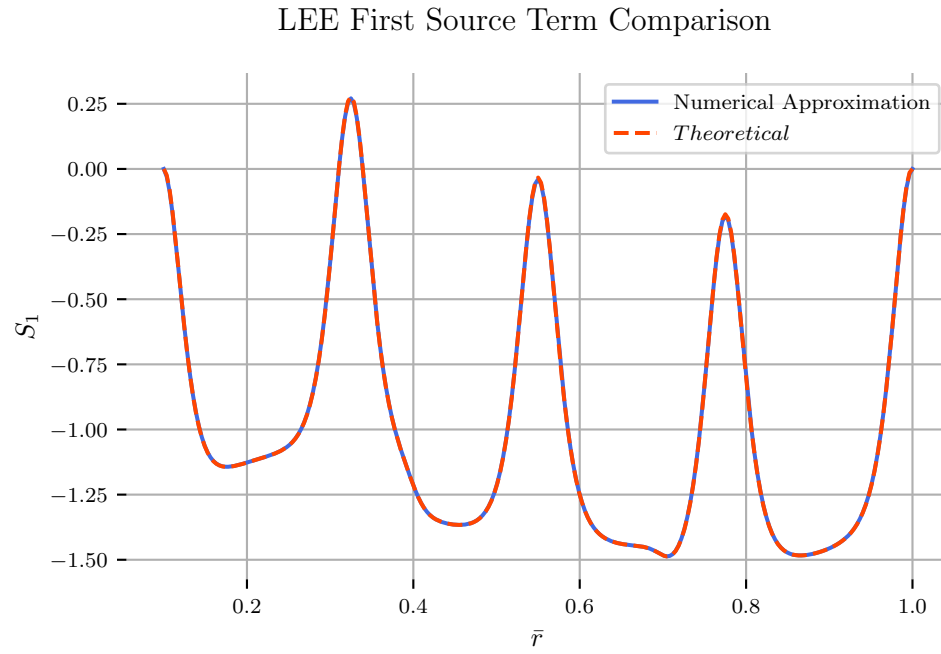LEE First Source Term Comparison

Figure 5-10: LEE Source Terms

frequency, mach number and duct liner admittance is reported below,

$$m = 2$$

$$k = \frac{\omega r_T}{A_T} = -1$$

$$M_x = 0.5$$

$$\eta_T = 0.72 + 0.42i$$

Source Term 1 Error at Multiple Grids
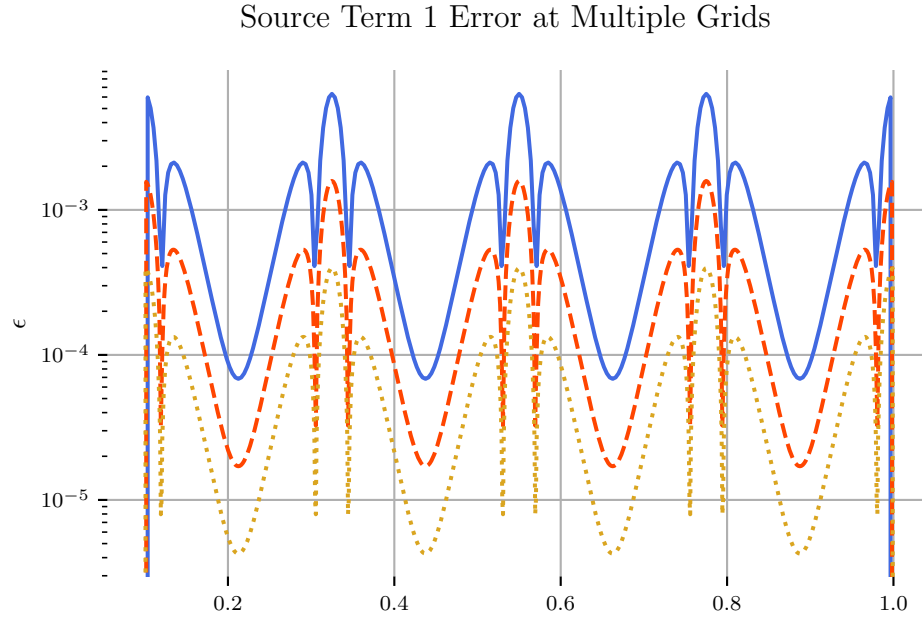

Figure 5-11: LEE Source Term Error
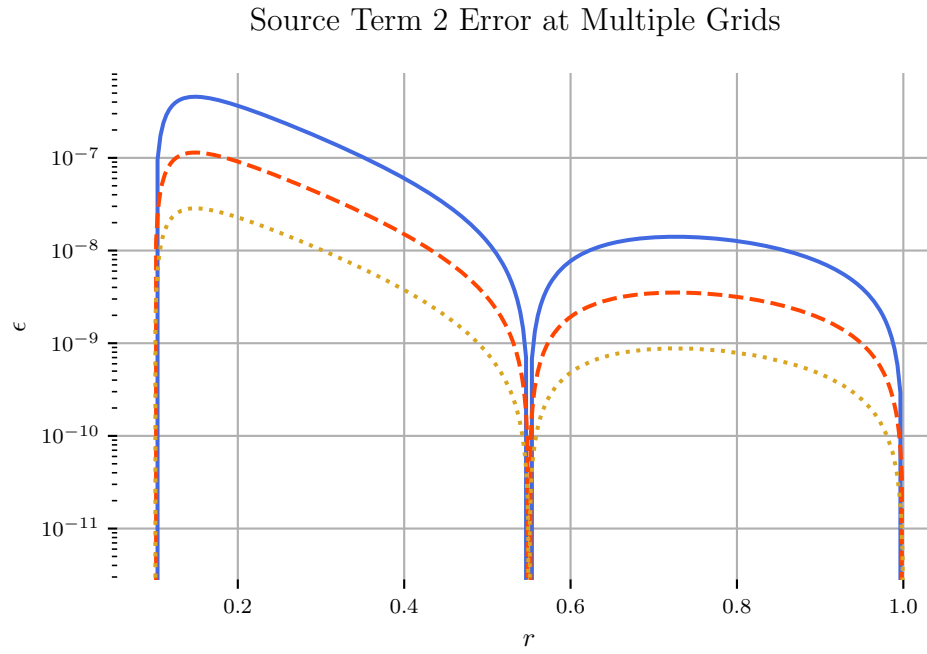
Source Term 2 Error at Multiple Grids

Figure 5-12: LEE Source Term Error

The results shown in 5.2 are in moderately good agreement. The results were obtained by visually comparing the output for 32 grid points. Note that the indicies
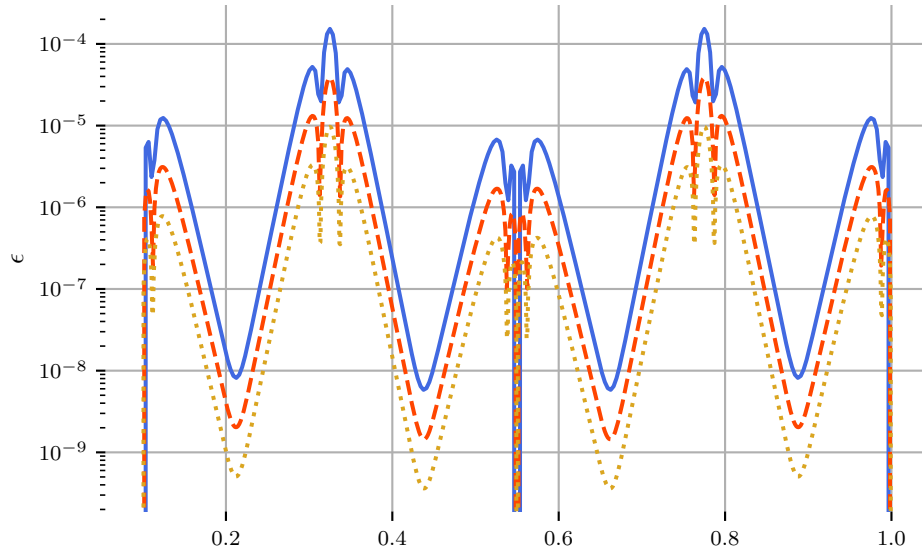
Source Term 3 Error at Multiple Grids

Figure 5-13: LEE Source Term Error

Source Term 4 Error at Multiple Grids
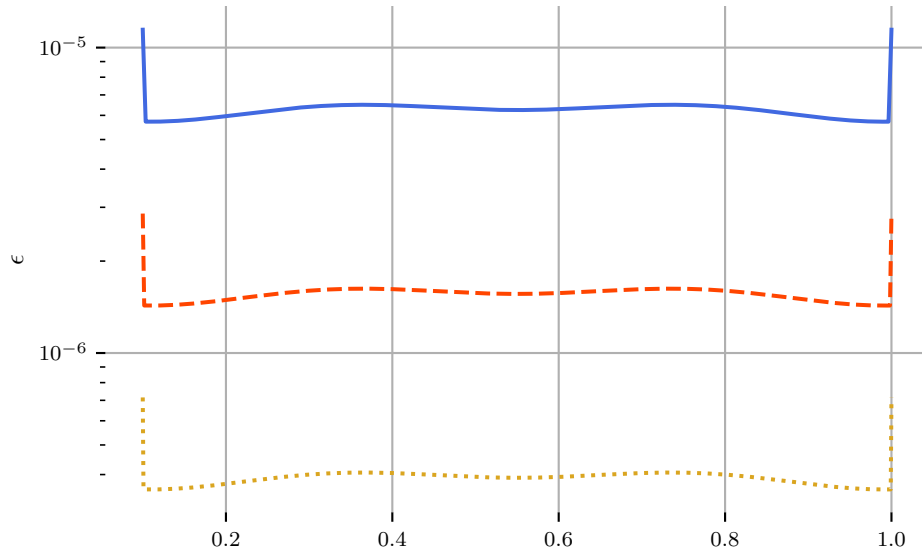
Figure 5-14: LEE Source Term Error

for the SWIRL deliverable are different that the ones obtained for the most recent
version of the code. While the convective axial wavenumbers show agreement to

L2 of LEE Matrix

Rate of Convergence of LEE Matrix
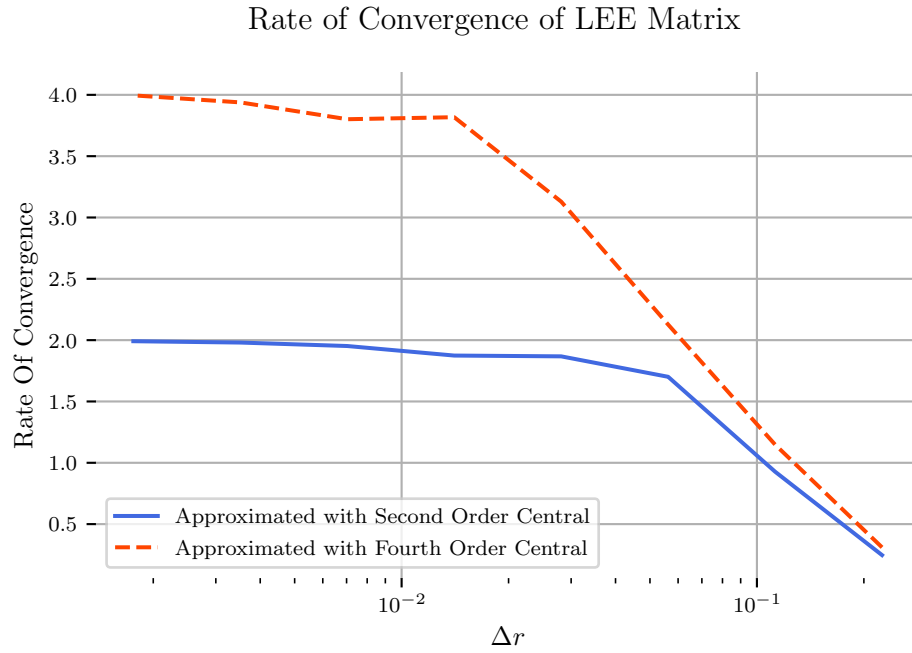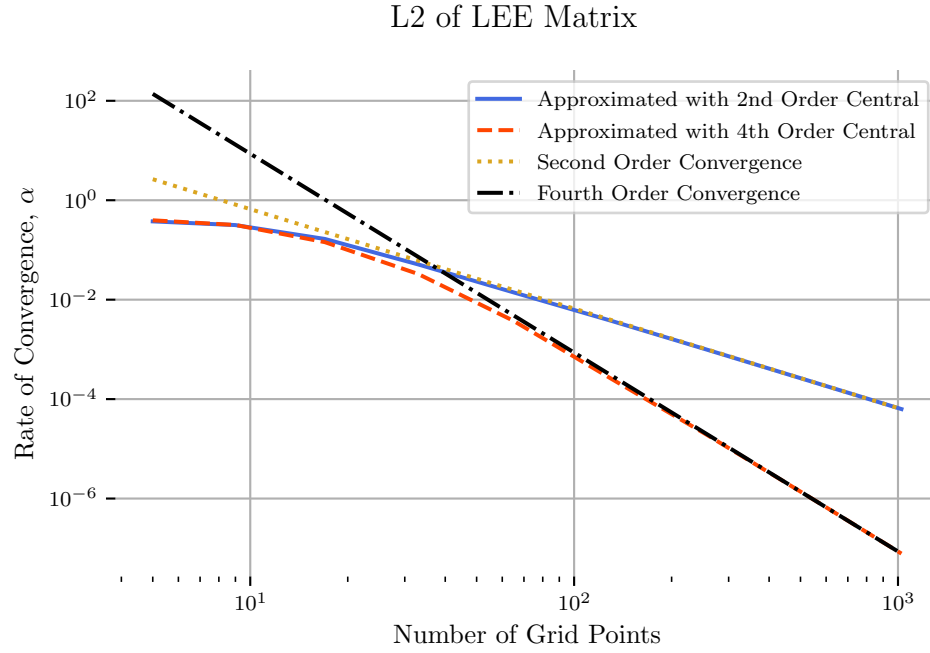
machine precision, this is not particularly insightful given that there are an infinite number of possible solutions that could satisfy the eigenvalue problem. The results that are of concern are propagating modes that are not convecting with the mean flow. The scatter plot of the axial wavenumbers show some sporadic behaviour around the

Axial Wavenumer γ
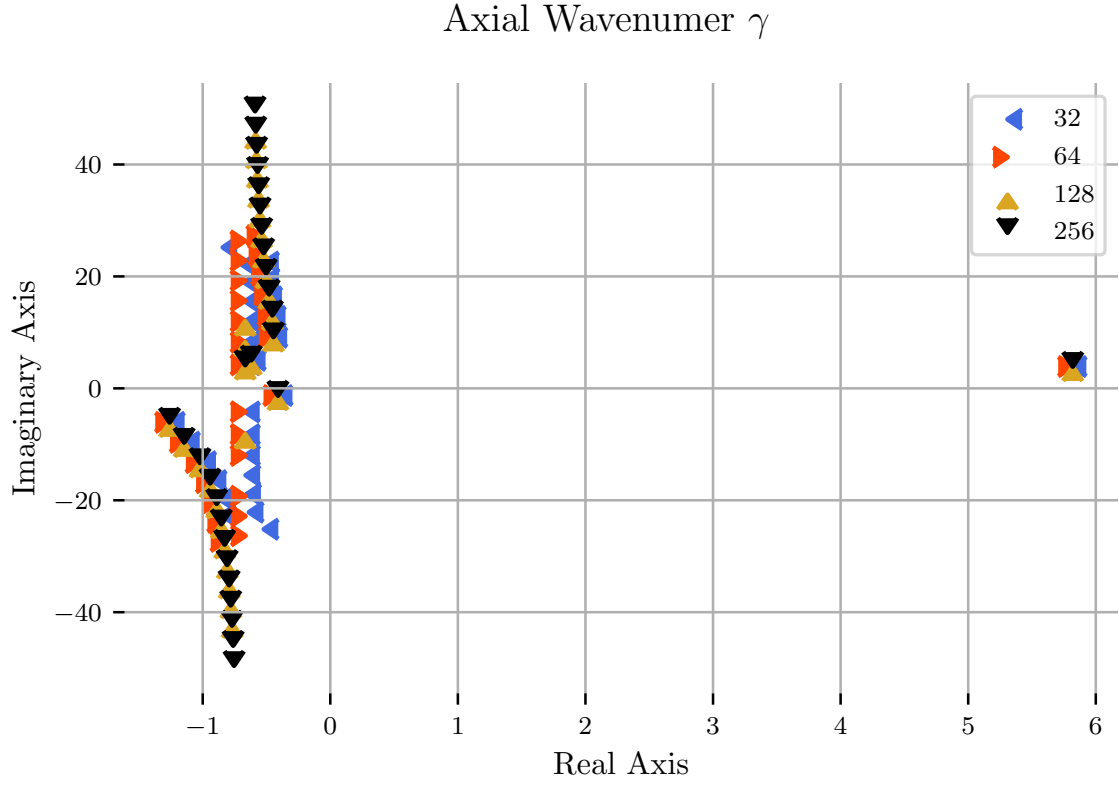
imaginary axis. The results from the MMS along with this plot indicate that more grid points are going to be needed if a finite difference technique is to be used.

The first 10 propagating and decaying modes are plotted in 5.1.2.1-5.1.2.1.
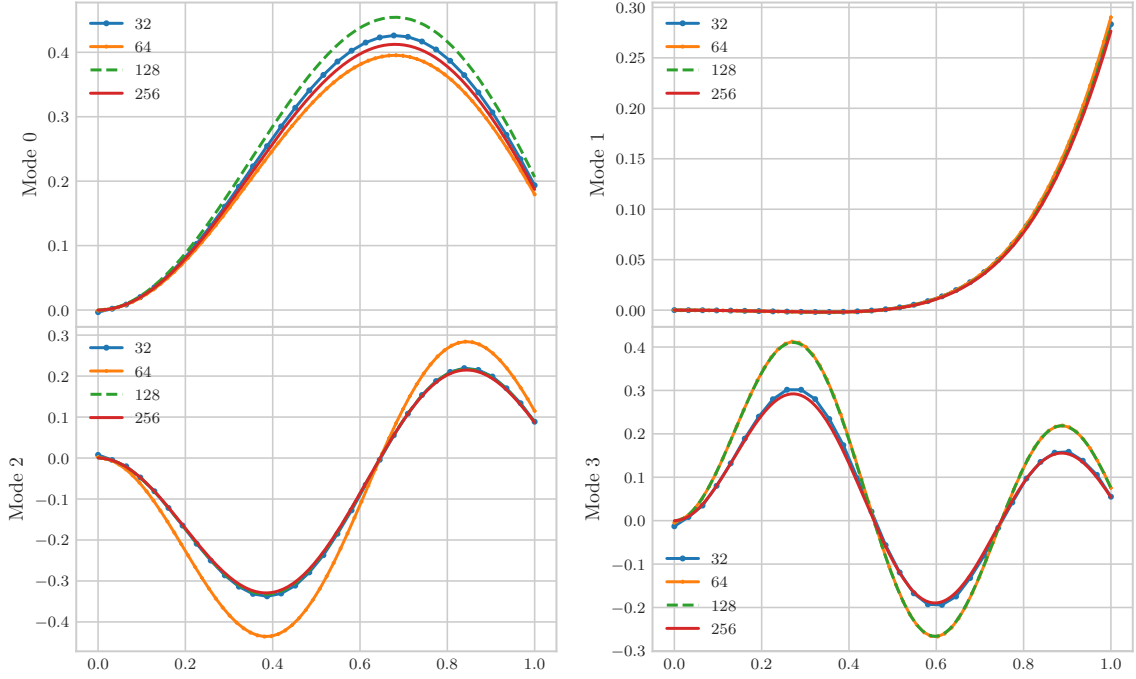
5.2 Sheared Flow Results

The axial Mach number for these sheared flow validation cases were taken to be,

$$M_x = M_0 \left(1 - \bar{r}_{Shankar}\right)^{\frac{1}{7}} \tag{5.1}$$

$$\tag{5.2}$$

where $\bar{r}_{Shankar} = \frac{r_{min}}{r_{max} - r_{min}} = \frac{r_{min}}{b}$

Since the radius is non-dimensionalized differently in **??**, the velocity profile defined as a function of $\bar{r}_{Shankar}$.

Propagating Modes [Imaginary]

5.3   Sheared Flow Results

The axial Mach number for these sheared flow validation cases were taken to be,

$$M_x = M_0 \left(1 - \bar{r}_{Shankar}\right)^{\frac{1}{7}} \tag{5.3}$$

$$\tag{5.4}$$

where $\bar{r}_{Shankar} = \frac{r_{min}}{r_{max} - r_{min}} = \frac{r_{min}}{b}$

Since the radius is non-dimensionalized differently in **??**, the velocity profile defined as a function of $\bar{r}_{Shankar}$.
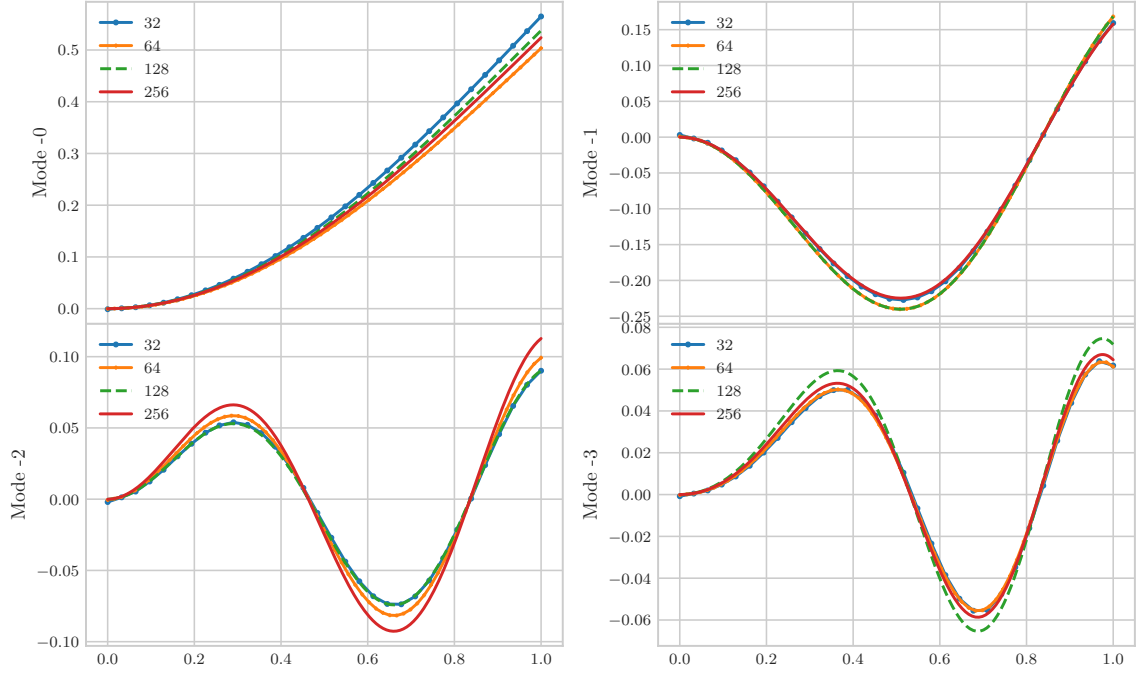
5.4 Sheared Flow Results

The axial Mach number for these sheared flow validation cases were taken to be,

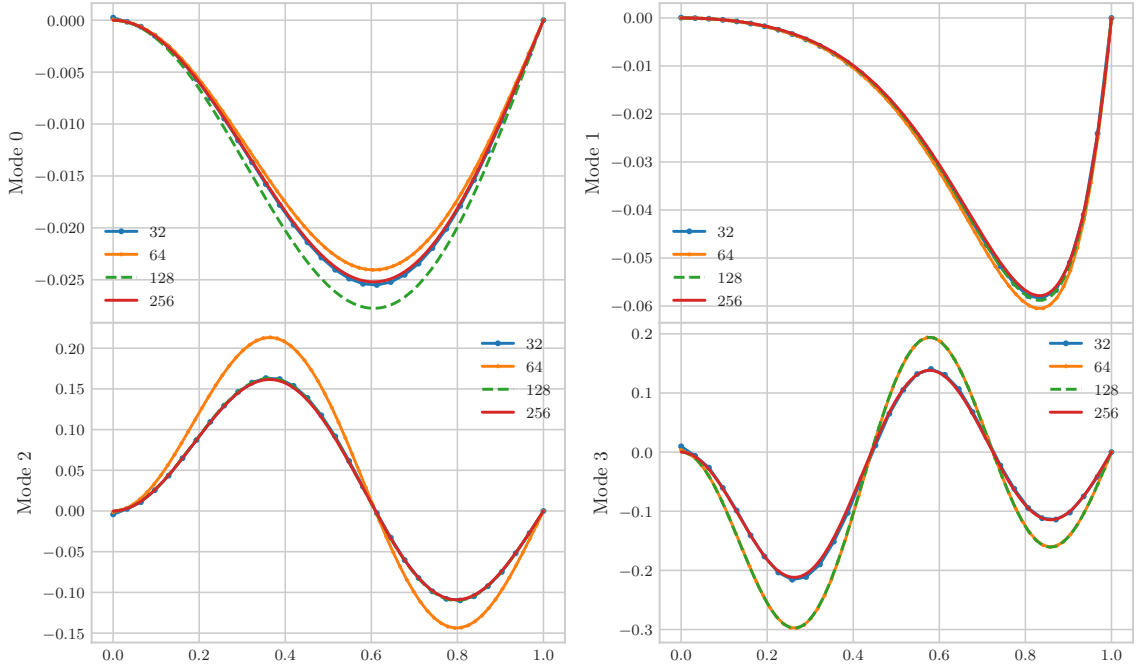$$M_x = M_0 \left(1 - \bar{r}_{Shankar}\right)^{\frac{1}{7}} \tag{5.5}$$

$$\tag{5.6}$$

where $\bar{r}_{Shankar} = \frac{r_{min}}{r_{max} - r_{min}} = \frac{r_{min}}{b}$

Since the radius is non-dimensionalized differently in **??**, the velocity profile defined as a function of $\bar{r}_{Shankar}$.
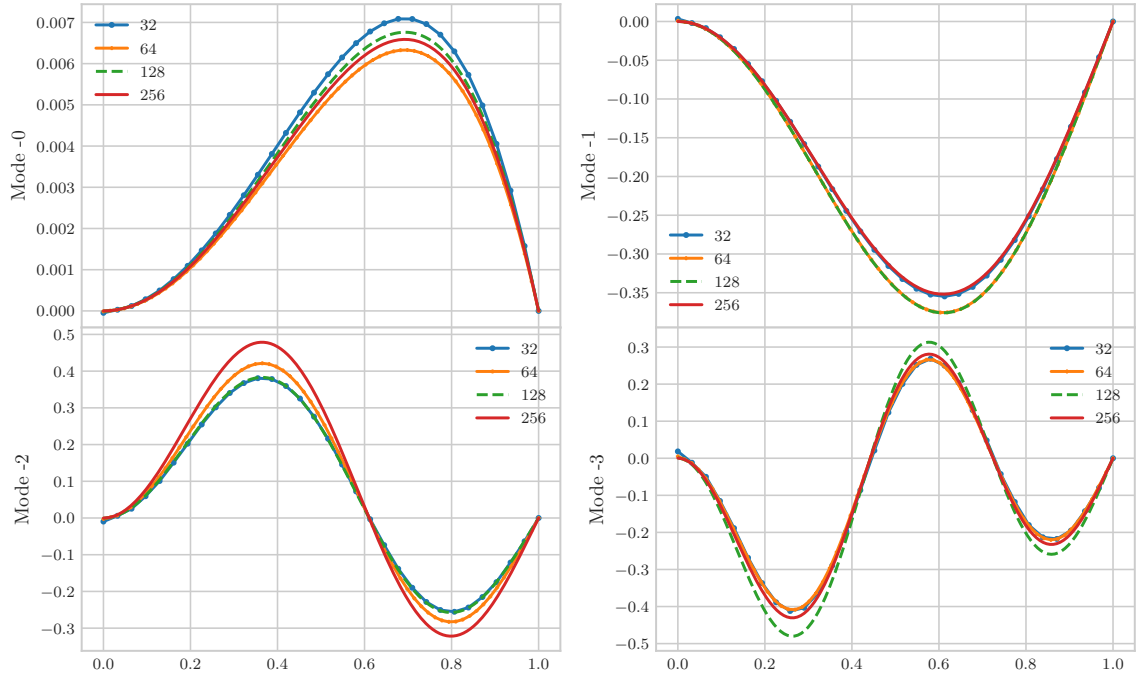
Kousen T4.4 Mean Flow Profile
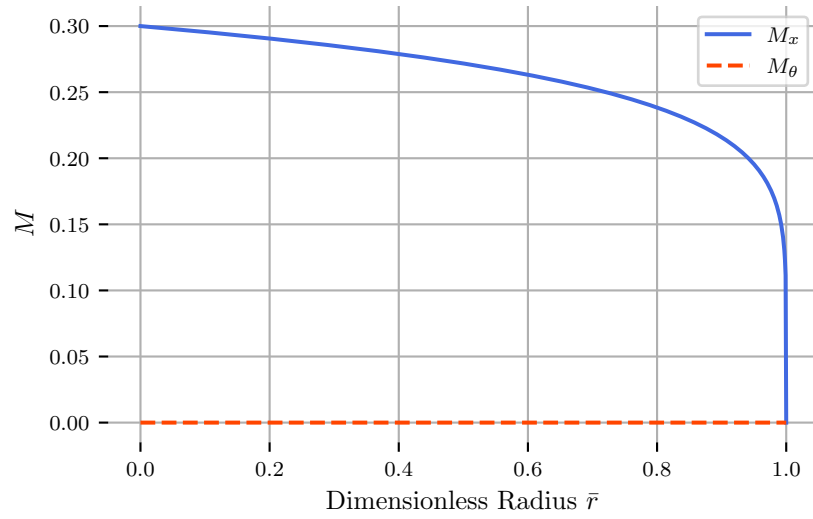
Figure 5-15: Mean mach number profile for the uniform flow in a lined cylinder

$\gamma_n^\pm$	Kousen Ref. [15]	Kousen report	current
γ_0^+	$0.620 - 5.014i$	$0.6195 - 5.0139i$	0.620755853112 - 5.00592416941i
γ_1^+	$-5.820 - 3.897i$	$-5.8195 - 3.8968i$	-0.581267772517 - 3.90050864568i
γ_2^+	$0.445 - 9.187i$	$0.4453 - 9.1868i$	0.451569491142 - 9.12191317214i
γ_3^+	$0.453 - 13.062i$	$0.4539 - 13.062i$	0.464247902898 - 12.8487472519i
γ_4^+	$0.480 - 16.822i$	$0.4795 - 16.822i$	0.492340380223 - 16.3292825150i
γ_0^-	$0.410 + 1.290i$	$0.4101 + 1.2904i$	0.409973310292 + 1.29020083859i
γ_1^-	$1.259 + 6.085i$	$1.2595 + 6.0852i$	1.25530612217 + 6.07214375548i
γ_2^-	$1.146 + 9.668i$	$1.1457 + 9.6679i$	1.13696444935 + 9.59622801724i
γ_3^-	$1.022 + 13.315i$	$1.0218 + 13.315i$	1.00950576515 + 13.0957277529i
γ_4^-	$0.943 + 16.977i$	$0.9425 + 16.977i$	0.928059983039 + 16.4791343118i

Table 5.2: Cylindical duct with Uniform flow, $M_x = 0.5$ and Acoustic Liner $\eta_T = 0.72 + 0.42i$, $k = -1$, and $m = 2$

Axial Wavenumer γ

Kousen T4.5 Mean Flow Profile
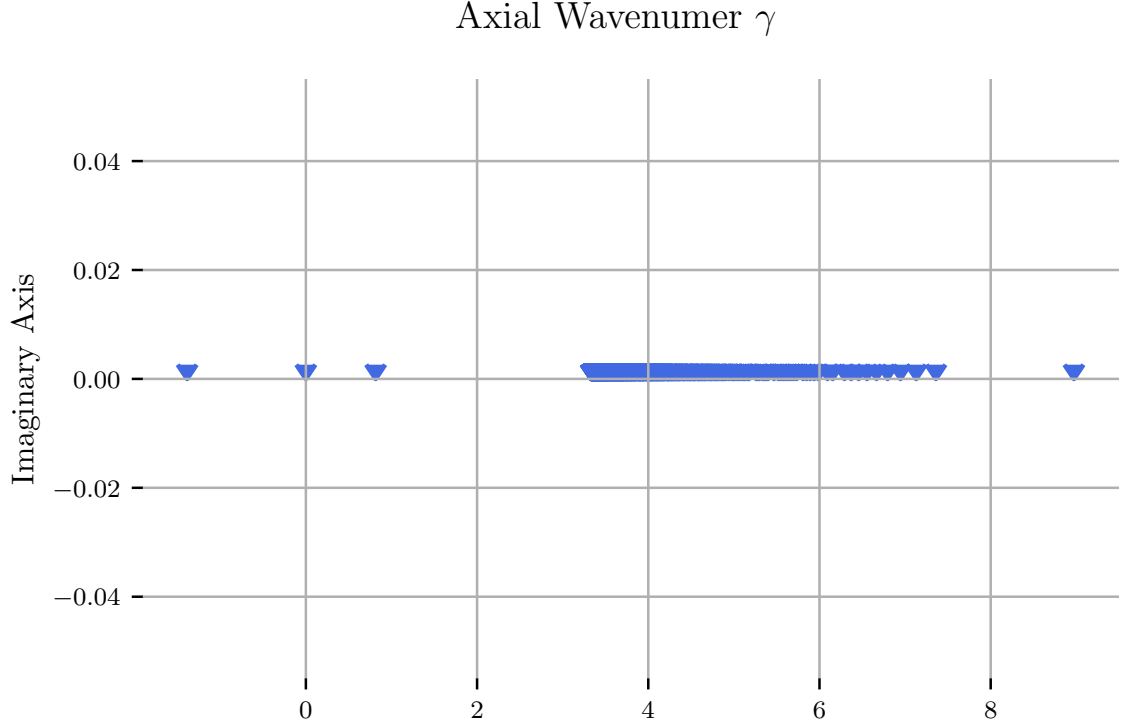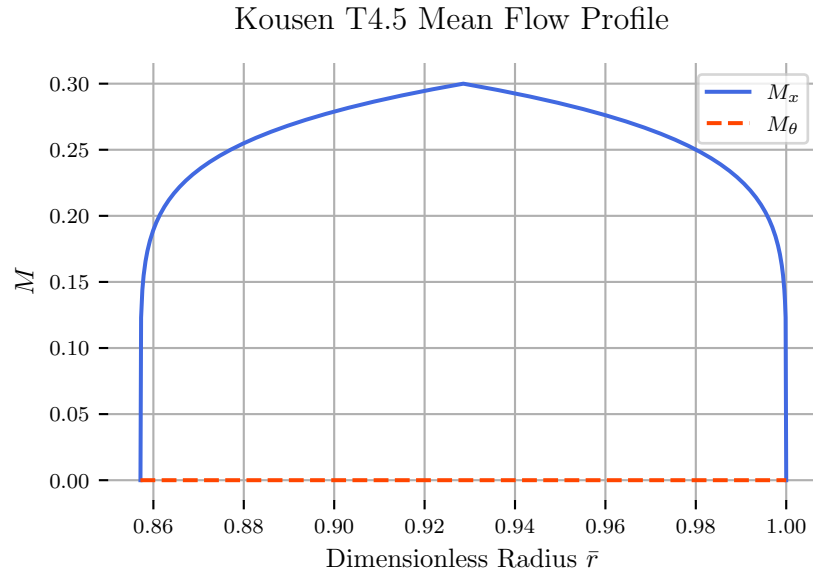
Figure 5-16: Mean mach number profile for the uniform flow in a lined cylin-
der

Axial Wavenumer γ
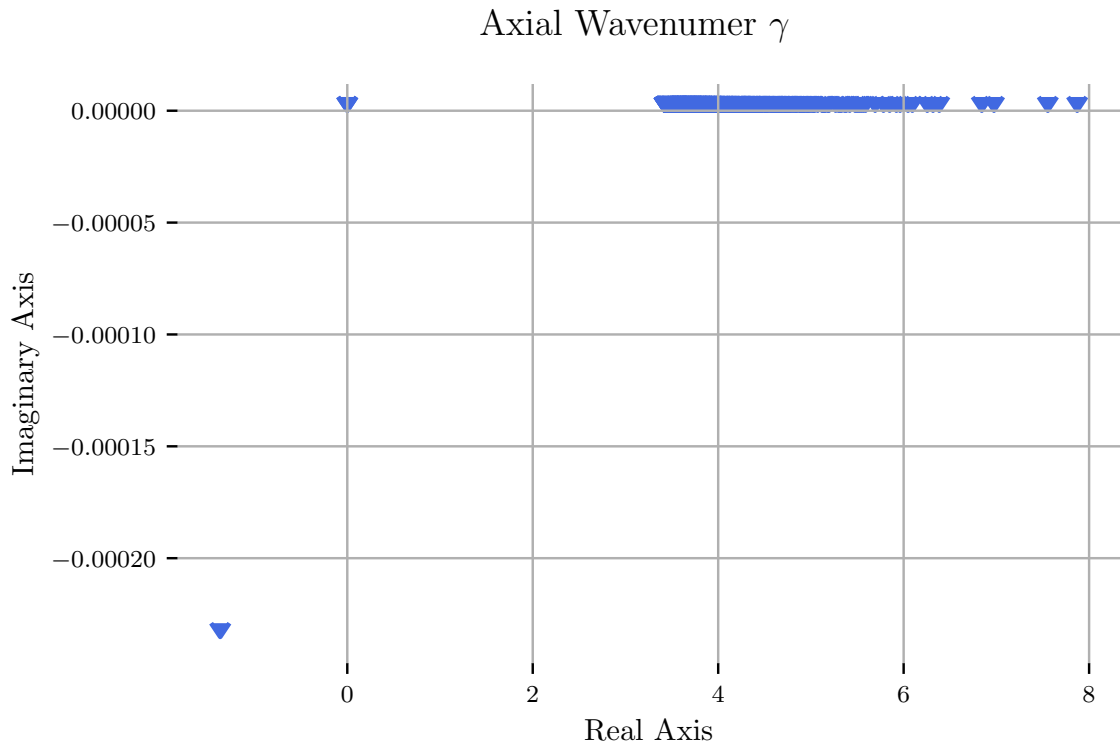
5.5 Validation

5.5.1 Comparison to Kousen

There are four key test cases to run and make sure that the data is post processed

for.
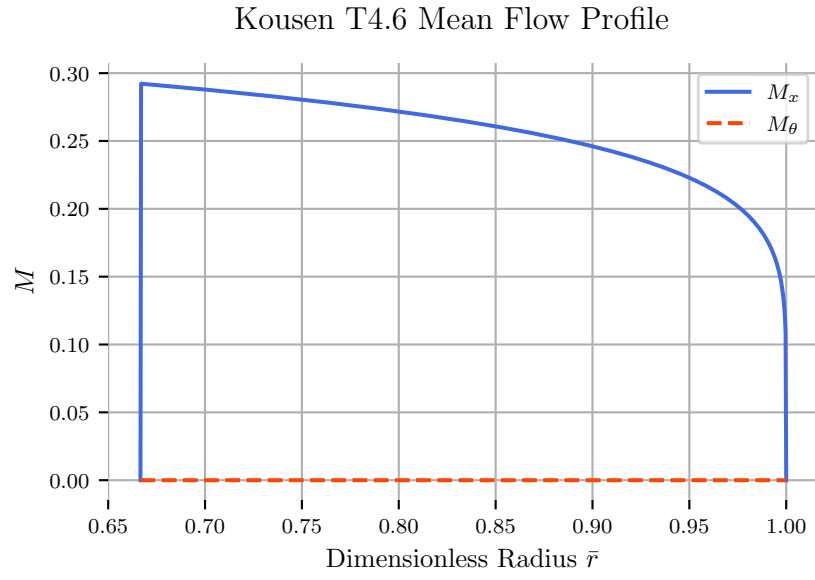
Figure 5-17: Mean mach number profile for the uniform flow in a lined cylinder
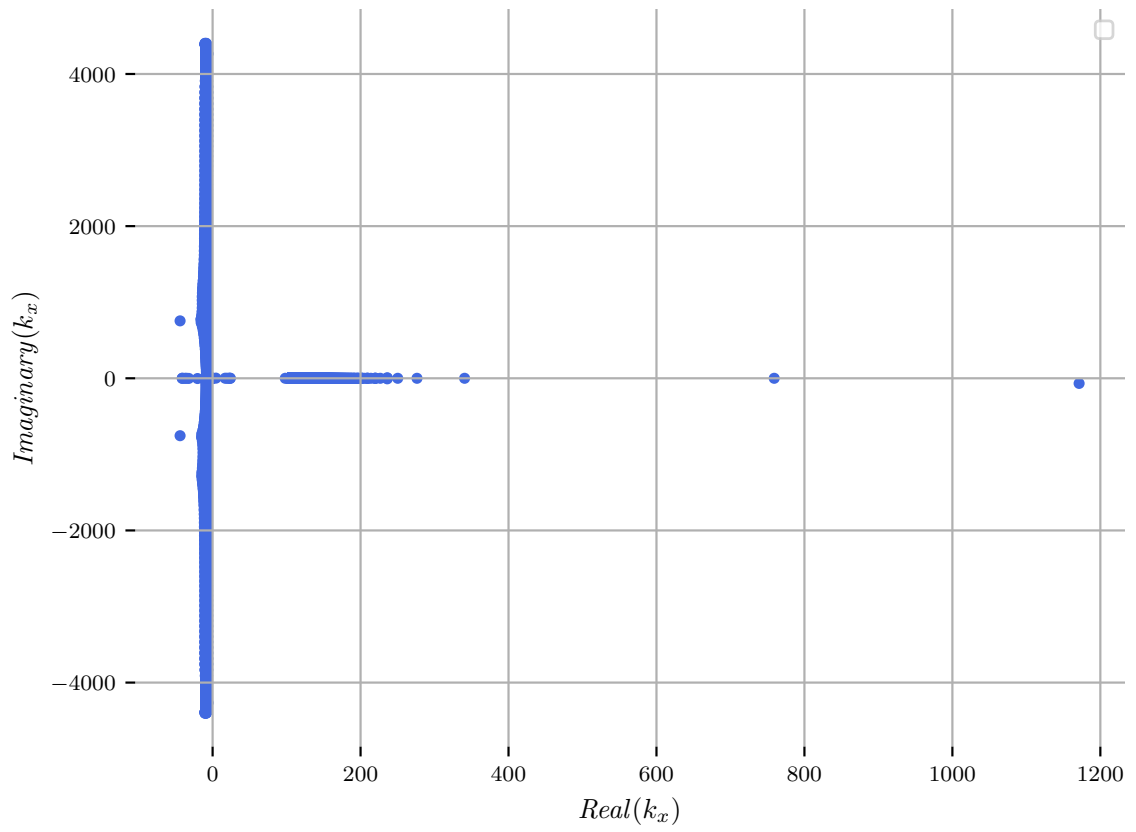
5.5.1.1 Test Case 1 ,Cylinder, Uniform Flow with Liner

5.5.1.2 Test Case 2

Cylinder, Shear Flow without Liner (Table 4.4)

$$m = 0$$

$$kb = \left(\frac{\omega r_T}{A_T}\right) b = 20$$

$$b = r_{max} - r_{min}$$

$$\tilde{r} = \frac{r}{b}$$

$$M_x = 0.3(1 - \tilde{r})^{\frac{1}{7}}$$

$$\eta_T = 0$$

5.5.1.3 Test Case 3

Annulus, Shear Flow without Liner (Table 4.5)

$$m = 0$$

$$kb = \left(\frac{\omega r_T}{A_T}\right) b = 10$$

$$b = r_{max} - r_{min} = \frac{1}{7}$$

$$k = 70$$

$$\tilde{r} = \frac{r}{b} = 6.0$$

$$M_x = 0.3 \left(1 - 2\left|\frac{r_{max} - r}{b} + 0.5\right|\right)^{\frac{1}{7}}$$

$$\eta_T = 0$$

5.5.1.4 Test Case 4

Annulus, Shear Flow with Liner (Table 4.6)

$$m = 0$$

$$kb = \left(\frac{\omega r_T}{A_T} \right) b = 10$$

$$b = r_{max} - r_{min} = \frac{1}{3}$$

$$k = 30$$

$$\tilde{r} = \frac{r}{b} = 2.0$$

$$M_x = 0.3 \left(1 - 2 \left| \frac{r_{max} - r}{b} + 0.5 \right| \right)^{\frac{1}{7}}$$

$$\eta_T = 0.3 + 0.1i$$

References

[1] Michael JT Smith. Aircraft noise. *Cambridge Aerospace Series*, 1989.

[2] Department Of Transportation Federal Aviation Administration. Aviation environmental and energy policy statement - july 2012, 2012.

[3] *INDEPENDENT EXPERT INTEGRATED TECHNOLOGY GOALS ASSESSMENT AND REVIEW FOR ENGINES AND AIRCRAFT REPORT*. 2019.

[4] Konrad Kozaczuk. Engine nacelles design – problems and challenges. *Proceedings of the Institution of Mechanical Engineers, Part G: Journal of Aerospace Engineering*, 231:2259–2265, 10 2017.

[5] VV Golubev and HM Atassi. Sound propagation in an annular duct with mean potential swirling flow. *Journal of Sound and Vibration*, 198(5):601–616, 1996.

[6] J. L. Kerrebrock. Small disturbances in turbomachine annuli with swirl. *https://doi.org/10.2514/3.7370*, 15:794–803, 5 2012.

[7] J. L. KERREBROCK. Waves and wakes in turbomachine annuli with swirl. 1974.

[8] Edmane Envia, Alexander G. Wilson, and Dennis L. Huff. Fan noise: A challenge to caa, 8 2004.

[9] A. J. COOPER and N. PEAKE. Propagation of unsteady disturbances in a slowly varying duct with mean swirling flow. *Journal of Fluid Mechanics*, 445:207–234, 10 2001.

[10] M. E. Goldstein. Characteristics of the unsteady motion on transversely sheared mean flows. *Journal of Fluid Mechanics*, 84:305, 1 1978.

[11] M. E. Goldstein. Scattering and distortion of the unsteady motion on transversely sheared mean flows. *Journal of Fluid Mechanics*, 91:601–632, 1979.

[12] A. KAPUR and P. MUNGUR. Sound interaction with a helical flow contained in an annular duct with radial gradients of flow, density and temperature. 1973.

[13] A. L.P. Maldonado, R. J. Astley, J. Coupland, G. Gabard, and D. Sutliff. Sound propagation in lined annular ducts with mean swirling flow. American Institute of Aeronautics and Astronautics Inc, AIAA, 2016.

[14] Daniel Ingraham and Ray Hixon. Verification of a viscous computational aeroacoustics code using external verification analysis aiaa paper 2015-2225 motivation.

[15] Daniel Ingraham. Verification of a computational aeroacoustics code using external verification analysis (eva), 2010.

[16] Kenneth Kousen. Pressure modes in ducted flows with swirl. In *Aeroacoustics Conference*, page 1679, 1996.

[17] Kenneth A Kousen. Eigenmode analysis of ducted flows with radially dependent axial and swirl components. In *CEAS/AIAA Joint Aeroacoustics Conference, 1 st, Munich, Germany*, pages 1085–1094, 1995.

[18] Chapter 3 exact methods of solution. *Mathematics in Science and Engineering*, 18:71–122, 1 1965.

[19] V. V. Golubev and H. M. Atassi. Acoustic-vorticity waves in swirling flows. *Journal of Sound and Vibration*, 209:203–222, 1 1998.

[20] Vladimir V. Golubev and Hafiz M. Atassi. Acoustic-vorticity modes in an annular duct with mean vortical swirling flow. *3rd AIAA/CEAS Aeroacoustics Conference*, pages 804–814, 1997.

[21] Christopher K.W. Tam and Laurent Auriault. The wave modes in ducted swirling flows. *Journal of Fluid Mechanics*, 371:1–20, 9 1998.

[22] Ronald Nijboer. Eigenvalues and eigenfunctions of ducted swirling flows. *7th AIAA/CEAS Aeroacoustics Conference and Exhibit*, 2001.

[23] Ying Guan, Kai H. Luo, and Tong Q. Wang. Sound transmission in a lined annular duct with mean swirling flow. *American Society of Mechanical Engineers, Noise Control and Acoustics Division (Publication) NCAD*, pages 135–144, 6 2009.

[24] A. J. Cooper. Effect of mean entropy on unsteady disturbance propagation in a slowly varying duct with mean swirling flow. *Journal of Sound and Vibration*, 291:779–801, 4 2006.

[25] H. Posson and N. Peake. The acoustic analogy in an annular duct with swirling mean flow. *Journal of Fluid Mechanics*, 726:439–475, 2013.

[26] C. J. Heaton and N. Peake. Algebraic and exponential instability of inviscid swirling flow. *Journal of Fluid Mechanics*, 565:279–318, 10 2006.

[27] Ray Hixon, Adrian Sescu, and Vasanth Allampalli. Towards the prediction of noise from realistic rotor wake/stator interaction using caa. volume 6, pages 203–213. Elsevier Ltd, 2010.

[28] R. YURKOVICH. Attenuation of acoustic modes in circular and annular ducts in the presence of sheared flow. *13th Aerospace Sciences Meeting*, 1 1975.

[29] J. M. Tyler and T. G. Sofrin. Axial flow compressor noise studies. *SAE Technical Papers*, 1 1962.

[30] P N Shankar. Acoustic refraction and attenuation in cylindrical and annular ducts, 1972.

[31] P. T. Vo and W. Eversman. A method of weighted residuals with trigonometric basis functions for sound transmission in circular ducts. *Journal of Sound and Vibration*, 56:243–250, 1 1978.

[32] R. J. Astley and W. Eversman. A finite element formulation of the eigenvalue problem in lined ducts with flow. *Journal of Sound and Vibration*, 65:61–74, 7 1979.

[33] Christopher J. Roy. Review of code and solution verification procedures for computational simulation. *Journal of Computational Physics*, 205:131–156, 5 2005.

[34] Kambiz Salari and Patrick Knupp. Code verification by the method of manufactured solutions, 2000.

[35] Jack L. Kerrebrock. *Aircraft engines and gas turbines*. MIT Press, 1992.

[36] N. K. Agarwal and M. K. Bull. Acoustic wave propagation in a pipe with fully developed turbulent flow. *Journal of Sound and Vibration*, 132:275–298, 7 1989.

Appendix A

Theory Appendix

Appendix B

Chapter 3 Appendix

B.1 Divergence operations in new coordinate systems

The divergence, (∇), represents the operation of taking derivatives of a vector field. However, understanding the mathematical and physical representation of the divergence operator into new coordinate systems serves as a good prerequisite for the application of the Navier Stokes equations for the evaluation of aerodynamic models in unusual flow domains. Although there are many resources that will provide equations in varying coordinate systems, the derivation offers insight into the advantages and drawbacks of using a new reference frame for a flow domain. The divergence operator in Cartesian coordinates is,

$$\vec{\nabla} \equiv \hat{e}_x \frac{\partial}{\partial x} + \hat{e}_y \frac{\partial}{\partial y} + \hat{e}_z \frac{\partial}{\partial z} = 0$$

The vectors, $\hat{e}_x, \hat{e}_y, \hat{e}_z$ (commonly denoted in literature as $\hat{i}, \hat{j}, \hat{k}$) are the basis vectors of the Cartesian coordinate system. The vector hat ($\vec{}$) reminds us that divergence operation includes a scalar product of the basis vectors and the individual derivative terms themselves. These basis vectors *scale* with the derivatives d/dx d/dy d/dz in the direction of these basis vectors themselves. This implicitly captures the coordinate system and assumptions that corresponds to the basis vectors themselves.

To relate the basis vectors of the cylindrical coordinate system to the Cartesian

coordinate system, we use the following relations,

$$r = \sqrt{x^2 + y^2}$$

$$\theta = \tan^{-1}\left(\frac{y}{x}\right)$$

$$= \cos^{-1}\left(\frac{x}{r}\right)$$

$$= \sin^{-1}\left(\frac{y}{r}\right)$$

Note that the equation above also establishes $x = r\cos\theta$ and $y = r\sin\theta$. The Cartesian basis vectors are related to the cylindrical basis vectors of the new coordinate system by,

$$\hat{e}_r = \hat{e}_x \cos\theta + \hat{e}_y \sin\theta$$

$$\hat{e}_\theta = -\hat{e}_x \sin\theta + \hat{e}_y \cos\theta$$

$$\hat{e}_z = \hat{e}_z$$

Defining these relationships, (they'll be useful later)

$$\frac{\partial \hat{e}_r}{\partial r} = \frac{\partial \hat{e}_\theta}{\partial r} = \frac{\partial \hat{e}_z}{\partial r} = 0$$

$$\frac{\partial \hat{e}_r}{\partial \theta} = -\hat{e}_x \sin\theta + \hat{e}_y \cos\theta = \hat{e}_\theta$$

$$\frac{\partial \hat{e}_\theta}{\partial \theta} = -\left(\hat{e}_x \cos\theta + \hat{e}_y \sin\theta\right) = -\hat{e}_r$$

The multi-variable chain rule for differentiation is then used to express the Cartesian variables, $\frac{\partial}{\partial x}, \frac{\partial}{\partial y}, \frac{\partial}{\partial z}$, with respect to the cylindrical variable.

$$\frac{\partial}{\partial x} = \frac{\partial}{\partial r}\frac{dr}{dx} + \frac{\partial}{\partial \theta}\frac{d\theta}{dx} + \frac{\partial}{\partial z}\frac{dz}{dx}$$

$$\frac{\partial}{\partial y} = \frac{\partial}{\partial r}\frac{dr}{dy} + \frac{\partial}{\partial \theta}\frac{d\theta}{dy} + \frac{\partial}{\partial z}\frac{dz}{dy}$$

By,finding the derivatives of r & θ with respect to x and y, we can substitute terms in the Cartesian divergence definition. First, $\frac{dr}{dx}$ & $\frac{dr}{dy}$ is calculated,

$$
\begin{aligned}
\frac{dr}{dx} &= \frac{d}{dx}\left(\left[x^2 + y^2\right]^{1/2}\right) \\
&= \frac{1}{2}\left[x^2 + y^2\right]^{-1/2}(2x) \\
&= \frac{x}{\sqrt{x^2 + y^2}} \\
&= \frac{r\cos\theta}{r} \\
&\boxed{\frac{dr}{dx} = \cos\theta}
\end{aligned}
$$

$$
\begin{aligned}
\frac{dr}{dy} &= \frac{d}{dy}\left(\left[x^2 + y^2\right]^{1/2}\right) \\
&= \frac{1}{2}\left[x^2 + y^2\right]^{-1/2}(2y) \\
&= \frac{y}{\sqrt{x^2 + y^2}} \\
&= \frac{r\sin\theta}{r} \\
&\boxed{\frac{dr}{dy} = \sin\theta}
\end{aligned}
$$

Then, $\frac{d\theta}{dx}$ & $\frac{d\theta}{dy}$ is found.

$$\frac{d\theta}{dx} = \frac{d}{dx}\left(tan^{-1}\left(\frac{y}{x}\right)\right)$$

$$= \frac{d}{du}tan^{-1}(u)\frac{d}{dx}\left(\frac{y}{x}\right)$$

$$= \frac{1}{u^2+1}\frac{-y}{x^2}$$

$$= -\frac{y}{y^2+x^2}$$

$$\boxed{\frac{d\theta}{dx} = -\frac{sin\theta}{r}}$$

$$\frac{d\theta}{dy} = \frac{d}{dy}\left(tan^{-1}\left(\frac{y}{x}\right)\right)$$

$$= \frac{d}{du}tan^{-1}(u)\frac{d}{dy}\left(\frac{y}{x}\right)$$

$$= \frac{1}{u^2+1}\frac{1}{x}$$

$$= \frac{x}{y^2+x^2}$$

$$\boxed{\frac{d\theta}{dy} = \frac{cos\theta}{r}}$$

Through substitution back into the chain rule expansion,

$$\frac{\partial}{\partial x} = \frac{\partial}{\partial r}\cos\theta - \frac{\partial}{\partial\theta}\frac{1}{r}\sin\theta$$

$$\frac{\partial}{\partial y} = \frac{\partial}{\partial r}\sin\theta + \frac{\partial}{\partial\theta}\frac{1}{r}\cos\theta$$

We can now convert our divergence operator, $\vec{\nabla}$

$$\vec{\nabla} = \frac{\partial}{\partial x}\hat{e}_x + \frac{\partial}{\partial y}\hat{e}_y + \frac{\partial}{\partial z}\hat{e}_z = 0$$

$$= \left(\frac{\partial}{\partial r}\cos\theta - \frac{\partial}{\partial \theta}\frac{1}{r}\sin\theta\right)\hat{e}_x + \left(\frac{\partial}{\partial r}\sin\theta + \frac{\partial}{\partial \theta}\frac{1}{r}\cos\theta\right)\hat{e}_y + \frac{\partial}{\partial z}\hat{e}_z = 0$$

Rearranging like terms (containing cylindrical derivative variables), and factoring out $1/r$

$$\vec{\nabla} = \left(\frac{\partial}{\partial r}\cos\theta - \frac{\partial}{\partial \theta}\frac{1}{r}\sin\theta\right)\hat{e}_x + \left(\frac{\partial}{\partial r}\sin\theta + \frac{\partial}{\partial \theta}\frac{1}{r}\cos\theta\right)\hat{e}_y + \frac{\partial}{\partial z}\hat{e}_z = 0$$

$$= (\hat{e}_x\cos\theta + \hat{e}_y\sin\theta)\frac{\partial}{\partial r} + \frac{1}{r}(\hat{e}_y\cos\theta - \hat{e}_x\sin\theta)\frac{\partial}{\partial \theta} + \frac{\partial}{\partial z}\hat{e}_z = 0$$

Recalling the definitions for $\hat{e}_r$ and $\hat{e}_\theta$, we can use these expressions to rewrite ∇ in polar coordinates

$$\vec{\nabla} = \hat{e}_r\frac{\partial}{\partial r} + \frac{1}{r}\hat{e}_\theta\frac{\partial}{\partial \theta} + \frac{\partial}{\partial z}\hat{e}_z = 0$$

80

$$\frac{DV}{dt} = \frac{1}{\rho}\nabla \cdot \boldsymbol{\sigma}$$

$$\boldsymbol{\sigma} = -p\boldsymbol{I_3} + \tau$$

where $[\boldsymbol{I_3}]$ is a 3 by 3 identity matrix and τ is the shear stress tensor. The velocity vector for a three dimensional flow.

$$\vec{V} = v_r(r, \theta, x, t)\hat{e}_r + v_\theta(r, \theta, x, t)\hat{e}_\theta + v_x(r, \theta, x, t)\hat{e}_x \tag{B.1}$$

In Kousen's work, a velocity vector is written as a function of radius, and the radial velocity component is neglected.

$$\vec{V} = v_\theta(r)\hat{e}_\theta + v_x(r)\hat{e}_x \tag{B.2}$$

We will go with the first definition and cancel out the radial velocity later on.

$$\frac{DV}{dt} = \frac{\partial\vec{V}}{\partial t}\frac{dt}{dt} + \frac{\partial\vec{V}}{\partial r}\frac{dr}{dt} + \frac{\partial\vec{V}}{\partial\theta}\frac{d\theta}{dt} + \frac{\partial\vec{V}}{\partial x}\frac{dx}{dt}$$

Starting with the first term,

$$\frac{\partial\vec{V}}{\partial t}\frac{dt}{dt} = \frac{\partial}{\partial t}\left(v_r\hat{e}_r + v_\theta\hat{e}_\theta + v_x\hat{e}_x\right) * 1$$

$$= \frac{\partial v_r}{\partial t}\hat{e}_r + \frac{\partial\hat{e}_r}{\partial t}\cancel{v_r} + \frac{\partial v_\theta}{\partial t}\hat{e}_\theta + \frac{\partial\hat{e}_\theta}{\partial t}\cancel{v_\theta} + \frac{\partial v_x}{\partial t}\hat{e}_x + \frac{\partial\hat{e}_x}{\partial t}\cancel{v_x}$$

$$\boxed{\frac{\partial\vec{V}}{\partial t} = \frac{\partial v_r}{\partial t}\hat{e}_r + \frac{\partial v_\theta}{\partial t}\hat{e}_\theta + \frac{\partial v_x}{\partial t}\hat{e}_x}$$

$$\frac{\partial \vec{V}}{\partial r} \frac{dr}{dt} = \frac{\partial \vec{V}}{\partial r} v_r$$

$$= \frac{\partial}{\partial r} \left[v_r \hat{e}_r + v_\theta \hat{e}_\theta + v_x \hat{e}_x \right] v_r$$

$$= \left(\frac{\partial v_r}{\partial r} \hat{e}_r + \frac{\cancel{\partial \hat{e}_r}}{\cancel{\partial r}} v_r + \frac{\partial v_\theta}{\partial r} \hat{e}_\theta + \frac{\cancel{\partial \hat{e}_\theta}}{\cancel{\partial r}} v_\theta + \frac{\partial v_x}{\partial r} \hat{e}_x + \frac{\cancel{\partial \hat{e}_x}}{\cancel{\partial r}} v_\theta \right) v_r$$

$$\boxed{\frac{\partial \vec{V}}{\partial r} \frac{dr}{dt} = \left[\frac{\partial v_r}{\partial r} \hat{e}_r + \frac{\partial v_\theta}{\partial r} \hat{e}_\theta + \frac{\partial v_x}{\partial r} \hat{e}_x \right] v_r}$$

Recalling that arc length is $ds = rd\theta$, and angular velocity is $d\theta/dt = v_\theta/r$

$$\frac{\partial \vec{V}}{\partial \theta} \frac{d\theta}{dt} = \frac{\partial \vec{V}}{\partial \theta} \frac{v_\theta}{r}$$

$$= \frac{\partial}{\partial \theta} \left[v_r \hat{e}_r + v_\theta \hat{e}_\theta + v_x \hat{e}_x \right] \frac{v_\theta}{r}$$

$$= \left[\frac{\partial v_r}{\partial \theta} \hat{e}_r + \underbrace{\frac{\partial \hat{e}_r}{\partial \theta}}_{\hat{e}_\theta} v_r + \frac{\partial v_\theta}{\partial \theta} \hat{e}_\theta + \underbrace{\frac{\partial \hat{e}_\theta}{\partial \theta}}_{-\hat{e}_r} v_\theta + \frac{\partial v_x}{\partial \theta} \hat{e}_x \right] \frac{v_\theta}{r}$$

$$\boxed{\frac{\partial \vec{V}}{\partial \theta} \frac{dr}{dt} = \left[\left(\frac{\partial v_r}{\partial \theta} - v_\theta \right) \hat{e}_r + \left(\frac{\partial v_\theta}{\partial \theta} + v_r \right) \hat{e}_\theta + \frac{\partial v_x}{\partial \theta} \hat{e}_x \right] \frac{v_\theta}{r}}$$

$$\frac{\partial \vec{V}}{\partial x}\frac{dx}{dt} = \frac{\partial \vec{V}}{\partial x}v_x$$

$$= \frac{\partial}{\partial x}\left[v_r\hat{e}_r + v_\theta\hat{e}_\theta + v_x\hat{e}_x\right]v_r$$

$$= \left(\frac{\partial v_r}{\partial x}\hat{e}_r + \frac{\cancel{\partial\hat{e}_r}}{\cancel{\partial x}}v_r + \frac{\partial v_\theta}{\partial x}\hat{e}_\theta + \frac{\cancel{\partial\hat{e}_\theta}}{\cancel{\partial x}}v_\theta + \frac{\partial v_x}{\partial r}\hat{e}_x + \frac{\cancel{\partial\hat{e}_x}}{\cancel{\partial x}}v_\theta\right)v_x$$

$$\boxed{\frac{\partial \vec{V}}{\partial x}\frac{dx}{dt} = \left[\frac{\partial v_r}{\partial x}\hat{e}_r + \frac{\partial v_\theta}{\partial x}\hat{e}_\theta + \frac{\partial v_x}{\partial x}\hat{e}_x\right]v_x}$$

Putting these terms together,

$$\frac{DV}{dt} = \left[\frac{\partial v_r}{\partial t} + v_r\frac{\partial v_r}{\partial r} + \frac{v_\theta^2}{r}\frac{\partial v_r}{\partial\theta} - \frac{v_\theta}{r} + v_x\frac{\partial v_r}{\partial x}\right]\hat{e}_r +$$

$$\left[\frac{\partial v_\theta}{\partial t} + v_r\frac{\partial v_\theta}{\partial r} + \frac{v_\theta}{r}\frac{\partial v_\theta}{\partial\theta} + \frac{v_r v_\theta}{r} + v_x\frac{\partial v_\theta}{\partial x}\right]\hat{e}_\theta +$$

$$\left[\frac{\partial v_x}{\partial t} + v_r\frac{\partial v_x}{\partial r} + \frac{v_\theta}{r}\frac{\partial v_x}{\partial\theta} + v_x\frac{\partial v_x}{\partial x}\right]\hat{e}_x$$

If we neglect viscosity on the right hand side, we will arrive at the linearized Euler equations

$$\nabla\sigma = -\nabla p[\mathbf{I_3}]$$

$$= -\frac{1}{\rho}\begin{Bmatrix} \frac{\partial p}{\partial r} & 0 & 0 \\ \\ 0 & \frac{1}{r}\frac{\partial p}{\partial\theta} & 0 \\ \\ 0 & 0 & \frac{\partial p}{\partial x} \end{Bmatrix}$$

B.2 Appendix A: Speed of Sound

Sound wave is a pressure disturbance that moves with at a speed a By applying a rectangular control volume around this pressure wave, we can apply our conservation equations. We are assuming that these properities are increasing by a small increment. This is why each variable is added by a infinitesimally small term.

Recalling the conservation of mass (continuity equation), $\dot{m} = constant$

$$\dot{m}_{left} = \dot{m}_{right}$$

Recalling he definition of density, $\rho = m/\bar{V}$ and rewriting $\bar{V} = uA$ (check the units)

$$\rho a \cancel{A} = (\rho + d\rho)(a + da)\cancel{A}$$

Futher expanding gives,

$$\rho a = (\rho a + \rho da + a d\rho + da d\rho)$$

We say that $da d\rho$ is so small, we can assume it is zero. This is often referred to as "neglecting higher order terms (H.O.T)". The expression then becomes

$$\frac{da}{a} = -\frac{d\rho}{\rho}$$

For the momentum equation $P + \rho u^2 = constant$

$$P + \rho a^2 = P + dP + (\rho + d\rho)(a + da)(a + da)$$

But we just said that $\rho a = (\rho + d\rho)(a + da)$

$$P + \rho a^2 = P + dP + \rho a(a + da)$$

84

$$dP + \rho a\, da = a$$

Multiplying the second term by a and divide by a, this is essentially multiplying the second term by one.

$$dP + \rho a^2 \frac{da}{a} = a$$

recalling the relation $\frac{da}{a} = -\frac{d\rho}{\rho}$

$$dp - a^2 d\rho = 0$$

$$a^2 = \frac{dp}{d\rho}$$

Since a sound wave is a very weak wave, when it travels through a medium, it only increases the pressure and density, etc. slightly. The effect of this is that friction and heat transfer can be neglected. Since friction cannot be undone, we call this an irreversible process. Whenever there is no transfer of heat, it is called this adiabatic. Thus, the propagation of sound is an adiabatic, reversible process, otherwise called isentropic. Isentropic implies no increase in entropy, which is *not* true in the presence of shock waves.

In the case of a thermally perfect gas, we can say $P = \rho RT$

For a callorically perfect gas we can say $pv^\gamma = constant$, where v is volume per unit mass, or specific volume

Differentiating and recalling that $v = 1/\rho$

$$a = \sqrt{\frac{\gamma P}{\rho}} = \sqrt{\gamma RT}$$

$$dm = (\rho u)_2 - (\rho u)_1$$

$$D(mV) = \left(\rho u^2 + P\right)_2$$

For Steady flow,

$$d\widehat{m} = (\rho u)_2 - (\rho u)_1$$

$$(\rho u)_1 = (\rho u)_2$$

Similarly, for the Momentum equation,

$$\left(\rho u^2 + P\right)_1 = \left(\rho u^2 + P\right)_2$$

Let us change the coordinate system motion for the traveling wave be independent of time, and thus corresponds to *steady state* wave propagation.

$$u_1 = \bar{u} + a - \frac{1}{2}\partial u$$

$$u_2 = \bar{u} + a + \frac{1}{2}\partial u$$

where, $\bar{u}$ is the average flow velocity and a is the wave speed.

Substituting this back into the conservation of mass

$$(\rho u)_1 = (\rho u)_2$$

$$\left(\rho - \frac{1}{2}\partial\rho\right)\left(\bar{u} - a - \frac{1}{2}\partial u\right) = \left(\rho + \frac{1}{2}\partial\rho\right)\left(\bar{u} - a + \frac{1}{2}\partial u\right)$$

Further expanding

$$\cancel{\rho\bar{u}} - \cancel{\rho\bar{a}} + \frac{1}{2}\left(-\rho\partial u - \bar{u} - \bar{u}\partial\rho + a\partial\rho\right) + \frac{1}{4}\cancel{\partial\rho\partial u} = \cancel{\rho\bar{u}} - \cancel{\rho\bar{a}} + \frac{1}{2}\left(\rho\partial u + \bar{u} - \bar{u}\partial\rho - a\partial\rho\right) + \frac{1}{4}\cancel{\partial\rho\partial u}$$

$$\frac{1}{2}\left(-\rho\partial u - \bar{u}\partial\rho + a\partial\rho\right) = \frac{1}{2}\left(\rho\partial u + \bar{u}\partial\rho - a\partial\rho\right)$$

$$\rho\partial u + u\partial\rho - a\partial\rho = 0$$

$$\rho\partial u + \left(u - a\right)\partial\rho = 0$$

Momentum Equation

$$\left(\rho u^2 + P\right)_1 = \left(\rho u^2 + P\right)_2$$

B.3 Appendix B: Isentropic Waves

$$dU = dW + dQ$$

For adiabatic, reversible processes, the work done by a system with constant pressure and a change in volume is $-pdV$ and the change in heat energy is zero. Hence,

$$dU = -pdV$$

.

The change in enthalpy of such a system can be found by taking the derivative of its expression for a thermodynamic process

$$H = U + pV$$

$$dH = dU + pdV + vdP$$

$$dH = -pdV + pdV + vdP$$

$$dH = vdP$$

The specific heats at constant pressure and constant volume

$$\left(\frac{\partial U}{\partial T}\right)_v = C_v$$

$$\left(\frac{\partial H}{\partial T}\right)_p = C_p$$

$$\gamma = \frac{C_p}{C_v} = \frac{dH}{dU} = -\frac{V\,dP}{p\,dV} = -\frac{V}{dV}\frac{dP}{p}$$

Integrating both sides

$$\gamma\frac{dV}{V} = \frac{-dP}{P} \rightarrow \gamma\int\frac{1}{V}dV = -\int\frac{1}{P}dP$$

$$\gamma ln(V) + ln(P) = C$$

Using log rules

$$ln(V^{\gamma}) + ln(P) = C$$

$$ln(pV^{\gamma}) = C$$

$$pV^{\gamma} = e^C = C$$

$$\frac{p}{\rho^{\gamma}}$$

B.3.1 Linearizing the governing equations

B.3.1.1 Linearizing Conservation of Mass

To linearize the Euler equations, we substitute each flow variable with its equivalent mean and perturbation components. Note that the mean term is only a function of space whereas the perturbation component is a dependent on both space and time (functional dependence is not explicity written with each variable). Assuming that we can divide the variable into a known laminar flow solution to the Navier-Stokes equations and a small amplitude perturbation solution:

$$v_r = V_r(x) + v'_r \tag{B.3}$$

$$v_\theta = V_\theta + v'_\theta \tag{B.4}$$

$$v_x = V_x + v'_x \tag{B.5}$$

$$p = \bar{p} + p' \tag{B.6}$$

$$\rho = \bar{\rho} + \rho' \tag{B.7}$$

Starting with continuity,

$$\frac{\partial \rho}{\partial t} + v_r \frac{\partial \rho}{\partial r} + \frac{v_\theta}{r} \frac{\partial \rho}{\partial \theta} + v_x \frac{\partial \rho}{\partial \theta} + \rho \left(\frac{1}{r} \frac{\partial (r v_r)}{\partial r} + \frac{1}{r} \frac{\partial v_\theta}{\partial \theta} + \frac{\partial v_x}{\partial x} \right) = 0$$

$$\frac{\partial \bar{\rho} + \rho'}{\partial t} + (V_r + v_r') \frac{\partial \bar{\rho} + \rho'}{\partial r} + \frac{V_\theta + v_\theta'}{r} \frac{\partial \bar{\rho} + \rho'}{\partial \theta} + (V_x + v_x') \frac{\partial \bar{\rho} + \rho'}{\partial \theta} +$$

$$(\bar{\rho} + \rho') \left(\frac{1}{r} \frac{\partial (r(V_r + v_r'))}{\partial r} + \frac{1}{r} \frac{\partial V_\theta + v_\theta'}{\partial \theta} + \frac{\partial (V_x + v_x')}{\partial x} \right) = 0$$

$$\frac{\partial \bar{\rho}}{\partial t} + \frac{\partial \rho'}{\partial t} +$$

$$V_r \frac{\partial \bar{\rho}}{\partial r} + v_r' \frac{\partial \bar{\rho}}{\partial r} + V_r \frac{\partial \rho'}{\partial r} + v_r' \frac{\partial \rho'}{\partial r} +$$

$$\frac{1}{r} \left(V_\theta \frac{\partial \bar{\rho}}{\partial \theta} + v_\theta' \frac{\partial \bar{\rho}}{\partial \theta} + V_\theta \frac{\partial \rho'}{\partial \theta} + v_\theta' \frac{\partial \rho'}{\partial \theta} \right) +$$

$$V_x \frac{\partial \bar{\rho}}{\partial x} + v_x' \frac{\partial \bar{\rho}}{\partial x} + V_x \frac{\partial \rho'}{\partial x} + v_x' \frac{\partial \rho'}{\partial x} +$$

$$\bar{\rho} \left(\frac{1}{r} \left(\frac{\partial (r V_r)}{\partial r} + \frac{\partial (r(v_r'))}{\partial r} + \frac{\partial V_\theta}{\partial \theta} + \frac{\partial v_\theta'}{\partial \theta} \right) + \frac{\partial V_x}{\partial x} + \frac{\partial v_x'}{\partial x} \right) +$$

$$\rho' \left(\frac{1}{r} \left(\frac{\partial (r V_r)}{\partial r} + \frac{\partial (r(v_r'))}{\partial r} + \frac{\partial V_\theta}{\partial \theta} + \frac{\partial v_\theta'}{\partial \theta} \right) + \frac{\partial V_x}{\partial x} + \frac{\partial v_x'}{\partial x} \right) = 0$$

Important things to note

- The small disturbances are infinitesimal (thus linearized)

- Neglect second order terms.

- The continuity equation is comprised of mean velocity components. This is subtracted off in each of the governing equations

Blue will be used for terms that are removed after subtracting in the original continuity equation, green will be used to cancel higher(2nd) order terms.Red will be used if we take the radial velocity to be zero.

$$= \frac{\cancel{\partial \bar{\rho}}}{\cancel{\partial t}} + \frac{\partial \rho'}{\partial t} +$$

$$V_r \frac{\cancel{\partial \bar{\rho}}}{\cancel{\partial r}} + v_r' \frac{\cancel{\partial \bar{\rho}}}{\cancel{\partial r}} + V_r \frac{\cancel{\partial \rho'}}{\cancel{\partial r}} + v_r' \frac{\cancel{\partial \rho'}}{\cancel{\partial r}} +$$

$$\frac{1}{r} \left(V_\theta \frac{\cancel{\partial \bar{\rho}}}{\cancel{\partial \theta}} + v_\theta' \frac{\cancel{\partial \bar{\rho}}}{\cancel{\partial \theta}} + V_\theta \frac{\partial \rho'}{\partial \theta} + v_\theta' \frac{\cancel{\partial \rho'}}{\cancel{\partial \theta}} \right) +$$

$$V_x \frac{\cancel{\partial \bar{\rho}}}{\cancel{\partial x}} + v_x' \frac{\cancel{\partial \bar{\rho}}}{\cancel{\partial x}} + V_x \frac{\partial \rho'}{\partial \theta} + v_x' \frac{\cancel{\partial \rho'}}{\cancel{\partial x}} +$$

$$\bar{\rho} \left(\frac{1}{r} \left(\frac{\cancel{\partial (rV_r)}}{\cancel{\partial r}} + \frac{\partial (r(v_r'))}{\partial r} + \frac{\cancel{\partial V_\theta}}{\cancel{\partial \theta}} + \frac{\partial v_\theta'}{\partial \theta} \right) + \frac{\cancel{\partial V_x}}{\cancel{\partial x}} + \frac{\partial v_x'}{\partial x} \right) +$$

$$\rho' \left(\frac{1}{r} \left(\frac{\cancel{\partial (rV_r)}}{\cancel{\partial r}} + \frac{\cancel{\partial (r(v_r'))}}{\cancel{\partial r}} + \frac{\cancel{\partial V_\theta}}{\cancel{\partial \theta}} + \frac{\cancel{\partial v_\theta'}}{\cancel{\partial \theta}} \right) + \frac{\cancel{\partial V_x}}{\cancel{\partial x}} + \frac{\cancel{\partial v_x'}}{\cancel{\partial x}} = 0 \right)$$

$$\boxed{\frac{\partial \rho'}{\partial t} + \frac{V_\theta}{r} \frac{\partial \rho'}{\partial \theta} + V_x \frac{\partial \rho'}{\partial x} + \bar{\rho} \left(\frac{1}{r} \left(\frac{\partial r v_r'}{\partial r} + \frac{\partial v_\theta'}{\partial \theta} \right) + \frac{\partial v_x'}{\partial x} \right) = 0}$$

B.3.1.2 Linearizing the Conservation of Momentum

in the r direction

Starting with the mean momentum equation

$$\frac{\partial v_r}{\partial t} + v_r\frac{\partial v_r}{\partial r} + \frac{v_\theta}{r}\frac{\partial v_r}{\partial \theta} - \frac{v_\theta^2}{r} + v_x\frac{\partial v_r}{\partial x} = -\frac{1}{\rho}\frac{\partial p}{\partial r}$$

Looking at the left hand side first

$$\frac{\partial (V_r + v_r')}{\partial t} + (V_r + v_r')\frac{\partial (V_r + v_r')}{\partial r} + \frac{V_\theta + v_\theta'}{r}\frac{\partial (V_r + v_r')}{\partial \theta} - \frac{(V_\theta + v_\theta')^2}{r} + (V_x + v_x')\frac{\partial (V_r + v_r')}{\partial x} = -\frac{1}{\rho}\frac{\partial p}{\partial r}$$

$$\frac{\partial V_r}{\partial t} + \frac{\partial v_r'}{\partial t} +$$

$$V_r\frac{\partial V_r}{\partial r} + v_r'\frac{\partial V_r}{\partial r} + V_r\frac{\partial v_r'}{\partial r} + v_r'\frac{\partial v_r'}{\partial r} +$$

$$\frac{1}{r}\left(V_\theta\frac{\partial V_r}{\partial \theta} + v_\theta'\frac{\partial V_r}{\partial \theta} + V_\theta\frac{\partial v_r'}{\partial \theta} + v_\theta'\frac{\partial v_r'}{\partial \theta}\right) -$$

$$\frac{1}{r}\left(V_\theta^2 + 2V_\theta v_\theta' + v_\theta'^2\right) +$$

$$V_x\frac{\partial V_r}{\partial x} + v_x'\frac{\partial V_r}{\partial x} + V_x\frac{\partial v_r'}{\partial x} + v_x'\frac{\partial v_r'}{\partial x} = -\frac{1}{\rho}\frac{\partial p}{\partial r}$$

$$\frac{\partial v_r'}{\partial t} + V_r\frac{\partial v_r'}{\partial r} + \frac{V_\theta}{r}\frac{\partial v_r'}{\partial \theta} - \frac{2V_\theta v_\theta'}{r} + V_x\frac{\partial v_r'}{\partial x} = -\frac{1}{\rho}\frac{\partial p}{\partial r}$$

Now looking at the right side, Expanding the $1/\rho$ using a Taylor series approximation

$$
\begin{aligned}
\frac{1}{\bar{\rho}+\rho'} &= \frac{1}{\bar{\rho}} + \left(\frac{1}{\bar{\rho}+\rho'} - \frac{1}{\rho}\right) \\
&= \frac{1}{\bar{\rho}} + \left(\frac{\bar{\rho}}{\bar{\rho}(\bar{\rho}+\rho')} - \frac{1}{\rho}\frac{\bar{\rho}+\rho'}{\bar{\rho}+\rho'}\right) \\
&= \frac{1}{\bar{\rho}} - \left(\frac{\bar{\rho}-\bar{\rho}+\rho'}{\bar{\rho}(\bar{\rho}+\rho')}\right) \\
&= \frac{1}{\bar{\rho}} - \frac{\rho'}{\bar{\rho}} \underbrace{\left(\frac{1}{\bar{\rho}+\rho}\right)}_{\text{This is what we're solving for!}} \\
&= \frac{1}{\bar{\rho}} - \frac{\rho'}{\bar{\rho}} \underbrace{\left[\frac{1}{\bar{\rho}} + \left(\frac{1}{\bar{\rho}+\rho'} - \frac{1}{\rho}\right)\right]}_{\text{This is from step 1}} \\
&= \frac{1}{\bar{\rho}} - \frac{\rho'}{\bar{\rho}^2} + \underbrace{\left[\left(\frac{\rho'}{\bar{\rho}}\right)^2 \frac{1}{\bar{\rho}+\rho'}\right]}_{\text{These are higher order terms that will go to } \infty}
\end{aligned}
$$

$$
\begin{aligned}
\frac{1}{\rho}\frac{\partial p}{\partial r} &= \left(-\frac{1}{\bar{\rho}} + \frac{\rho'}{\bar{\rho}^2}\right)\left(\frac{\partial \bar{p}+p'}{\partial r}\right) \\
\frac{1}{\rho}\frac{\partial p}{\partial r} &= -\frac{1}{\bar{\rho}}\frac{\partial \bar{p}}{\partial r} - \frac{1}{\bar{\rho}}\frac{\partial p'}{\partial r} + \frac{\rho'}{\bar{\rho}^2}\frac{\partial \bar{p}}{\partial r} + \frac{\rho'}{\bar{\rho}^2}\frac{\partial p'}{\partial r} \\
\frac{1}{\rho}\frac{\partial p}{\partial r} &= -\frac{1}{\bar{\rho}}\frac{\partial p'}{\partial r} + \frac{\rho'}{\bar{\rho}^2}\frac{\partial \bar{p}}{\partial r}
\end{aligned}
$$

$$
\boxed{\frac{\partial v_r'}{\partial t} + \frac{V_\theta}{r}\frac{\partial v_r'}{\partial \theta} - \frac{2V_\theta v_\theta'}{r} + V_x\frac{\partial v_r'}{\partial x} = \frac{1}{\bar{\rho}}\frac{\partial p'}{\partial r} + \frac{\rho'}{\bar{\rho}^2}\frac{\partial \bar{p}}{\partial r}}
$$

B.3.1.3 Linearizing the Conservation of Momentum in the θ direction

Starting with the mean momentum equation

$$\frac{\partial v_\theta}{\partial t} + v_r \frac{\partial v_\theta}{\partial r} + \frac{v_\theta}{r}\frac{\partial v_\theta}{\partial \theta} + \frac{v_r v_\theta}{r} + v_x \frac{\partial v_\theta}{\partial x} = -\frac{1}{\rho r}\frac{\partial p}{\partial \theta}$$

Looking at the left hand side first

$$\frac{\partial(V_\theta + v_\theta')}{\partial t} + (V_r + v_r')\frac{\partial(V_\theta + v_\theta')}{\partial r} +$$

$$\frac{V_\theta + v_\theta'}{r}\frac{\partial(V_\theta + v_\theta')}{\partial \theta} + \frac{(V_r + v_r')(V_\theta + v_\theta')}{r} + (V_x + v_x')\frac{\partial(V_\theta + v_\theta')}{\partial x} = -\frac{1}{\rho r}\frac{\partial p}{\partial \theta}$$

$$\cancel{\frac{\partial V_\theta}{\partial t}} + \frac{\partial v_\theta'}{\partial t} +$$

$$V_r \cancel{\frac{\partial V_\theta}{\partial r}} + \underbrace{v_r'\frac{\partial V_\theta}{\partial r}}_{v_r'=0} + V_r \cancel{\frac{\partial v_\theta'}{\partial r}} + v_r' \cancel{\frac{\partial v_\theta'}{\partial r}} +$$

$$\frac{1}{r}\left(V_\theta \cancel{\frac{\partial V_\theta}{\partial \theta}} + v_\theta' \cancel{\frac{\partial V_\theta}{\partial \theta}} + V_\theta \frac{\partial v_\theta'}{\partial \theta} + v_\theta' \cancel{\frac{\partial v_\theta'}{\partial \theta}}\right) +$$

$$\frac{1}{r}\left(\cancel{V_r V_\theta} + v_r' V_\theta + \cancel{V_r v_\theta'} + \cancel{v_r' v_\theta'}\right) +$$

$$V_x \cancel{\frac{\partial V_\theta}{\partial x}} + v_x' \cancel{\frac{\partial V_\theta}{\partial x}} + V_x \frac{\partial v_\theta'}{\partial x} + v_x' \cancel{\frac{\partial v_\theta'}{\partial x}} = -\frac{1}{\rho r}\frac{\partial p}{\partial \theta}$$

$$\frac{\partial v_\theta'}{\partial t} + v_r'\frac{\partial V_\theta}{\partial r} + \frac{V_\theta}{r}\frac{\partial v_\theta'}{\partial \theta} + \frac{v_r' V_\theta}{r} + V_x \frac{\partial v_r'}{\partial x} = -\frac{1}{\rho r}\frac{\partial p}{\partial \theta}$$

Now looking at the right side, Expanding the $1/\rho$ using a Taylor series approximation

$$-\frac{1}{\rho r}\frac{\partial p}{\partial \theta} = \left(-\frac{1}{\bar\rho} + \frac{\rho'}{\bar\rho^2}\right)\left(\frac{\partial \bar p + p'}{\partial \theta}\right)$$

$$\frac{1}{\rho r}\frac{\partial p}{\partial \theta} = -\frac{1}{\bar\rho}\cancel{\frac{\partial \bar p}{\partial \theta}} - \frac{1}{\bar\rho r}\frac{\partial p'}{\partial \theta} + \frac{\rho'}{\bar\rho^2 r}\cancel{\frac{\partial \bar p}{\partial \theta}} + \frac{\rho'}{\bar\rho^2 r}\cancel{\frac{\partial p'}{\partial \theta}}$$

$$\frac{1}{\rho r}\frac{\partial p}{\partial \theta} = -\frac{1}{\bar\rho}\frac{\partial p'}{\partial \theta}$$

$$\frac{\partial v'_\theta}{\partial t} + v'_r \frac{\partial V_\theta}{\partial r} + \frac{V_\theta}{r} \frac{\partial v'_\theta}{\partial \theta} + \frac{v'_r V_\theta}{r} + V_x \frac{\partial v'_r}{\partial x} = -\frac{1}{\bar{\rho} r} \frac{\partial p'}{\partial \theta}$$

B.3.1.4 Linearizing the Conservation of Momentum in the x direction

Starting with the mean momentum equation

$$\frac{\partial v_x}{\partial t} + v_r \frac{\partial v_x}{\partial r} + \frac{v_\theta}{r} \frac{\partial v_x}{\partial \theta} + v_x \frac{\partial v_x}{\partial x} = -\frac{1}{\rho} \frac{\partial p}{\partial x}$$

$$\frac{\partial(V_x + v'_x)}{\partial t} + (V_r + v'_r)\frac{\partial(V_x + v'_x)}{\partial r} + \frac{V_\theta + v'_\theta}{r}\frac{\partial(V_x + v'_x)}{\partial \theta} + (V_x + v'_x)\frac{\partial(V_x + v'_x)}{\partial x} = -\frac{1}{\rho}\frac{\partial p}{\partial x}$$

$$\cancel{\frac{\partial V_x}{\partial t}} + \frac{\partial v'_x}{\partial t} +$$

$$V_r\cancel{\frac{\partial V_x}{\partial r}} + v'_r\frac{\partial V_x}{\partial r} + V_r\cancel{\frac{\partial v'_x}{\partial r}} + v'_r\cancel{\frac{\partial v'_x}{\partial r}} +$$

$$\frac{1}{r}\left(V_\theta\cancel{\frac{\partial V_x}{\partial \theta}} + v'_\theta\cancel{\frac{\partial V_x}{\partial \theta}} + V_\theta\frac{\partial v'_x}{\partial \theta} + v'_\theta\cancel{\frac{\partial v'_x}{\partial \theta}}\right) +$$

$$V_x\cancel{\frac{\partial V_x}{\partial x}} + v'_x\cancel{\frac{\partial V_x}{\partial x}} + V_x\frac{\partial v'_x}{\partial x} + v'_x\cancel{\frac{\partial v'_x}{\partial x}} = -\frac{1}{\rho}\frac{\partial p}{\partial x}$$

$$\boxed{\frac{\partial v'_x}{\partial t} + v'_r\frac{\partial V_x}{\partial r} + \frac{V_\theta}{r}\frac{\partial v'_x}{\partial \theta} + V_x\frac{\partial v'_x}{\partial x} = -\frac{1}{\rho}\frac{\partial p}{\partial x}}$$

$$\rightarrow -\frac{1}{\rho}\frac{\partial p}{\partial x} = \left(-\frac{1}{\bar{\rho}} + \frac{\rho'}{\bar{\rho}^2}\right)\left(\frac{\partial \bar{p} + p'}{\partial x}\right)$$

$$\frac{1}{\rho}\frac{\partial p}{\partial x} = -\frac{1}{\bar{\rho}}\frac{\partial \bar{p}}{\partial x} - \frac{1}{\bar{\rho}}\frac{\partial p'}{\partial x} + \frac{\rho'}{\bar{\rho}^2 r}\frac{\partial \bar{p}}{\partial x} + \frac{\rho'}{\bar{\rho}^2 r}\frac{\partial p'}{\partial x}$$

$$\frac{1}{\rho}\frac{\partial p}{\partial x} = -\frac{1}{\bar{\rho}}\frac{\partial p'}{\partial x}$$

$$\boxed{\frac{\partial v_x'}{\partial t} + v_r'\frac{\partial V_x}{\partial r} + \frac{V_\theta}{r}\frac{\partial v_x'}{\partial \theta} + V_x\frac{\partial v_x'}{\partial x} = -\frac{1}{\bar{\rho}}\frac{\partial p'}{\partial x}}$$

98

B.3.1.5   Linearizing the Energy Equation

$$\frac{\partial p}{\partial t} + v_r\frac{\partial p}{\partial r} + \frac{v_\theta}{r}\frac{\partial p}{\partial x} + v_x\frac{\partial p}{\partial x} + \gamma p\left(\frac{1}{r}\frac{\partial rv_r}{\partial r} + \frac{1}{r}\frac{\partial v_\theta}{\partial \theta} + \frac{\partial v_x}{\partial x}\right) = 0$$

$$\frac{\partial(\bar{P}+P')}{\partial t} + (V_r+v_r')\frac{\partial(\bar{P}+P')}{\partial r} + \frac{(V_\theta+v_\theta')}{r}\frac{\partial(\bar{P}+p')}{\partial x} + (V_x+v_x')\frac{\partial(\bar{P}+P')}{\partial x} + \dots$$
$$\gamma(\bar{P}+P')\left(\frac{1}{r}\frac{\partial r(V_r+v_r')}{\partial r} + \frac{1}{r}\frac{\partial(V_\theta+v_\theta')}{\partial \theta} + \frac{\partial(V_x+v_x')}{\partial x}\right) = 0$$

$$\frac{\partial\bar{P}}{\partial t} + \frac{\partial P'}{\partial t} +$$
$$V_r\frac{\partial\bar{P}}{\partial r} + V_r\frac{\partial P'}{\partial r} + V_r'\frac{\partial\bar{P}}{\partial r} + V_r'\frac{\partial P'}{\partial r} +$$
$$\frac{V_\theta}{r}\frac{\partial\bar{P}}{\partial x} + \frac{V_\theta}{r}\frac{\partial P'}{\partial x} + \frac{v_\theta'}{r}\frac{\partial\bar{P}}{\partial x} + \frac{v_\theta'}{r}\frac{\partial P'}{\partial x} +$$
$$V_x\frac{\partial\bar{P}}{\partial x} + V_x\frac{\partial P'}{\partial x} + v_x'\frac{\partial\bar{P}}{\partial x} + v_x'\frac{\partial P'}{\partial x} +$$
$$\gamma\bar{P}\left(\frac{1}{r}\frac{\partial rV_r}{\partial r} + \frac{1}{r}\frac{\partial rv_r'}{\partial r} + \frac{1}{r}\frac{\partial V_\theta}{\partial \theta} + \frac{\partial v_\theta'}{\partial \theta} + \frac{\partial V_x}{\partial x} + \frac{\partial v_x'}{\partial x}\right)$$
$$\gamma P'\left(\frac{1}{r}\frac{\partial rV_r}{\partial r} + \frac{1}{r}\frac{\partial rv_r'}{\partial r} + \frac{1}{r}\frac{\partial V_\theta}{\partial \theta} + \frac{\partial v_\theta'}{\partial \theta} + \frac{\partial V_x}{\partial x} + \frac{\partial v_x'}{\partial x}\right)$$

$$\boxed{\frac{\partial p'}{\partial t} + v_r'\frac{\partial P}{\partial r} + \frac{V_\theta}{r}\frac{\partial p'}{\partial \theta} + V_x\frac{\partial p'}{\partial x} + \gamma P\left(\frac{1}{r}\frac{\partial(rv_r')}{\partial r} + \frac{1}{r}\frac{\partial v_\theta'}{\partial \theta} + \frac{\partial v_x'}{\partial x}\right) = 0}$$

The linearized Euler equations are,

$$\frac{\partial \rho'}{\partial t} + \frac{V_\theta}{r}\frac{\partial \rho'}{\partial \theta} + V_x\frac{\partial \rho'}{\partial x} + \bar{\rho}\left(\frac{1}{r}\left(\frac{\partial r v_r'}{\partial r} + \frac{\partial v_\theta'}{\partial \theta}\right) + \frac{\partial v_x'}{\partial x}\right) = 0$$

$$\frac{\partial v_r'}{\partial t} + \frac{V_\theta}{r}\frac{\partial v_\theta'}{\partial \theta} - \frac{2V_\theta v_\theta'}{r} + V_x\frac{\partial v_r'}{\partial x} = -\frac{1}{\bar{\rho}}\frac{\partial p'}{\partial r} + \frac{\rho'}{\bar{\rho}^2}\frac{\partial \bar{p}}{\partial r}$$

$$\frac{\partial v_\theta'}{\partial t} + v_r'\frac{\partial V_\theta}{\partial r} + \frac{V_\theta}{r}\frac{\partial v_\theta'}{\partial \theta} + \frac{v_r' V_\theta}{r} + V_x\frac{\partial v_r'}{\partial x} = -\frac{1}{\bar{\rho}r}\frac{\partial p'}{\partial \theta}$$

$$\frac{\partial v_x'}{\partial t} + v_r'\frac{\partial V_x}{\partial r} + \frac{V_\theta}{r}\frac{\partial v_x'}{\partial \theta} + V_x\frac{\partial v_x'}{\partial x} = -\frac{1}{\bar{\rho}}\frac{\partial p'}{\partial x}$$

$$\frac{\partial p'}{\partial t} + v_r'\frac{\partial P}{\partial r} + \frac{V_\theta}{r}\frac{\partial p'}{\partial \theta} + V_x\frac{\partial p'}{\partial x} + \gamma P\left(\frac{1}{r}\frac{\partial (r v_r')}{\partial r} + \frac{1}{r}\frac{\partial v_\theta'}{\partial \theta} + \frac{\partial v_x'}{\partial x}\right) = 0$$

Recalling:

$$\frac{\partial P}{\partial r} = \frac{\bar{\rho}V_\theta^2}{r}$$

$$\gamma P = \bar{\rho}A^2$$

$$\rho' = \frac{1}{A^2}p'$$

We can rearrange the equations to reflect Equations 2.33-2.36. Note that the momentum equation in the θ and x directions remain unchanged. The term $\frac{\partial (r v_r')}{\partial r} = \frac{\partial (r)}{\partial r}v_r' + \frac{\partial v_r'}{\partial r}r$ in the Energy equation

$$\frac{1}{\bar{\rho}A^2}\left(\frac{\partial p'}{\partial t} + \frac{V_\theta}{r}\frac{\partial p'}{\partial \theta} + V_x\frac{\partial p'}{\partial x}\right) + \frac{V_\theta^2}{A^2 r}v_r' + \frac{\partial v_r'}{\partial r} + \frac{v_r'}{r} + \frac{1}{r}\frac{\partial v_\theta'}{\partial \theta} + \frac{\partial v_x'}{\partial x} = 0$$

$$\frac{\partial v_r'}{\partial t} + \frac{V_\theta}{r}\frac{\partial v_r'}{\partial \theta} - \frac{2V_\theta v_\theta'}{r} + V_x\frac{\partial v_r'}{\partial x} = \frac{1}{\bar{\rho}}\frac{\partial p'}{\partial r} + \frac{V_\theta}{\bar{\rho}r A^2}v_\theta^2 p'$$

$$\frac{\partial v_\theta'}{\partial t} + v_r'\frac{\partial V_\theta}{\partial r} + \frac{V_\theta}{r}\frac{\partial v_\theta'}{\partial \theta} + \frac{v_r' V_\theta}{r} + V_x\frac{\partial v_\theta'}{\partial x} = -\frac{1}{\bar{\rho}r}\frac{\partial p'}{\partial \theta}$$

$$\frac{\partial v_x'}{\partial t} + v_r'\frac{\partial V_x}{\partial r} + \frac{V_\theta}{r}\frac{\partial v_x'}{\partial \theta} + V_x\frac{\partial v_x'}{\partial x} = -\frac{1}{\bar{\rho}}\frac{\partial p'}{\partial x}$$

B.4 Substituting Pertubation Variables

One key assumption is that the perturbation quantites, $\tilde{p}$, $\tilde{v}_r$,$\tilde{v}_\theta$, and $\tilde{v}_x$, are all exponential and that they are solely a function of radius,

$$v'_r = v_r(r)e^{i(k_x x + m\theta - \omega t)}$$

$$v'_\theta = v_\theta(r)e^{i(k_x x + m\theta - \omega t)}$$

$$v'_x = v_x(r)e^{i(k_x x + m\theta - \omega t)}$$

$$p' = p(r)e^{i(k_x x + m\theta - \omega t)}$$

Substituting the quantities into the linearized equations will give us the final governing equations. Starting with the Conservation of Momentum in the r direction,

$$\frac{\partial v_r'}{\partial t} + \frac{V_\theta}{r}\frac{\partial v_r'}{\partial \theta} - \frac{2V_\theta}{r}v_r' + V_x\frac{\partial v_r'}{\partial x} = \frac{\partial p'}{\partial r} + \frac{\rho'}{\bar{\rho}^2}\frac{\partial P}{\partial r}$$

Looking at the left hand side (LHS) of the equation, the derivatives are:

$$\frac{\partial v_r'}{\partial t} = \underbrace{\frac{\partial v_r(r)}{\partial t}}_{0} e^{i(k_x x + m\theta - \omega t)} + v_r(r)\left(-i\omega e^{i(k_x x + m\theta - \omega t)}\right)$$

$$\frac{\partial v_r'}{\partial \theta} = \underbrace{\frac{\partial v_r(r)}{\partial \theta}}_{0} e^{i(k_x x + m\theta - \omega t)} + v_r(r)\left(im e^{i(k_x x + m\theta - \omega t)}\right)$$

$$\frac{\partial v_r'}{\partial x} = \underbrace{\frac{\partial v_r(r)}{\partial x}}_{0} e^{i(k_x x + m\theta - \omega t)} + v_r(r)\left(ik_x e^{i(k_x x + m\theta - \omega t)}\right)$$

Similarly for the right hand side (RHS),

$$\frac{\partial p'}{\partial r} = \frac{\partial P(r)}{\partial r}e^{i(k_x x + m\theta - \omega t)} + P(r)\underbrace{\frac{\partial}{\partial r}e^{i(k_x x + m\theta - \omega t)}}_{0}$$

Recalling $p'/\rho' = A^2 \to \rho' = \frac{1}{A^2}p'$ $\frac{\partial \bar{P}}{\partial r} = \frac{\bar{\rho}v_\theta^2}{r}$

$$\frac{\rho'}{\bar{\rho}^2}\frac{\partial \bar{P}}{\partial r} = \frac{V_\theta^2}{A^2}\frac{1}{\bar{\rho}r}p'$$

After substituting and canceling common terms,

$$v_r\left(-i\omega e^{i(k_x x + m\theta - \omega t)}\right) + \frac{V_\theta}{r}v_r\left(im e^{i(k_x x + m\theta - \omega t)}\right) - \frac{2V_\theta}{r}v_r e^{i(k_x x + m\theta - \omega t)} + V_x\left(v_r\left(ik_x e^{i(k_x x + m\theta - \omega t)}\right)\right)$$
$$= \left(-\frac{1}{\bar{\rho}}\frac{\partial P(r)}{\partial r}e^{i(k_x x + m\theta - \omega t)} + \frac{V_\theta^2}{A^2}\frac{1}{\bar{\rho}r}P(r)e^{i(k_x x + m\theta - \omega t)}\right)$$

$$\left(-i\omega + \frac{imV_\theta}{r} + ik_x V_x\right)v_r - \frac{2V_\theta}{r}v_\theta = -\frac{1}{\bar{\rho}}\frac{\partial P}{\partial r} + \frac{V_{\theta 2}}{A^2}\frac{1}{\bar{\rho}r}p$$

Continuing with conservation of momentum in the θ direction,

$$\frac{\partial v_\theta'}{\partial t} + v_r'\frac{\partial V_\theta}{\partial r} + \frac{V_\theta}{r}\frac{\partial v_\theta'}{\partial \theta} + \frac{v_r' V_\theta}{r} + V_x\frac{\partial v_\theta'}{\partial x} = -\frac{1}{\bar{\rho}r}\frac{\partial p'}{\partial \theta}$$

$$\frac{\partial v_\theta'}{\partial t} = \underbrace{\frac{\partial v_\theta(r)}{\partial t}}_{0}e^{i(k_x x + m\theta - \omega t)} + v_\theta(r)\left(-i\omega e^{i(k_x x + m\theta - \omega t)}\right)$$

$$\frac{\partial v_\theta'}{\partial \theta} = \underbrace{\frac{\partial v_\theta'(r)}{\partial \theta}}_{0}e^{i(k_x x + m\theta - \omega t)} + v_\theta(r)\left(ime^{i(k_x x + m\theta - \omega t)}\right)$$

$$\frac{\partial v_\theta'}{\partial x} = \underbrace{\frac{\partial v_\theta(r)}{\partial x}}_{0}e^{i(k_x x + m\theta - \omega t)} + v_\theta(r)\left(ik_x e^{i(k_x x + m\theta - \omega t)}\right)$$

$$\frac{\partial p'}{\partial \theta} = \underbrace{\frac{\partial P(r)}{\partial \theta}}_{0}e^{i(k_x x + m\theta - \omega t)} + P(r)\underbrace{\frac{\partial}{\partial \theta}e^{i(k_x x + m\theta - \omega t)}}_{me^{i(k_x x + m\theta - \omega t)}}$$

After substituting and canceling common terms

$$\left(-i\omega + \frac{imV_\theta}{r} + ik_x V_x\right)v_\theta + \left(\frac{V_\theta}{r} + \frac{\partial V_\theta}{\partial r}\right)v_\theta = -\frac{m}{\bar{\rho}r}p$$

Next, the conservation of momentum in the x direction,

$$\frac{\partial v_x'}{\partial t} + v_r'\frac{\partial V_x}{\partial r} + \frac{V_\theta}{r}\frac{\partial v_x'}{\partial \theta} + V_x\frac{\partial v_x'}{\partial x} = -\frac{1}{\bar{\rho}}\frac{\partial p'}{\partial x}$$

$$\frac{\partial v_x'}{\partial t} = \underbrace{\frac{\partial v_x(r)}{\partial t}}_{0}e^{i(k_x x + m\theta - \omega t)} + v_x(r)\left(-i\omega e^{i(k_x x + m\theta - \omega t)}\right)$$

$$\frac{\partial v'_x}{\partial \theta} = \underbrace{\frac{\partial v_x(r)}{\partial \theta}}_{0} e^{i(k_x x + m\theta - \omega t)} + v_x(r) \left(im e^{i(k_x x + m\theta - \omega t)} \right)$$

$$\frac{\partial v'_x}{\partial x} = \frac{\partial v_x(r)}{\partial x} e^{i(k_x x + m\theta - \omega t)} + v_x(r) \left(ik_x e^{i(k_x x + m\theta - \omega t)} \right)$$

$$\frac{\partial p'}{\partial x} = 0 + ik_x p e^{i(k_x x + m\theta - \omega t)}$$

$$\boxed{\left(-i\omega + \frac{imV_\theta}{r} + ik_x V_x \right) v_x + \frac{\partial V_x}{\partial r} v_r = -\frac{ik_x}{\bar{\rho}} p}$$

Continuing with the Conservation of Energy,

$$\frac{1}{\bar{\rho}A^2} \left(\frac{\partial p'}{\partial t} + \frac{V_\theta}{r} \frac{\partial p'}{\partial \theta} + V_x \frac{\partial p'}{\partial x} \right) + \frac{V_\theta^2}{A^2 r} v'_r + \frac{\partial v'_r}{\partial r} + \frac{1}{r} \frac{\partial v'_\theta}{\partial \theta} + \frac{\partial v'_x}{\partial x} = 0$$

Left hand side (LHS) derivatives:

$$\frac{\partial p'}{\partial t} = \underbrace{\frac{\partial p(r)}{\partial t}}_{0} e^{i(k_x x + m\theta - \omega t)} + p(r) \left(-i\omega e^{i(k_x x + m\theta - \omega t)} \right)$$

$$\frac{\partial p'}{\partial \theta} = \underbrace{\frac{\partial p(r)}{\partial \theta}}_{0} e^{i(k_x x + m\theta - \omega t)} + p(r) \left(im e^{i(k_x x + m\theta - \omega t)} \right)$$

$$\frac{\partial p'}{\partial x} = \underbrace{\frac{\partial p(r)}{\partial x}}_{0} e^{i(k_x x + m\theta - \omega t)} + p(r) \left(ik_x e^{i(k_x x + m\theta - \omega t)} \right)$$

$$\frac{\partial v'_r}{\partial r} = \frac{\partial v_r(r)}{\partial r} e^{i(k_x x + m\theta - \omega t)} + v_r(r) \underbrace{\frac{\partial}{\partial r} \left(e^{i(k_x x + m\theta - \omega t)} \right)}_{0}$$

$$\frac{\partial v'_\theta}{\partial \theta} = \frac{\partial v_\theta(r)}{\partial \theta} e^{i(k_x x + m\theta - \omega t)} + v_\theta(r) \left(im e^{i(k_x x + m\theta - \omega t)} \right)$$

$$\frac{\partial v_x'}{\partial x} = \underbrace{\frac{\partial v_x(r)}{\partial x}}_{0} e^{i(k_x x + m\theta - \omega t)} + v_x(r)\left(ik_x e^{i(k_x x + m\theta - \omega t)}\right)$$

After substituting and canceling common terms,

$$\frac{1}{\bar{\rho}A^2}\left(p(r)\left(-i\omega e^{i(k_x x + m\theta - \omega t)}\right) + \frac{V_\theta}{r}p(r)\left(ime^{i(k_x x + m\theta - \omega t)}\right) + V_x p(r)\left(ik_x e^{i(k_x x + m\theta - \omega t)}\right)\right) +$$

$$\frac{V_\theta^2}{A^2 r}v_r' + \frac{\partial v_r(r)}{\partial r}e^{i(k_x x + m\theta - \omega t)} + \frac{1}{r}\left(v_\theta(r)\left(ime^{i(k_x x + m\theta - \omega t)}\right)\right) + v_x(r)\left(ik_x e^{i(k_x x + m\theta - \omega t)}\right) = 0$$

$$\boxed{\frac{1}{\bar{\rho}A^2}\left(-i\omega + \frac{imV_\theta}{r} + ik_x V_x +\right)p(r) + \frac{V_\theta^2}{A^2 r}v_r + \frac{v_r}{r} + \frac{\partial v_r(r)}{\partial r} + \frac{im}{r}v_\theta(r) + ik_x v_x(r) = 0}$$

The Linearized Euler equations now become

r-direction: $i\left(-\omega + \dfrac{m}{r} + k_x V_x\right)v_r - \dfrac{2\bar{v}_\theta}{r}v_\theta = -\dfrac{1}{\bar{\rho}}\dfrac{\partial P}{\partial r} + \dfrac{V_{\theta 2}}{A^2}\dfrac{1}{\bar{\rho}r}p$

θ-direction: $i\left(-\omega + \dfrac{m}{r} + k_x V_x\right)v_\theta + \left(\dfrac{V_\theta}{r} + \dfrac{\partial V_\theta}{\partial r}\right)v_\theta = -\dfrac{m}{\bar{\rho}r}p$

x-direction: $i\left(-\omega + \dfrac{mV_\theta}{r} + k_x Vx\right)v_x + \dfrac{\partial V_x}{\partial r}v_r = -\dfrac{ik_x}{\bar{\rho}}p$

Energy: $\dfrac{1}{\bar{\rho}A^2}\left(-i\omega + \dfrac{imV_\theta}{r} + ik_x V_x +\right)p(r) + \dfrac{V_\theta^2}{A^2 r}v_r + \dfrac{v_r}{r} + \dfrac{\partial v_r(r)}{\partial r} + \dfrac{im}{r}v_\theta(r) + ik_x v_x(r) \quad = 0$

B.5 Non-Dimensionalization

Defining

$$r_T = r_{max}$$

$$A_T = A(r_{max})$$

$$k = \frac{\omega r_T}{A_T}$$

$$\bar{\gamma} = k_x r_T$$

$$\tilde{r} = \frac{r}{r_T}$$

$$\frac{\partial}{\partial r} = \frac{\partial \tilde{r}}{\partial r}\frac{\partial}{\partial \tilde{r}} = \frac{1}{r_T}\frac{\partial}{\partial \tilde{r}}$$

$$V_\theta = M_\theta A$$

$$V_x = M_x A$$

$$\tilde{A} = \frac{A}{A_T}$$

$$v_x = \tilde{v}_x A$$

$$v_r = \tilde{v}_r A$$

$$v_\theta = \tilde{v}_\theta A$$

$$p = \tilde{p}\bar{\rho}A^2$$

r-direction: $i\left(-\omega + \dfrac{mV_\theta}{r} + k_x V_x\right) v_r - \dfrac{2\bar{v}_\theta}{r} v_\theta = -\dfrac{1}{\bar{\rho}}\dfrac{\partial P}{\partial r} + \dfrac{V_{\theta 2}}{A^2}\dfrac{1}{\bar{\rho}r}p$

θ-direction: $i\left(-\omega + \dfrac{m}{r} + k_x V_x\right) v_\theta + \left(\dfrac{V_\theta}{r} + \dfrac{\partial V_\theta}{\partial r}\right) v_\theta = -\dfrac{m}{\bar{\rho}r}p$

x-direction: $i\left(-\omega + \dfrac{mV_\theta}{r} + k_x V x\right) v_x + \dfrac{\partial V_x}{\partial r}v_r = -\dfrac{ik_x}{\bar{\rho}}p$

Energy: $\dfrac{1}{\bar{\rho}A^2}i\left(-\omega + \dfrac{mV_\theta}{r} + k_x V_x\right) p(r) + \dfrac{V_\theta^2}{A^2 r}v_r + \dfrac{v_r}{r} + \dfrac{\partial v_r(r)}{\partial r} + \dfrac{im}{r}v_\theta(r) + ik_x v_x(r) = 0$

Substituting the non dimensional quantities, and noting r_T and A^2 in each term, the radial momentum equation becomes,

$$\boxed{i\left[-\dfrac{k}{\tilde{A}} + \dfrac{mM_\theta}{\tilde{r}} + \bar{\gamma}M_x\right]\tilde{v}_r - \dfrac{2M_\theta \tilde{v}_\theta}{\tilde{r}} = -\dfrac{1}{\bar{\rho}A^2}\dfrac{\partial \tilde{p}\bar{\rho}A^2}{\partial \tilde{r}} + M_\theta \dfrac{\tilde{p}}{\tilde{r}}}$$

Similarly for the θ and x directions:

$$\boxed{i\left[-\dfrac{k}{\tilde{A}} + \dfrac{mM_\theta}{\tilde{r}} + \bar{\gamma}M_x\right]\tilde{v}_\theta + \left(\dfrac{M_\theta}{\tilde{r}} + \dfrac{1}{A}\dfrac{\partial M_\theta A}{\partial \tilde{r}}\right)\tilde{v}_r = \dfrac{im}{\tilde{r}}\tilde{P}}$$

$$\boxed{i\left[-\dfrac{k}{\tilde{A}} + \dfrac{mM_\theta}{\tilde{r}} + \bar{\gamma}M_x\right]\tilde{v}_x + \dfrac{1}{A}\dfrac{\partial M_x A}{\partial \tilde{r}}\tilde{v}_r = -i\bar{\gamma}\tilde{P}}$$

and for the Energy equation:

$$\boxed{i\left[-\dfrac{k}{\tilde{A}} + \dfrac{mM_\theta}{\tilde{r}} + \bar{\gamma}M_x\right]\tilde{p} + \dfrac{M_\theta^2}{\tilde{r}}\tilde{v}_r + \dfrac{1}{A}\dfrac{\partial(\tilde{v}_r A)}{\partial \tilde{r}} + \dfrac{\tilde{v}_r}{\tilde{r}} + \dfrac{im}{\tilde{r}}\tilde{v}_\theta + i\bar{\gamma}\tilde{v}_x = 0}$$

Expanding mean derivatives (using product rule) $\dfrac{\partial \tilde{p}\bar{\rho}A^2}{\partial \tilde{r}}$

$$\boxed{i\left[-\dfrac{k}{\tilde{A}} + \dfrac{mM_\theta}{\tilde{r}} + \bar{\gamma}M_x\right]\tilde{v}_r - \dfrac{2M_\theta \tilde{v}_\theta}{\tilde{r}} = -\left(\dfrac{\partial \tilde{p}}{\partial \tilde{r}} + \dfrac{\tilde{p}}{\bar{\rho}A^2}\dfrac{\partial \bar{\rho}A^2}{\partial \tilde{r}}\right) + M_\theta \dfrac{\tilde{p}}{\tilde{r}}}$$

$$i\left[-\frac{k}{\widetilde{A}} + \frac{mM_\theta}{\tilde{r}} + \bar{\gamma}M_x\right]\tilde{v}_\theta + \left(\frac{M_\theta}{\tilde{r}} + \frac{1}{A}\frac{\partial M_\theta A}{\partial\tilde{r}}\right)\tilde{v}_r = \frac{im}{\tilde{r}}\tilde{P}$$

$$i\left[-\frac{k}{\widetilde{A}} + \frac{mM_\theta}{\tilde{r}} + \bar{\gamma}M_x\right]\tilde{v}_x + \frac{1}{A}\frac{\partial M_x A}{\partial\tilde{r}}\tilde{v}_r = -i\bar{\gamma}\tilde{P}$$

$$i\left[-\frac{k}{\widetilde{A}} + \frac{mM_\theta}{\tilde{r}} + \bar{\gamma}M_x\right]\tilde{p} + \frac{M_\theta^2}{\tilde{r}}\tilde{v}_r + \frac{\partial\tilde{v}_r}{\partial\tilde{r}} + \frac{1}{A}\frac{\partial A}{\partial\tilde{r}}v_r + \frac{\tilde{v}_r}{\tilde{r}} + \frac{im}{\tilde{r}}\tilde{v}_\theta + i\bar{\gamma}\tilde{v}_x = 0$$

$$\frac{1}{A}\frac{\partial A}{\partial \tilde{r}}$$

Recall, $\partial/\partial r = (1/r_T)(\partial/\partial \tilde{r}$,

$$\frac{1}{A}\frac{\partial A}{\partial \tilde{r}} = r_T \left(\frac{1}{A}\frac{\partial A}{\partial r} \right)$$
$$= \frac{r_T}{A^2} \left(A\frac{\partial A}{\partial r} \right)$$

Using the trick, $\frac{\partial}{\partial r}\left(\frac{A^2}{2} \right) = A\frac{\partial A}{\partial r}$

$$= \frac{r_T}{A^2} \left(\frac{\partial}{\partial r}\left(\frac{A^2}{2} \right) \right)$$
$$= \frac{r_T}{2A^2}\frac{\partial A^2}{\partial r}$$

Using the definition derived earlier (Needs eqn reference) $\frac{\partial A^2}{\partial r} = \frac{\gamma-1}{2}\frac{v_\theta^2}{r}$

$$= \frac{r_T}{2A^2}\frac{\gamma-1}{2}\frac{v_\theta^2}{r}$$
$$= \frac{\gamma-1}{2}\frac{M_\theta^2}{\tilde{r}}$$

$$\frac{\partial \rho A^2}{\partial \tilde{r}} = \gamma\frac{\partial p}{\partial \tilde{r}}$$
$$= \gamma\frac{\rho v_\theta^2}{\tilde{r}}$$
$$= r_T\gamma\frac{\rho v_\theta^2}{r}$$

$$\frac{1}{\rho A^2} \frac{\partial \rho A^2}{\partial r} = \frac{\gamma M_\theta^2}{\tilde{r}}$$

Substituting in yields ,

$$i \left[-\frac{k}{\tilde{A}} + \frac{m M_\theta}{\tilde{r}} + \bar{\gamma} M_x \right] \tilde{v}_r - \frac{2 M_\theta \tilde{v}_\theta}{\tilde{r}} = -\frac{\partial \tilde{p}}{\partial \tilde{r}} - (\gamma - 1) \frac{\gamma M_\theta}{\tilde{r}} \tilde{p}$$

$$i \left[-\frac{k}{\tilde{A}} + \frac{m M_\theta}{\tilde{r}} + \bar{\gamma} M_x \right] \tilde{v}_\theta + \left(\frac{M_\theta}{\tilde{r}} + \frac{1}{A} \frac{\partial M_\theta A}{\partial \tilde{r}} \right) \tilde{v}_r = \frac{im}{\tilde{r}} \tilde{p}$$

$$i \left[-\frac{k}{\tilde{A}} + \frac{m M_\theta}{\tilde{r}} + \bar{\gamma} M_x \right] \tilde{v}_x + \frac{1}{A} \frac{\partial M_x A}{\partial \tilde{r}} \tilde{v}_r = -i \bar{\gamma} \tilde{p}$$

$$i \left[-\frac{k}{\tilde{A}} + \frac{m M_\theta}{\tilde{r}} + \bar{\gamma} M_x \right] \tilde{p} + \frac{M_\theta^2}{\tilde{r}} \tilde{v}_r + \frac{\partial \tilde{v}_r}{\partial \tilde{r}} + \frac{1}{A} \frac{\partial A}{\partial \tilde{r}} v_r + \frac{\tilde{v}_r}{\tilde{r}} + \frac{im}{\tilde{r}} \tilde{v}_\theta + i \bar{\gamma} \tilde{v}_x = 0$$

Defining, $\lambda = -i\bar{\gamma}$

and defining

$$\{\bar{x}\} = \begin{Bmatrix} \tilde{v}_r \\ \tilde{v}_\theta \\ \tilde{v}_x \\ \tilde{p} \end{Bmatrix}$$

The governing equations can be written in the form of $[A]x - \lambda[B]x$

$$
\begin{bmatrix}
-i\left(\frac{k}{A} - \frac{mM_\theta}{\tilde{r}}\right) - \lambda M_x & -\frac{2M_\theta}{\tilde{r}} & 0 & \frac{\partial}{\partial \tilde{r}} + \frac{\gamma-1}{\tilde{r}} \\
\frac{M_\theta}{\tilde{r}} + \frac{\partial M_\theta}{\partial \tilde{r}} + \left(\frac{\gamma-1}{2}\right)\frac{M_\theta^3}{\tilde{r}} & -i\left(\frac{k}{A} - \frac{mM_\theta}{\tilde{r}}\right) - \lambda M_x & 0 & \frac{im}{\tilde{r}} \\
\frac{\partial M_x}{\partial \tilde{r}} + \left(\frac{\gamma-1}{2}\frac{M_x M_\theta^2}{\tilde{r}}\right) & 0 & -i\left(\frac{k}{A} - \frac{mM_\theta}{\tilde{r}}\right) - \lambda M_x & -\lambda \\
\frac{\partial}{\partial \tilde{r}} + \frac{\gamma+1}{2}\frac{M_\theta^2}{\tilde{r}} + \frac{1}{\tilde{r}} & \frac{im}{\tilde{r}} & -\lambda & -i\left(\frac{k}{A} - \frac{mM_\theta}{\tilde{r}}\right) - \lambda M_x
\end{bmatrix}
\bar{x} =
$$